T.C.
YEDITEPE UNIVERSITY
INSTITUTE OF HEALTH SCIENCES
DEPARTMENT OF PHARMACEUTICAL CHEMISTRY

IN SILICO TARGET PREDICTION OF 6-GINGEROL AND SIMILAR COMPOUNDS AS POSSIBLE ANTICANCER AGENTS

MASTER OF SCIENCE THESIS

NOUR AL-MASSRI, MSc.

İstanbul-2022

T.C.
YEDITEPE UNIVERSITY
INSTITUTE OF HEALTH SCIENCES
DEPARTMENT OF PHARMACEUTICAL CHEMISTRY

IN SILICO TARGET PREDICTION OF 6-GINGEROL AND SIMILAR COMPOUNDS AS POSSIBLE ANTICANCER AGENTS

MASTER OF SCIENCE THESIS

NOUR AL-MASSRI, MSc.

SUPERVISOR

Assist. Prof. Enise Ece Gürdal

CO-ADVISOR

Assist. Prof. Gülçin Tuğcu

İstanbul-2022

THESIS APPROVAL

Institute : Yeditepe University Institute of Health Sciences

Program : Pharmaceutical Chemistry

Title of the Thesis : In Silico Target Prediction Of 6-Gingerol and Similar Compounds as Possible Anticancer Agents

Owner of the Thesis : Nour Al-Massri

Examination Date : 29.09.2022

This study was approved as a Master Thesis in regard to content and quality by the Jury.

Chair of the Jury	Prof. Dr. Hülya Akgün (Yeditepe University)
Supervisor	Assist. Prof. Dr. Enise Ece Gürdal (Yeditepe University)
Co.Advisor	Assist. Prof. Dr. Gülçin Tuğcu (Yeditepe University)
Examiner	Prof. Dr. Filiz Esra Önen Bayram (Yeditepe University)
Examiner	Prof. Dr. Gökçen Eren (Gazi University)

APPROVAL

This thesis has been deemed by the jury in accordance with the relevant articles of Yeditepe University Graduate Education and Examinations Regulation and has been approved by Administrative Board of Institute with decision dated ..... and numbered .....

Prof. Dr. Bayram Yılmaz

Director of Institute of Health Sciences

DECLARATION

I declare that this thesis is my own work and that, to the best of my knowledge and belief, it contains no material previously published or written by another person nor material which has been accepted for the award of any other degree except where due acknowledgment has been made in the text.

29.09.2022

Nour Al Massri

ACKNOWLEDGEMENTS

I extend my deepest thanks and gratitude to my dedicated supervisors Assist. Prof. Enise Ece Gürdal and Assist. Prof. Gülçin Tuğcu. For all their effort they made in supervising this research and helping to complete it. For being always present to answer questions, give advice and directions to accomplish this work, and present it in the best way. It is a great honor to be one of their master's students and I am willing to take our scientific relationship forward.

All thanks and appreciation to the head of the department Prof. Hülya Akgün, for all the information I have learned, for her kindness during the years of study.

All thanks and appreciation to Prof. Filiz Esra Önen Bayram, for all the information I have learned, for her kindness during the years of study.

All thanks and appreciation to Prof. Gökçen Eren for her suggestions to improve the work.

TABLE OF CONTENTS

LIST OF TABLES

LIST OF FIGURES

LIST OF ABBREVIATIONS

5-FU	5-Fluorouracil
ADME	Absorption, Distribution, Metabolism, And Excretion
ADRB1	Beta-1 Adrenergic Receptor
AGC	Protein Kinase A/G/C-Related Kinase
AKT	Serine/Threonine Kinase 1
AlOX15	Arachidonate 15-Lipoxygenase
ALOX5	Arachidonate 5-Lipoxygenase
AR	Androgen Receptor
Asp	Aspartic Acid
ATP	Adenosine Triphosphate
BA	Bioavailability Score
Bax	Bcl-2-Associated X Protein
BBB	Blood Brain Barrier
Bcl-2	B-Cell Lymphoma 2
BCRs	B Cell Receptors
B-RAF	V-Raf Murine Sarcoma Viral Oncogene Homolog B1
CADD	Computer-Aided Drug Design
CAMK	Ca^{2+}/Calmodulin- Dependent Kinase
Cdk	Cyclin-Dependent Kinase
cIAP1	Cellular Inhibitor Of Apoptosis Proteins
CK1	Casein Kinase 1
CLtot	Total Clearance
CML	Chronic Myelogenous Leukemia
CNS	Central Nervous System
CRLM	Colorectal Cancer Liver Metastasis
CYP450	Cytochrome P450
CYS	Cysteine
DFG	Asp-Phe-Gly
DOX	Doxorubicin
EP300	Histone Acetyltransferase P300
ERK	Extracellular Signal-Regulated Kinase

FDA	Food And Drug Administration
FP2	Fingerprints
GI	Gastrointestinal
Gln	Glutamine
Glu	Glutamic Acid
HBAs	Hydrogen Bond Acceptors
HBD	Hydrogen Bond Donors
iLOGP	n-Octanol/Water Partition Coefficient
JAK	Janus Tyrosine Kinase
LBVS	Ligand-Based Virtual Screening
Leu	Leucine
Lico B	Licochalcone B
MAPK	Mitogen-Activated Protein Kinase
MDM2	p53-binding protein Mdm-2
MMP	Mitochondrial Membrane Potential
MOE	Molecular Operating Enviroment
Mol.wt	Molecular Weight
mTOR	Mammalian Target Of Rapamycin
MW	Molecular Weight
NFκB	Nuclear Factor NF-Kappa-B
NMR	Nuclear Magnetic Resonance
NRB	Number Of Rotatable Bonds
NRB	Number Of Rotatable Bonds
OSCC	Oral Squamous Cell Carcinoma
OCT2	Organic Cation Transporter 2
OX	Oxaliplatin
P53	Phosphoprotein Tumor Suppressor
Pa	Probable Activity
PARP	Poly (ADP-Ribose) Polymerase
P-gp	P-Glycoprotein
Phe	Phenylalanine
Pi	Probable inactivity
PI3K	Phosphatidylinositol-3-Kinase

PSA	Polar Surface Area
QSAR	Quantitative Structure–Activity Relationship
Rb	Retinoblastoma
RBVS	Receptor-Based Virtual Screening
RGC	Receptor Guanylyl Cyclase
Ro5	Rule Of Five
SA	Synthetic Accessibility
SBVS	Structure-based Virtual Screening
Ser	Serine
STE	Serine/ threonine Related Kinase
SYK	Spleen Tyrosine Kinase
Thr	Threonine
Tk	Tyrosine Kinase
TKL	Tyrosine Kinase-Like Kinase
TPSA	Topological Polar Surface Area
TUBB1	Tubulin Beta-1 Chain
Tyr	Tyrosine
VS	Virtual Screening
WHO	World Health Organization

ABSTRACT

Al-Massri, N (2022). In Silico Target Prediction of 6-Gingerol and Similar Compounds as Possible Anticancer Agents. Yeditepe University Institute of Health Sciences, Department of Pharmaceutical Chemistry, MSc. Thesis, Istanbul.

Cancer still affects millions of people and causes death around the globe. Due to its prevalence, the discovery of novel anticancer drugs has always been a hot topic in pharmaceutical chemistry. Natural products provide a reliable source of bioactive substances and a rich resource for novel therapeutic leads. Also, the phyto-substances have fewer side effects, are relatively affordable, and offer a potent alternative. Hence, in our study, the 6-gingerol was focused on, as one of the polyphenols in ginger (*Zingiber officinale Roscoe*) characterized by a diversity of biological activities, specifically anti-cancer activity. Similar analogues of 6-gingerol were firstly screened by using similarity screening and then the putative biological targets of 6-gingerol and its similar compounds were investigated by using *in silico* target fishing servers. Their effect on the kinases as an anti-cancer target were specifically focused on. The docking study was performed for the 6-gingerol and its similars with the B-Raf proto-oncogene serine/threonine kinase (BRAF), Janus kinase (JAK1/2), extracellular signal-regulated kinase (ERK1(MAPK3)), and human p38 mitogen-activated kinase (p38γ) crystal structures. Computational studies revealed that vanylglycol, L-(+)-vanillylmandelic acid, dehydrozingerone, 2-methoxyestrone, methylvanillate, dihydroconiferyl aldehyde, pratensein, acetovanillone, acetosyringone, licochalcone B, isoferulic acid, curcumin PE, and coniferaldehyde can interact with at least one of these targets. Also, all these studied compounds satisfied Lipinski's rule of five. The computational approaches that were used for toxicity predictions revealed that none of the compounds have toxicity on cardiac and hepatic organs. Furthermore, these selected compounds have toxicities on one or more tumor cells. Eventually, the *in silico* target and toxicity predictions revealed that these similar molecules to 6-gingerol, are possible anticancer candidates that could be developed further within future lead optimization studies.

Key words: 6-gingerol, anticancer, chemical similarity, kinase, target fishing, docking studies, computational toxicity

ÖZET

Al-Massri, N (2022). Antikanser Etkili 6-Gingerol ve Benzeri Bileşiklerin Olası In Silico Hedeflerinin Tahmini. Yeditepe Üniversitesi Sağlık Bilimleri Enstitüsü, Farmasötik Kimya Anabilim Dalı, Yüksek Lisans Tezi, İstanbul.

Kanser halen milyonlarca insanı etkilemekte ve dünya çapında hastalık ve ölümlere neden olmaktadır. Yaygınlığı nedeniyle, yeni antikanser ilaçların keşfi farmasötik kimyada her zaman popüler bir konu olmuştur. Doğal ürünler, güvenilir bir biyoaktif madde kaynağı ve yeni terapötik ipuçları için zengin bir kaynak sağlar. Ayrıca, bitkisel maddeler daha az yan etkiye sahiptir, nispeten ekonomiktir ve güçlü bir alternatif sunar. Bu nedenlerle, çalışmada, zencefildeki *(Zingiber officinale Roscoe)* polifenollerden biri olan ve özellikle antikanser aktivite olmak üzere çeşitli biyolojik aktivitelerle karakterize edilen 6-gingerol üzerine odaklanıldı. İlk olarak benzerlik taraması kullanarak 6-gingerol'ün benzer analoglarını tarandı ve daha sonra *in silico* hedef belirleme sunucuları kullanılarak 6-gingerol ve benzer bileşiklerinin varsayılan biyolojik hedefleri araştırıldı. Özellikle bir antikanser hedef olarak kinazlar üzerindeki etkisine odaklanıldı. 6-gingerol ve benzerleri için B-Raf proto-onkojen serin/treonin kinaz (B-RAF), Janus kinaz (JAK1/2), hücre dışı sinyale düzenlenen kinaz (ERK1(MAPK3)) ve insan p38 mitojen-aktive kinazı (p38γ) ile kenetlenme çalışmaları gerçekleştirildi. Hesaplamalı çalışmalar, vanilglikol, L-(+)-vanilmandelik asit, dehidrozingeron, 2-metoksiestron, metilvanilat, dihidrokoniferil aldehit, pratensein, asetovanillon, asetosiringon, likokalkon B, izoferulik asit, kurkumin PE ve koniferaldehitin bu hedeflerden en az biriyle etkileşime girebileceğini ortaya koymuştur. Ayrıca, incelenen tüm bu bileşikler Lipinski'nin beş kuralını karşılamıştır. Toksisite tahminleri için kullanılan hesaplamalı yaklaşımlar, bileşiklerin hiçbirinin kardiyak ve hepatik organlar üzerinde toksisiteye sahip olmadığını ortaya koymuştur. Ayrıca, seçilen bu bileşikler bir veya daha fazla tümör hücresi üzerinde toksisiteye sahiptir. Sonuç olarak, *in silico* hedef ve toksisite tahminleri, 6-gingerol ile benzer moleküller olan bu bileşiklerin, gelecekteki öncü optimizasyon çalışmalarında daha da geliştirilebilecek potansiyel antikanser adaylar olduğunu ortaya koymuştur.

Anahtar kelimeler: 6-gingerol, antikanser, kimyasal benzerlik, kinaz, hedef tahmini, yerleştirme çalışmaları, bilgisayar destekli toksikoloji

1. INTRODUCTION AND PURPOSE

Cancer is considered as one of the primary diseases that cause death worldwide. Many cancer treatments exist depending on the particular situation of the patient who may receive one treatment or combination of treatments. One of these treatments is chemotherapy which is still the most widely used one to treat all kinds of cancers at any stage of cancer progression. Although, this current therapy failed to cure the malignancy of the disease and the life span can expand only for few months [1]. Chemotherapy treatment has several disadvantages like requiring high doses, severe side effects related to toxicity, activation of pro-survival pathways upon long-term exposure, and development of chemoresistance [1, 2]. Hence, researchers are always working to find another source that they could depend on to discover and develop new anti-tumor drugs. They found natural resources as a good alternative because it contains products such as alkaloids, flavonoids, terpenoids, polysaccharides, saponins, and others that have been conducted as natural bioactive products with potent anticancer activity. Over 60% of anticancer drugs that are in clinical use now and have shown a significant efficacy for combating cancer are derived from natural products. Natural sources consider one of the best sources of drugs which is in line with our concern to improve a new natural anti-tumor drug that can decrease cell toxicity and the adverse effects that happen when traditional therapy was used. Studies have admitted that the most natural products act as anti-cancer drugs by activating regulating immune function, inducing autophagy, or inhibiting cell proliferation [1]. Ginger (*Zingiber officinale Roscoe*), which belongs to the Zingiberaceae family and the Zingiber genus, has been commonly used as a spice and herbal medicine. Ginger root is the essential part that was used to palliate and treat several ordinary diseases, such as headaches, colds, nausea, and emesis. Ginger contains many bioactive compounds such as phenolic compounds like gingerols, shogaols, and paradols. But the major polyphenols found in fresh ginger are 6-gingerol, 8-gingerol, 10-gingerol and terpene compounds. Most recently, the bioactive compounds in ginger have been found to possess different biological activities, such as antioxidant, anti-inflammatory, antimicrobial, anticancer activities, and others. Researchers find that these major activities are referred to 6-Gingerol (1-[4’-hydroxy-3’-methoxyphenyl]-5-hydroxy-3-decanone) (Figure 1.1.). The activity of this molecule is related to the aliphatic chain moiety containing a hydroxyl group [3, 4].

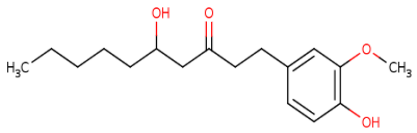

Figure 1.1. Structure of 6-gingerol.

Many studies show the effect of 6-Gingerol as an anticancer in multiple human carcinomas, including leukemia, breast, colon, pancreatic, prostate, and liver cancers. The studies show that the most potential mechanisms of action involve the inhibition of proliferation and the induction of apoptosis in cancer [3- 5].

Kinases are cellular transmitters that accelerate the phosphorylation reaction by moving the γ-phosphate of an ATP molecule to Ser, Thr, or Tyr residues in the substrate. Kinases are crucially regulated the cellular signaling pathways as a result of controlling a diversity of cellular functions including transcription, metabolism, nervous system activity, immunological response, cell division, and migration [6- 8] Additionally, the dysregulation and mutations of protein kinase have been linked with a diversity of human diseases such as cancer, diabetes, autoimmune, cardiovascular, inflammatory, and neurological disorders which make the protein kinases one of the principal therapeutic targets for cancer [9].

The traditional drug discovery process needs many efforts like high costs and long development cycles. Also, the rate of its success is low. As a result, various computer-aided drug design techniques are used to decrease the challenges that the traditional process face [10, 11]. Virtual screening (VS) is a computational method for selecting chemicals from a huge library that bind to a particular target, typically an enzyme or receptor. Nowadays, it is one of the most effective tools. It determines the most advantageous bioactive ligands utilizing the information of the target or known active ligand. It is also known as an alternative to high-throughput screenin because it is performed with low cost, and the highest ability to find the most appropriate novel hit through the filtration of large molecules found in libraries. VS techniques can typically be separated into two more common VS types: ligand-based virtual screening (LBVS) and receptor-based virtual screening (RBVS) [10, 12, 13].

Small molecules can interact with multiple proteins of particular interest for rationally designing more effective and less toxic drugs. To detect this interaction between the ligand and target, docking is a method used to predict the preferred orientation of one molecule to a second. Indeed, docking helps to predict the bioactive conformation structure of a molecule in the binding site of a target which is equivalent to find the global free energy minimum of the system consisting of the ligand and the target. Docking is also used as a tool in structure-based drug design as well as in structure-based virtual screening [13, 14]. Also, the computational methods give information about absorption, distribution, metabolism, excretion, and toxicity (ADMET) properties as well as physicochemical characterization [15].

Under light of aforementioned literature, this study aims to determine new lead compounds similar to 6-gingerol that show anticancer activity with a high bioavailability and low toxicity profile. For this aim, an *in silico* screening were performed to search for compounds that have similar structures to 6-gingerol by using ChemMine Tools depending on the PubChem fingerprints. Then, 6-gingerol and similar compounds are further evaluated for their potential anticancer activities on kinases. For that, compounds are investigated for their putative biological targets by *in silico* target fishing servers. Selected kinase targets are further utilized in docking studies to present the possible interactions of the dataset. Additionally, the pharmacokinetics, drug-likeness, and toxicity profile of these compounds were computationally determined to point out the safety and bioavailability of 6-gingerol and its similar compounds. The workflow of the study is given in Figure 1.2. The outcomes of this work reveal some lead compounds together with new targets and pathways for further development.

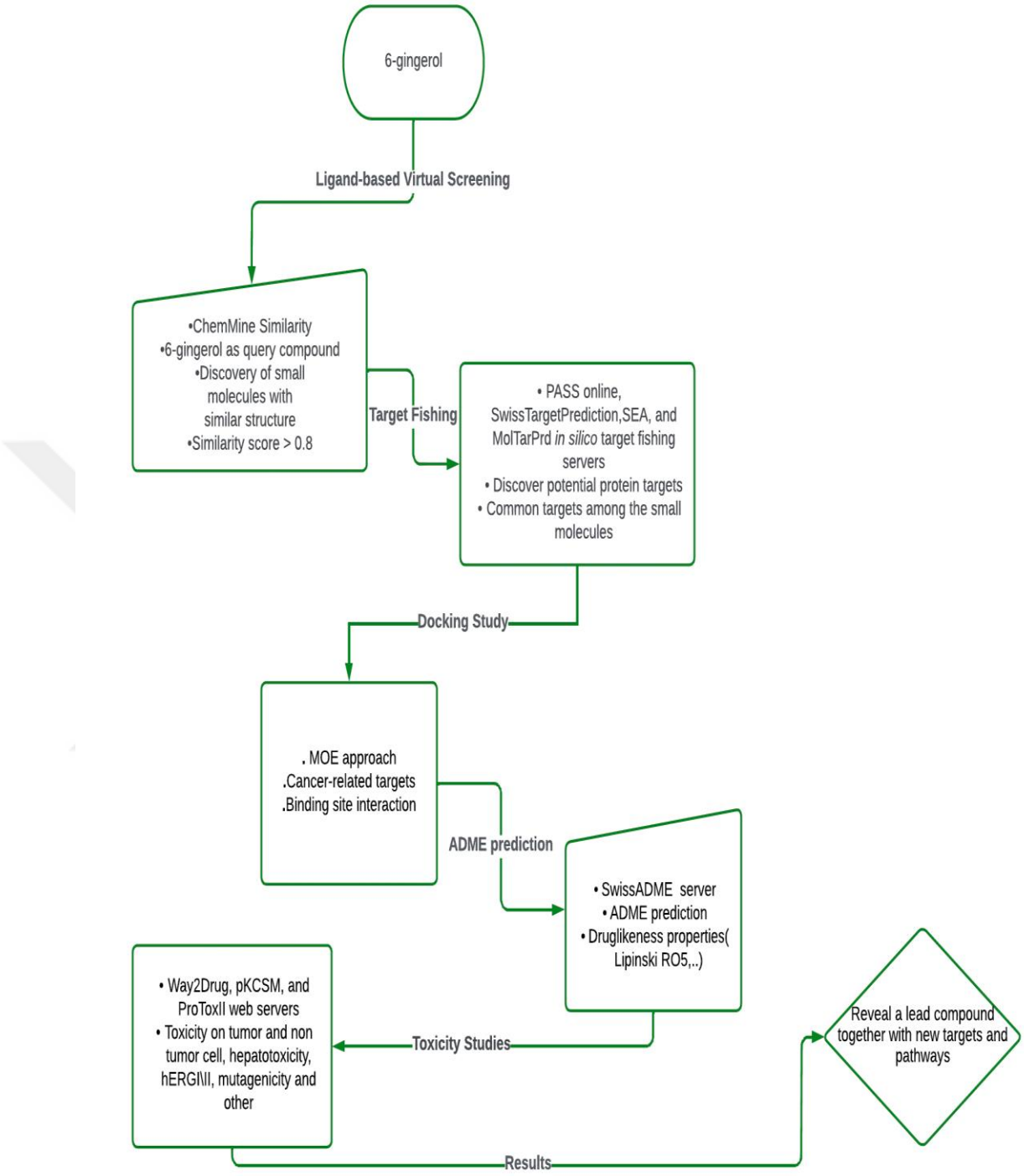

Figure 1.2. Workflow of the study

2. LITERATURE REVIEW

2.1 Cancer

2.1.1 Epidemiology and Etiology

Millions of people are affected by cancer which is one of the chief causes of illness and mortality around the globe. According to the estimations from the World Health Organization (WHO), there were 96 million people who died from cancer and 18.1 million new cases of cancer globally in 2018. By 2040, there will be an increase of about 27 million new cases of cancer annually from the estimated cases in 2018 [1, 16]. Cancer is a broad term that covers more than 100 different diseases that can affect a variety of organs and cell types. However, all types of cancer are distinguished by aberrant cell proliferation caused by hereditary or environmental-induced genomic instability and mutations. Cancer is characterized by cellular transformation, apoptosis, and other types of cell death dysregulation, enhanced proliferation, angiogenesis, immune evasion, inflammatory responses, and, eventually, metastatic spreading [17, 18]. Lungs, prostate, colorectal, stomach, and liver are the most common cancer spreading among men while breast, colorectal, lungs, cervix, and stomach are the most spread among women [1]. According to published reports, between 90 and 95 % of all cancers are caused by lifestyle factors, such as smoking, drinking, obesity, pollution, and dietary additives, with the remaining 5 to 10 % being due to genetic defects [18].

2.1.2 Therapies and Needs to Alternative Sources

Many cancer treatments exist depending on the status of the patient, who may take one treatment or a combination of treatments. The most often utilized forms of cancer treatment are surgery, chemotherapy, radiation, and targeted therapy. Surgery is typically required for cancer patients, whether to detect, treat, or prevent cancer, and it proved to be quite beneficial if the disease has not moved to other body parts. Chemotherapy refers to the use of drugs or medications to treat cancer. There are over 100 chemotherapeutic medications for cancer in use today, each with a unique composition and mode of action. In radiotherapy, cancer cells are eliminated by high-energy particles. Targeted therapy, a relatively recent technique, uses chemicals to target specific cancer cells while reducing harm to healthy cells [1, 19]. In spite of this, chemotherapy remains one of the most commonly utilized therapies in all types of tumors and at all stages of cancer progression [1]. Besides the wide usage of chemotherapy, it failed to cure the malignancy of the disease, and the life span can expand only for a few months. Studies confirmed that

chemotherapy is linked to a wide range of adverse effects, including hepatotoxicity and cardiotoxicity, which are severe or even lethall. Here are a few examples of the drugs that cause critical side effects while using them to cure cancer. FOLFOX, which consists of 5-fluorouracil (5-FU), leucovorin, and oxaliplatin (OX) are used to treat colorectal cancer liver metastasis (CRLM), researchers found that they promote cardiotoxicity by affecting different mechanisms such as forming coronary thrombosis, arthritis, and lead to vasospasm. Also, Doxorubicin (DOX) treatment causes arrhythmia or cardiomyopathy due to the production of reactive oxygen species and the release of cytochrome c from mitochondria. It was also shown that therapeutic dosages of DOX increase lipid peroxidation in microsomes and mitochondria in the liver, especially when Fe^{3+} ions are present. Even a single dose of DOX has been shown to cause irreversible liver damage and an increase in apoptotic processes in hepatic tissue [17, 20, 21]. Additionally, chemotherapy observes a myriad of challenges, including the need for high doses, severe side effects from toxicity, activation of pro-survival pathways after prolonged exposure, and the development of chemoresistance [1, 2]. The development of a new class of anticancer agents with less toxicity in comparison with the current chemotherapeutic agents and not affected by common mechanisms of chemoresistance would be a significant advancement in cancer therapy [17]. In this regard, natural substances, particularly spices and herbs, have gained the interest of experts due to their diverse health-promoting qualities [18]. They determined that using natural resources was a good alternative because it contains substances like alkaloids, flavonoids, terpenoids, polysaccharides, saponins, and others that have been proven as natural bioactive products with potent anticancer activity. Over 60% of anticancer drugs that are in clinical use now and have shown significant efficacy for combating cancer are derived from natural products. Natural sources are regarded as one of the best sources of drugs which is in line with our concern to improve a new natural anti-tumor drug that can decrease cell toxicity and the adverse effects that happen when traditional therapy was used. Studies have admitted that the most natural products act as anti-cancer drugs by activating regulatory immune function, inducing autophagy, or inhibiting cell proliferation [1].

2.2 *Zingiber officinalle Roscoe*

2.2.1 *Zingiber Officinalle Roscoe* and Cancer

Ginger (*Zingiber officinale Roscoe*), which is a member of the Zingiberaceae family and zingiber genus, has been used as a spice and herbal medicine for a long time. Ginger root is generally used to alleviate and treat a variety of common illnesses like headaches, colds, nausea, and emesis. Ginger has diverse bioactive substances, including phenolic and terpene substances. The major phenolic chemicals that are responsible for ginger's different bioactivities include gingerols, shogaols, paradols, and zingerone. Lately, numerous studies indicate that the biological properties of ginger's constituents have antioxidant, anti-inflammatory, antibacterial, and anticancer properties. Additionally, other studies have shown that ginger can prevent and treat a variety of ailments, including respiratory problems, obesity, diabetes mellitus, chemotherapy-induced nausea and emesis, cardiovascular, metabolic, and neurodegenerative diseases, indigestion, infertility, insomnia, and memory booster [3, 4, 22]. In recent times, when the ginger was recommended as a nutural home cure that may aid against COVID-19, it obtained a considerable public attention and although at this time, there is little data to support its use. Also, ginger's anti-inflammatory characteristics may be useful in treating respiratory symptoms carried on by the SARS-CoV-2 infection [23].

2.2.2 The Bioactive Components of the Ginger

Ginger contains various active ingredients like phenolic and terpene chemicals (Table 2.1.). The main phenolic substances found in ginger are gingerols, shogaols, and paradols. Gingerols, including 6-gingerol, 8-gingerol, and 10-gingerol, are chiefly polyphenols present in fresh ginger. Terpene components are noticed as the primary constituents of ginger essential oils. In addition to these, ginger also contains polysaccharides, lipids, organic acids, raw fibers, protein, phytosterols, vitamins (like nicotinic acid and vitamin A), and minerals. These constituents have been utilized extensively in a variety of culinary products, such as soft beverages, as well as numerous pharmaceutical compositions. 6-gingerol, which is found in considerable amounts in the fresh rhizome, is in charge of the majority of the pharmacological effects of ginger that were previously documented [3, 18, 24].

Table 2.1. The phenolic and terpene compounds in ginger

Phenolic compounds	Terpene compounds
Gingerols	β-bisabolene
Shogaols	α-curcumene
Paradols	Zingiberene
Quercetin	α-farnesene
Zingerone	β-sesquiphellandrene
gingerenone-A	
6-dehydrogingerdione	

2.2.3 The Relationship Between 6-Gingerol and Cancer

Many studies about the anticancer properties of ginger are mainly concentrated on gingerols, especially 6-gingerol. The activity of 6-gingerol (1-[4'-hydroxy-3'-methoxyphenyl]-5-hydroxy-3-decanone) is related to the aliphatic chain containing a hydroxyl group [4, 18]. Many experimental studies show the effect of 6-gingerol as an anticancer agent in multiple human carcinomas, including leukemia, breast, colon, cervical, pancreatic, prostate, and liver cancers [4]. *In vivo* and *in vitro* studies along with clinical trials unveiled that 6-gingerol can target cellular molecules, inhibit proliferation, induce apoptosis, and act as an anti-invasive agent in multiple cancer types via modulating the expression of NF-κB, STAT3, Rb, MAPK, PI3K, Akt, ERK, cIAP1, cyclin A, cyclin-dependent kinase (Cdk), cathepsin D, and caspase-3/7 (Figure 2.1.) [3, 5, 18, 23- 26]. Lin and colleagues' study, which investigated the anticancer actions of 6-gingerol on human colon cancer cells (LoVo), found a considerable, dose-dependent decrease in cell viability. The outcomes highlighted how crucial 6-gingerol is used as a therapy for colon cancer. Whereas 6-gingerol primarily caused cell cycle arrest at the G2/M phase, has minimal impact on the subG1 phase and lowers cyclin A, cyclin B1, and CDK1 levels. Additionally, 6-gingerol administration enhanced the amount of ROS and p53 phosphorylation and raised the ratio of the negative cell cycle regulators p27Kip1 and p21Cip1 [18]. *In vivo* experiments were conducted to validate the outcomes of the *in vitro* studies. In one of the *in vivo* experiments, 6-gingerol was found to decrease tumor formation in a murine xenograft tumor model. The outcomes showed that 6-gingerol administration dramatically lowered anti-apoptotic proteins such as proliferating cell nuclear antigen, Bcl2, Bcl-XL, and XIAP and promoted pro-apoptotic proteins like Bax, Bak, and PARP cleavage and caspase-3 activation. Furthermore, 6-gingerol had no

adverse effects on hematological markers or body weights, indicating that it could be used as a future chemotherapeutic [18]. Other research has been conducted to determine the mechanisms of 6-gingerol. It observed alterations after treating SW-480 cells with 6-gingerol. Procaspase-8 and -9 were significantly cleaved into their active fragments, p43/41 and p35/37, respectively. Additionally, it has been demonstrated that 6-gingerol increases effector caspase-3 and -7 activation in a dose-dependent manner by cleaving procaspase-3 and -7 into their respective active segments, p17/19 and p20. Likewise, the caspase-3 substrate PARP protein was also found to be cleaved, which is consistent with caspase-mediated apoptosis [18].

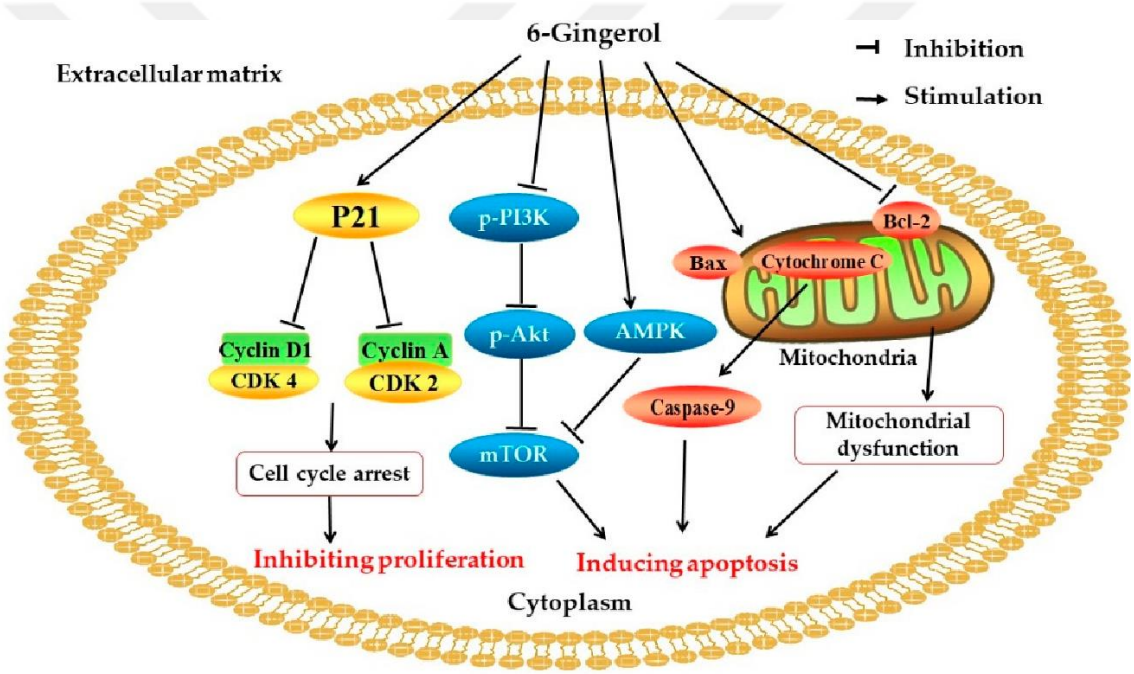

Figure 2.1. Several signaling pathways involve in the anticancer mechanisms of 6-gingerol [3].

2.3 Protein Kinase Inhibitors

2.3.1 Human Protein Kinase

Cellular signaling pathways are crucially regulated by phosphorylation. Kinases are cellular transmitters that accelerate the phosphorylation reaction by moving the γ-phosphate of an ATP molecule to Ser, Thr, or Tyr residues in the substrate. Kinases control transcription, metabolism, nervous system activity, immunological response, cell division, and migration. As a result, protein kinases must be strictly regulated due to their critical role in cellular activity [6- 8]. The human genome is made up of protein and lipid kinases. It is also known that it includes 518 protein kinases in total, 478 of which are typical and 40 of which are atypical. Typical kinases are further divided into eight primary categories counted on the similarity of their kinase domain sequences: tyrosine kinase (TK) has 90 members, tyrosine kinase-like kinase (TKL) has 43 members, serine/ threonine STE (STE7, STE11, and STE20-) related kinase has 47 members, casein kinase 1 (CK1) has 12 members, protein kinase A/G/C-related kinase (AGC) has 63 members, Ca^{2+}/calmodulin-dependent kinase (CAMK) has 74 members, CDK/MAPK/GSK/CDKlike- related (CMGC) has 61 members, and receptor guanylyl cyclase (RGC) has 5 members. Additionally, 40 atypical protein kinases have been reported, such as pyruvate dehydrogenase kinases, bromodomain kinases, B cell receptors (BCRs), and PI3 kinase-related kinases [6].

2.3.1.1 General Structure of the Kinase Domain

Generally, almost all the protein kinases have an identical fold. Kinase structures have a bilobal design for the catalytic domain, with an N-terminal lobe composed of β-strands and one α-helix (referred to as C-helix), and a C-lobe composed primarily of α-helices (Figure 2.2.). The catalytic center and ATP-binding pocket that it conserved throughout the progression are sited in a cleft that is formed by these two lobes and linked by a flexible hinge region. The flexible activation (A)-loop, is usually 20 to 30 amino acids long and distinguished by a conserved Asp-Phe-Gly (DFG) motif at its beginning, which makes up the C-terminal domain. Also, the A-loop can exhibit significant alterations in conformation, affecting the catalytic activity and access to the substrate-binding pocket. The conformational change is frequently followed by a specific orientation of the DFG motif's sidechains, which leads to the binding of several inhibitor classes. In the catalytically active "DFG-in" state, the transfer of ATP phosphate groups is controlled by the DFG aspartate and the catalytic loop while two Mg^{2+} ions are

positioned by them (Figure 2.3.). Type I inhibitors are compounds that typically bind to the ATP-binding pocket when the DFG motif is in its active conformation. Moreover, in the inactive "DFG-out" conformation, the Asp and Phe side chains of the DFG motif are reversed compared to the DFG-in state, causing the Asp to point far from the binding site. This change inhibits Mg^{2+}coordination and, as a result, catalytic activity. Additionally, the DFG-out conformation makes a hydrophobic pocket at the ATP binding site that can be targeted by type II inhibitors. In the inactive (DFG-out) state, the position of the C-helix, which has a conserved Glu residue and forms a significant salt bridge with Lys of the N-lobe β3-strand in the active state, is often shifted outward. That is also considered another significant structural feature affecting the catalytical activity [7].

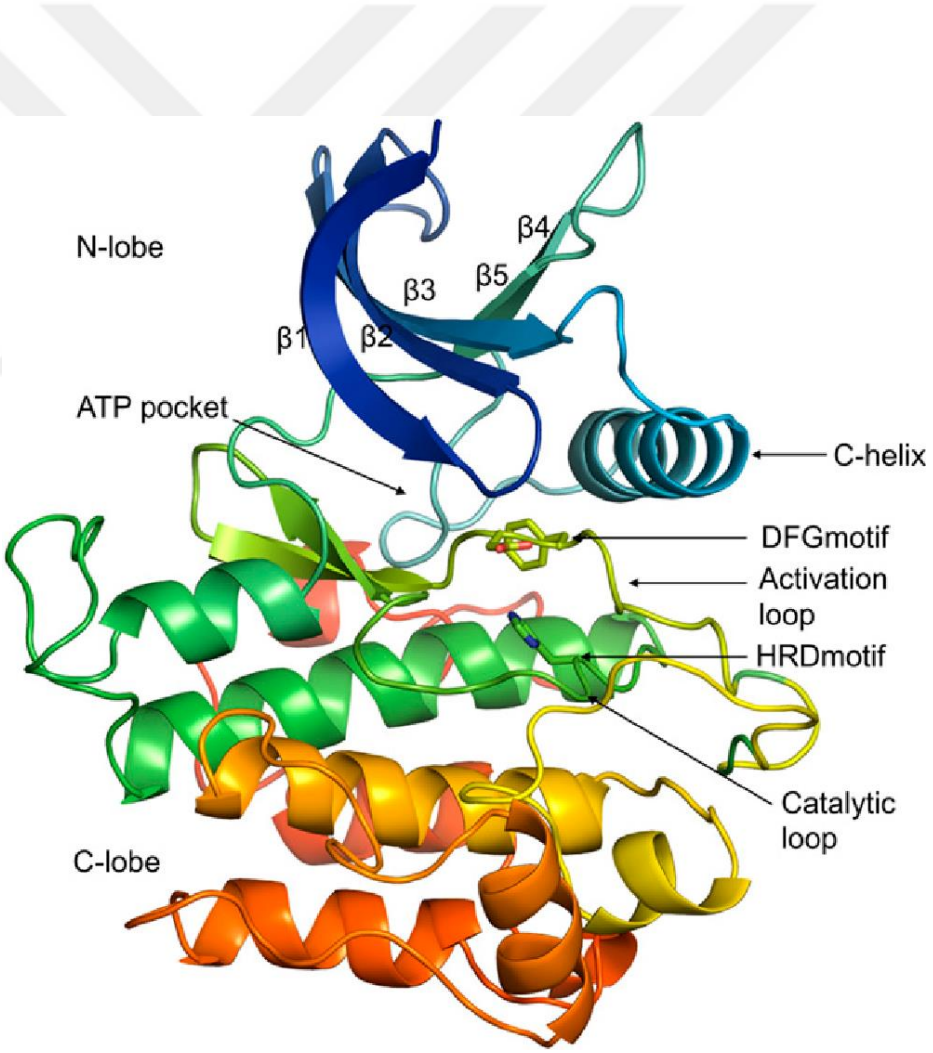

Figure 2.2. Structure of a typical protein kinase domain displaying ATP binding site and conserved elements around it (INSR kinase, PDB ID code 1GAG) [6].

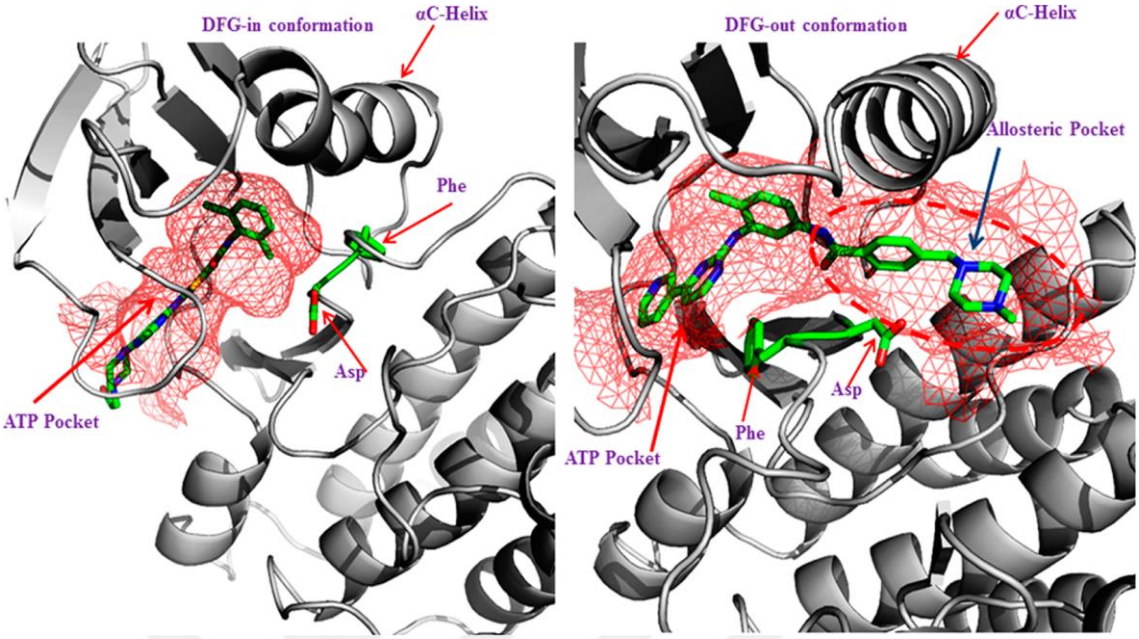

Figure 2.3. Left photo shows a DFG-in conformation of ABL kinase bound to dasatinib, with the Asp pointing in to the ATP binding site, and the right photo shows a DFG-out conformation of the ABL kinase domain bound to imatinib, with the Phe pointing into the ATP binding pocket [27].

2.3.2 Definition and Classifications

The dysregulation and mutations of protein kinase have been linked with a diversity of human diseases such as cancer, diabetes, autoimmune, cardiovascular, inflammatory, and neurological disorders. As a result, over the past 20 years, protein kinases have become one of the principal therapeutic targets. In 2001, the FDA authorized imatinib as the main small molecule targeted protein kinase inhibitor as a therapy for chronic myelogenous leukemia (CML) [9]. There are now 27 orally efficient direct protein kinase inhibitors that focus on a small number of enzymes on the FDA-approved medication list. Moreover, these drugs are generally used to treat malignancies with only two exceptions ruxolitinib and tofacitinib which are applied for myelofibrosis and rheumatoid arthritis treatment, respectively. The majority of protein kinase antagonists that are approved interact with the ATP-binding pocket and are steady-state competitive enzyme inhibitors with ATP [9].

The protein kinase inhibitors listed below can be defined into Types I to VI [9].

1. **Type I inhibitors** bind to the ATP-binding site in the active conformation of TKs in a competitive manner. In this type of inhibitor, the DFG motif is arranged so that the aspartate residue points toward the kinase catalytic site.
2. **Type II inhibitors** bind to kinases in their inactive configuration, typically at the ATP-binding site. In type II inhibitors, the DFG motif extends outward and away from the ATP-binding site. Many type II inhibitors can interact with the regions next to the ATP-binding site that would not be accessible due to the DFG motif's outward rotation.
3. **Type III and IV inhibitors** do not engage in any interaction with the ATP-binding pocket. However, they are exclusively bound to the allosteric pockets that are located next to the ATP-binding site.
4. **Type V inhibitors** are bivalent compounds that occupy two regions of the protein kinase domain.
5. **Type VI inhibitors are** small molecules that interact with the target enzymes by forming covalent bonds.

2.3.3 Kinases Under Study

There is a multiplicity of protein kinases. However, in this study, the effect of the choosing molecules on BRAF, ERK1, JAK1/2, and P38γ were investigated and how they interact with both active and inactive conformation of these proteins. The RAF kinase is a member of kinases that are considered as a major component of the highly conserved mitogen-activated protein kinase (MAPK) signaling pathway (RAS-RAF-MEK-ERK). It transmits signals from the extracellular environment to the nucleus *via* receptor tyrosine kinases (RTKs) to encourage the expression of genes essential for cell survival and proliferation. CRAF (RAF-1 or c-RAF-1), BRAF, and ARAF are the three isoforms of the RAF kinases, which were first discovered as cellular homologs of v-raf oncogenes acquired by retroviruses. BRAF is one of the RAF isoforms, which differs dramatically from CRAF and ARAF because its activation requires fewer regulatory processes. Additionally, BRAF has been demonstrated to be the main MEK1/2 activator and to have a substantially higher level of activity baseline in comparison with the other RAF isoforms. The observation that BRAF mutations are present in a wide range of malignancies like melanomas, thyroid cancers, ovarian cancers, colorectal cancers, and other cancer types, emphasizes the significance of BRAF as the primary RAF effector of the MAPK signaling pathway. BRAF is mutated in as much as 7% of human malignancies, according to an elaborate mapping of cancer genome alteration. BRAF represents one of the most significant oncogenes, mainly in human melanoma, and the most prevalent mutation is V600E-BRAF, which constantly activates downstream MAPK signaling. Overall, the BRAF kinase makes a promising target for designing anticancer drugs [28, 29].

Extracellular-regulated kinases (ERK1/2) are also one of the MAPK signaling pathways. ERKs are strictly regulated, with absolute activation occurring after dual phosphorylation by MKK1/2 and deactivation occurring after dephosphorylation by MAP kinase phosphatases (including MKP3/DUSP6) [30]. The ERK enzyme has two isoforms in mammals, ERK-1 and ERK-2, which share several biological activities but not all of them. These two isoforms share > 80% of their sequence and both contain conserved ATP binding sites. They are also had equal catalytic activity *in vitro* and are simultaneously activated in cellular systems, demonstrating their functional redundancy. However, ERK-1 and ERK-2 compete negatively for MEK, reducing its signaling. It is currently unknown whether the substrates for these two isoforms differ. Additionally, It was discovered that

the ERK pathway is essential for a diversity of biological functions, including cell proliferation, differentiation, migration, and survival. The prognosis of many human malignancies, including lung, kidney, ovarian, colon, and pancreatic tumors, is correlated with the aberration of the extracellular regulated kinase (ERK) pathway. As a result, this pathway is regarded as a crucial therapeutic target for cancer treatment [31].

The human p38 mitogen-activated protein kinase (MAPK) family contains four isoforms including, p38α, p38β, p38γ, and p38δ. p38α and p38β are expressed broadly, while p38γ and p38δ are expressed only in distinct tissue types. These identical isoforms are activated by the MAPK vis dual phosphorylation of tyrosine (Tyr) and threonine (Thr) residues in a common Thr-X-Tyr motif mediated. In addition, the p38 MAPK family is split into two subgroups according to substrate selectivity, cellular expression patterns, and sequence similarity. P38α and β represent one subgroup with a 75% sequence identical, whereas p38γ and δ represent the second subgroup with a roughly 70% sequence identity [32, 33]. The versatile kinase p38 interacts with numerous substrates to regulate multiple cellular processes, like cell proliferation, differentiation, stress response, apoptosis, inflammation, cell growth, and cell migration and survival [34]. Moreover, it has a direct role in the formation of pro-inflammatory cytokines like tumor necrosis factor α and interleukin 1β. It has been suggested that these cytokines are overproduced in several disorders with an inflammatory component. The specific function of the inflammatory response controlled by p38 MAPK is to promote tumor development. Notably, the expression of p38γ, which is ordinarily undetectable in normal T cells, is elevated in cutaneous T-cell lymphoma (CTCL), offering p38γ as a possible therapeutic target for CTCL treatment. Also, It is demonstrated that the expression of p38γ promotes the growth of various malignancies, including colon, prostate, esophageal, breast, and liver cancers [32, 33].

Nonreceptor tyrosine kinases known as Janus kinases (JAKs) are divided into four groups JAK1, JAK2, JAK3, and TYK2. These enzymes are a component of the JAK/STAT route, which is triggered by cytokines and promotes a series of signals for an organism's development or homeostasis. The JAK kinases serve as a link between cytokine signals and the phosphorylated transcriptional factor STAT. The majority of cell types include JAKs. JAK1 and JAK2 are elaborated in a number of actions, including hematopoiesis, growth, and neural development, whereas JAK3 and TYK2 mainly control immunological responses. Therefore, abnormal JAK/STAT signaling has the

potential to cause a variety of illnesses, including cancer, inflammation, and autoimmune conditions. JAK1 has been linked to various forms of acute leukemia or B-cell lymphoma depending on the mutant locations, whereas JAK2 mutations, like the V617F mutation in the kinase-like domain of JAK2, have been linked to thrombocytosis, myelofibrosis, leukemia, and lymphoma. Enhancing the JAK3 signaling has also been linked to T-cell acute lymphocytic leukemia. Moreover, the JAK/STAT3 pathway is activated by inflammatory cytokines present in the tumor microenvironment, which also perform critical part in most solid tumors. The proliferation, survival, angiogenesis, tumor metabolism, and inhibition of antitumor immunity of cancer cells are all promoted when the JAK/STAT3 signaling is excessed. Accordingly, there has been a focus on finding efficient JAK inhibitors [35, 36].

2.4 Drug Design

2.4.1 Drug Discovery and Development

The development of new drugs needs many efforts like high costs and long development cycles. Also, the rate of its success is low. This field faces multiple challenges while simultaneously, new opportunities are appearing. Generally, the traditional drug discovery process includes several stages (Figure 2.4.). It begins with the determination of targets or molecular pathways that are probably associated with the disease under investigation and looking for hit compounds that modify the potential target(s) and pathway(s). Then, variable features of the initial hit compounds must be modified (for example, their affinity, solubility, and toxicity at the required dose, typically conducted during the so-called hit to lead stage and beyond) until clinical candidates are identified. To detect and improve these early-stage chemicals, many experimental techniques are needed (screening, biophysical methods, biochemistry, medicinal chemistry). The early discovery and preclinical research, without mentioning the clinical phases, take a long time and are costly [10].

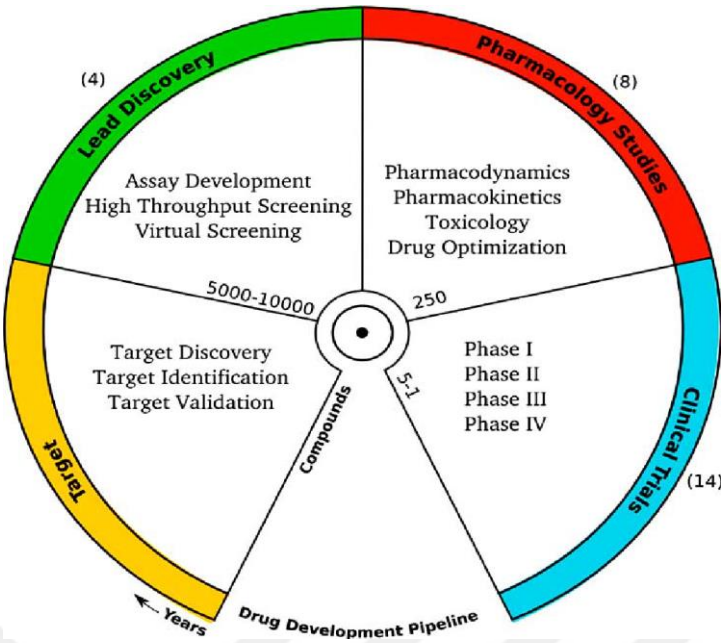

Figure 2.4. Overview of the drug development process [12]

To assist the numerous challenges that the traditional drug discovery process face, various computer-aided drug design techniques are used [11]. The non-specific and rational drug design methodology are considered the two most effective and potent approaches in drug discovery and development [12]. (Figure 2.5.). The non-specific drug design that includes high-throughput screening (HTS) and combinatorial chemistry methods are specified by many drawbacks like high cost and time consumption. Also, there is no assurance that new hit-molecules or lead compounds against a particular target will be discovered or identified at the end of the procedure. However, these days virtual screening is considered as the most convenient tool in drug discovery and development [11, 12].

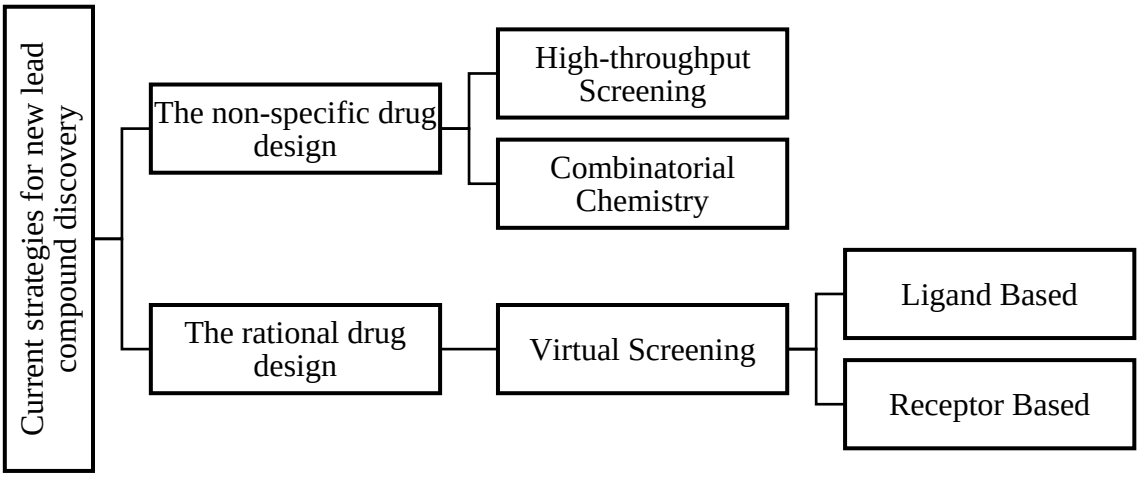

Figure 2.5. Present strategies to develop new lead compounds reproduced from Virtual Screening in Drug Design and Development [12]

2.4.2 Virtual Screening

Virtual screening (VS) is a computational method for selecting chemicals from a huge library that bind to a particular target, typically an enzyme or receptor. Nowadays, it is one of the most effective tools. It helps in determination the most advantageous bioactive ligands utilizing the information of the target or known active ligand. It is also known as an alternative to high-throughput screening because it is performed with low cost, and the highest ability to find the most appropriate novel hit through the filtration of large molecules found in libraries. To get satisfying results, the several stages that VS had, had to be considered while selecting. VS techniques can typically be separated into two more common VS types (Figure 2.5.): ligand-based virtual screening (LBVS) and receptor-based virtual screening (RBVS) [10, 12, 13]. The most popular ways for searching for molecules that are the most likely to interact with a particular target in the libraries of compounds are ligand-based and structure-based virtual screening (SBVS) approaches. Unless these methods might need to be modified to identify the query molecule's most likely targets. The essential goals for these methods include identifying a compound's bioactivity or mechanism of action, identifying drug polypharmacology, predicting probable side effects, assisting with the rational design of multitarget medications, or supporting efforts at drug repositioning [10].

2.4.2.1 Ligand-based Virtual Screening Method (LBVS)

In this method, 2D or 3D chemical structures or molecular descriptors of the known actives are used to identify other 'similar' compounds in a database using various forms of similarity measurements or by looking for a shared substructure or pharmacophore between the query molecule and the scanned libraries. The basic techniques utilized in ligand-based screening is the 2D molecular similarity method. This approach depends on finding compounds with identical fingerprints in the electronic libraries by comparing them to known ligands that bind to a target. A variety of similarity or distance measurements can be employed. The most used similarity index, for instance, is the Tanimoto coefficient, which ranges from 0 to 1. The closer the database's chemicals are to the input query, the higher the threshold. 3D pharmacophore modeling is another tool used in LBVS screening. Here, the prevalent and important structural characteristics of ligands, that bind to a target, are distinguised and used to construct a model. This model is then used to screen a library of compounds to find the one that meets the model's requirements.

Shape similarity is another 3D similarity method. Numerous techniques, such as electrostatic similarity or "force field" colored shape similarity, have been evolved to describe molecule shape and estimate shape similarity. This method can be applied to molecular target prediction, drug repositioning, and scaffold hopping in addition to virtual screening. In addition, quantitative structure–activity relationship (QSAR) modeling is a computational technique that represent the correlation among a set of chosen features (such as molecular descriptors like fingerprints or different physicochemical properties) of the ligands that bind to the target, and the associated biological activity effect. The popular approaches in QSAR modelind are linear regression and machine learning. The basic drawback of the LBSV techniques is that it tends to favor hits that have characteristics similar to those of known ligands due to their underlying guiding principles. Additionally, the concept of biological similarity between two pairs of molecules can be problematic because when bound to the receptor, substances that are structurally extremely different can also behave similarly [10, 12].

2.4.2.2 Structure-based Virtual Screening (SBVS)

They focus on the interaction between the ligand and the receptor, instead of concentrating just on the ligand, by docking molecules from a database into a binding site. The results are then evaluated generally using one of the scoring techniques like consensus scoring or consensus docking and scoring, rescoring with more rigorous binding free energy calculations or with machine learning scoring functions. Proteins in general are the targets, but other macromolecules, such as nucleic acids, can also be studied. Also, in SBVS, there is no prior information about the ligand that will be studied with a known target. However, there will be knowledge about what kind of binding the studied target requires through structures that have cocrystallized or known ligands. SBVS methods are more applied when the protein target is in its 3D structure. The target's 3D structure is determined by using one of the following methods: X-ray, cryo-electron microscopy, nuclear magnetic resonance (NMR), and homology models. Active-site derived pharmacophore approaches and protein-ligand docking are the two main categories of receptor-based techniques [10, 12].

2.4.2.2.1 Active-site derived Pharmacophore Methods

It depends on the 3D structure of the receptor that contains all the essential structural features specifically on the potential points which are related to ligand-receptor interaction to form the pharmacophore model. Also, it focuses on the fundamental ligand-receptor interaction pattern and the overall topology of the active site [10, 12].

2.4.2.2.2 Protein-ligand Docking Methods

This method is used to accurately place small molecule structures from an existing compound database into the target protein's active site. The lead compound resulting from this method relies on the quality of the docked models and on the protocol of docking more than on a subjective view that the ligand is supposed to have like in ligand-based techniques. In addition, it represents a promising approach for finding structurally novel ligands [10, 12].

2.4.3 Molecular Docking

Molecular docking is *an in silico* technique that estimates where small molecules or ligands will be located within the active site of a target protein (receptor). It is primarily utilized to accurately estimate the most desirable binding modes and bio-affinities of ligands with their receptors, and it is currently widely employed in virtual screening for the optimization of lead compounds (Figure 2.6.). Prediction of binding position, bio affinity, and virtual screening are the three main objectives of the molecular docking process. The search algorithm and scoring functions are considered as fundamental tools in the molecular docking method for producing and evaluating ligand conformations. Compared to traditional high throughput screening, it provides compounds with high hit rates through scanning massive libraries of compounds *in silico*. It also decreases the chance of failures in the final phase [13].

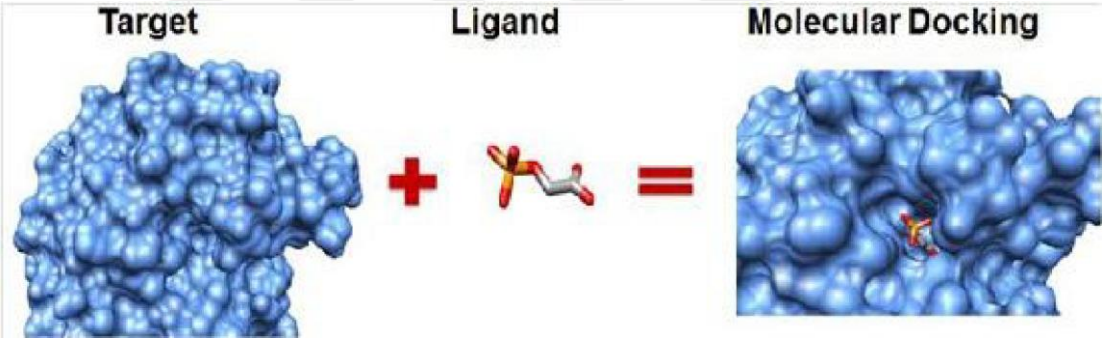

Figure 2.6. Docking process [11]

3. MATERIALS AND METHODS

3.1 Compounds Under Study

The study will focus on 6-gingerol (1-[4'-hydroxy-3'-methoxyphenyl]-5-hydroxy-3-decanone) as an active anti-tumor compound and will look for compounds that have a similar chemical structure to the 6-gingerol. Accordingly, structurally similar compounds to 6-gingerol with a proper cut-off value will be considered. Tanimoto score calculations for similarity search will be employed using PubChem fingerprints in ChemMine Tools [37].

3.2 *In Silico* Target Fishing

The biological activities of 6-gingerol and its similar compounds will be predicted via PASSOnline, Swiss Target Prediction, Mol Tar Pred, and SEA web servers [38- 41]. These servers provide a list of putative biological targets for the molecules depending on their fingerprint similarity to known bioactive compounds. The possible biological targets of the compounds will be selected related to the anti-cancer activity. PASSonline is a freely accessible web resource that is used for predicting the probable biological activity of organic compounds depending on their structural formula. It offers estimations with a mean accuracy of 95% for approximately 4000 different types of biological activity. The prediction of action of the compound depends on structure-activity relationship analysis of the training set containing more than 300000 compounds [38]. The PASS user receives output data in the form of a list of anticipated activity kinds along with an estimated probability in terms of probable activity (Pa) and probable inactivity (Pi). Pa and Pi have values ranging from 0 to 1. Only activities with Pa>Pi were considered possible for a particular compound. If Pa is greater than 0.7, there is a good probability that the compound may exhibit novel pharmacological activity, and it may also resemble an existing drug structurally. If 0.5<Pa <0.7, The probability of experimental pharmacological action is less. If the value of Pa is less than 0.5, there is a low chance to find the activity of the structure experimentally and may prove a parent compound for a new chemical group for examining the biological activity [38].

The second server used is a web tool, Swiss Target Prediction, that has been serving since 2014. It looks to determine the most likely protein targets for any bioactive small molecules depending on ligand-based target prediction. The predictions are performed by investigating the 2D and 3D similarity of input query to compounds with known *in vitro* activity data in the ChEMBL Library (ChEMBL23 in the version used).

The 2D measure uses the Tanimoto index between path-based binary fingerprints (FP2), while the 3D measure is based on a Manhattan distance similarity quantity between Electroshape 5D (ES5D). The thresholds are 0.65 for Tanimoto in dex on FP2 (2D) and 0.85 for the Manhattan-based similarity on ES5D (3D). The outcomes of the server include a list of the top 100 potential protein targets, as well as the similar known actives per target found for the query compound [39].

The third method used in this screening is the Mol Tar Pred web server. It is freely available (http://moltarpred.marseille.inserm.fr) and used for predicting protein targets utilizing ChEMBL22 data. When a query is submitted, the server determines the Tanimoto similarity between the query molecule's Morgan fingerprint and each of the 607,659 ChEMBL compounds that will be tested. The predicted targets are regained from the top 10 most similar molecules to the query. Additionally, the estimated target is more likely to be the target of the query molecule with a higher confidence score. To claim that a drug candidate is among the 607,659 ChEMBL and has single-protein targets annotated with activity equal to or lower than 10 micromolar, the confidence score must be valued between 7.8 and 9. However, when the query involves more than one protein target with an activity lower than 7.8 micromolar. Here, further prospective validation of these targets is required [40].

The Similarity Ensemble Approach (SEA) server is the fourth tool used for selecting the putative biological target for the query. It is a 2D ligand-based similarity ensemble approach, that predicts the biological targets of a compound based on its likeness to ligands found in a reference database, such as ChEMBL. The input ligand is compared to all ligands of all target sets by using the Tanimoto similarity of the ECFP4 fingerprints. The Tanimoto similarities are summed up, and z-scores are calculated for each ligand. This tool has been successfully applied in new target identification for old drugs, and natural products. Moreover, it predicts the side effects and the potential anatomical therapeutic indications (ATCs) of approved drugs [41- 43]. Here, in this work, the query (6-gingerol) and its similar molecules were screened with these *in silico* approaches. The respective SMILES were added as the query input. A list of predicted targets was downloaded and further analyzed manually.

3.3 Molecular Docking

Each compound will be washed and prepared according to the physiological pH. The compounds will be subjected to conformational search in Molecular Operating Environment (MOE) software using the Stochastic Conformational Search module. The global minimum energy of each molecule will be minimized with the MMFF94x force field. All proteins will be downloaded from Protein Data Bank [44]. Unnecessary chains, ions, water molecules and solvents will be deleted. Hydrogen atoms and partial charges will be added to protein. Missing loops and side chains will be fixed. Each conformation of compounds will be docked into the structures with MOE using London dG rescoring and triangle matcher placement settings [45].

3.4 The Pharmacokinetic Properties and Drug-likeness

Drug-likeness (such as Lipinski's rule of five) also absorption, distribution, metabolism, and excretion (ADME) properties will be calculated *in silico* for 6-gingerol and similar molecules. The web server SwissADME will be used to evaluate these properties [46]. The excretion properties of the compounds will be predicted by using open web servers pkCSM [47]. The user-friendly web interface allows input structures in SMILES format and after submission, the results are given in an output table. Drug-likeness is considered an essential concept that gives a useful outline in screening drugs (candidates) at an early stage of the drug discovery to become an oral drug concerning bioavailability. Lipinski's Rule of Five (Ro5) is one of the most frequent rules used to evaluate the drug-likeness properties of the molecules. It refers that if the molecule violates more than two of the following criteria: The molecular weight (MW) <500, number of hydrogen bond donors (HBD) <5 (counting the sum of all NH and OH groups), partition coefficient octanol/water Log P <5, number of hydrogen bond acceptors (HBAs) <10 (counting all N and O atoms), the molecule will exhibit poor absorption or permeation [46, 48, 49]. Also, there are two other descriptors identified by Veber *et al.* [50]: Number of Rotatable bonds (NRB) <10 and Polar surface area (PSA) <140 $Å^2$. Blood Brain Barrier (BBB) will also be determined as one of the distribution parameters to screen the ability of the studied compounds to cross the BBB [46].

Additionally, Cytochrome P450 (CYP450) plays a vital role in drug elimination through metabolic biotransformation because it is the main liver protein system. Only 17 CYP families were identified in humans, even though only (CYP1, CYP2, CYP3, and CYP4, respectively) are involved in the drug metabolism. However, These five major

isoforms of CYP (1A2, 2C9, 2C19, 2D6, and 3A4, respectively) are responsible for the biotransformation of more than 90% of the drugs. The inhibition of these isoenzymes considers one of the essential causes of a toxic or unwanted adverse effect related to drug-drug interaction. Scientists defined a variety of inhibitors of the CYE where some of these inhibitors affect different CYP isoforms, while others exhibit as a specific inhibitor for isoenzymes. According to that, there is a great need to predict the properties of the studied compounds which molecule will cause significant drug interactions through inhibition of CYPs, and determine which isoforms are affected [46]. Drug clearance was measured by the proportionality constant (CLtot) and expressed as a log(mL/min/kg). It is related to bioavailability and is important for determining dosing rates to achieve steady-state concentrations. The Organic Cation Transporter 2 (OCT2) was also determined to reveal if the compounds are substrates for it or not. It plays an essential role in drug clearance and endogenous substance clearance by using the pkCSM server [47].

3.5 Toxicity Potential Evaluation

Toxicity prediction is one of the most essential criteria during the drug development process because many medicines that reach the clinical trial stage fail to reach the market due to ineffectiveness or unfavorable side effects. Various computational approaches are utilized to identify the potential cytotoxicity and adverse effect of chemical structures on both normal cells and tumor cells, as well as organs in general. It also assists in determining the structure that may boost efficacy and therapeutic success. There is also quantitative structure-activity relationship (QSAR) models that supply such a computational method for the *in silico* prediction of chemical toxicity. These models use robust machine learning algorithms to develop a relationship between chemical structure and the predicted endpoint (toxicity). Then, the accurate and precisely validated- QSAR models are utilized to produce *in silico* predictions of the endpoint of interest [51]. As a result, the cytotoxicity of the drugs on tumor and non-tumor cells would be computationally screened using PASS CLC Pred, a free online server (http://www.way2drug.com/Cell-line/) [52]. The most frequent adverse consequences of anti-cancer drugs are hepatotoxicity and cardiotoxicity. Hepatotoxicity and hERG I- II inhibitory activities of the compounds will be predicted by using pkCSM which is available on (http://structure. bioc.cam.ac.uk/pkcsm) [47]. The hepatotoxicity will also be predicted via the ProTox-II program [53]. The studied compounds will also be evaluated for mutagenicity, carcinogenicity, cytotoxicity, and immunotoxicity. Also, its impacts on stress response pathways, particularly mitochondrial membrane potential

(MMP) and phosphoprotein tumor suppressor (p53) will be predicted via ProTox-II program [53]. The SMILES structure of the compounds will be input to predict their mentioned toxicity endpoints.

4. RESULTS AND DISCUSSION

4.1 Similarity Study

The similar chemical structures to query 6-Gingerol were determined by using the Chemmine server. The cut-off value of similarity is set at 0.80. The search resulted in 49 compounds including 6-gingerol (Table 4.1.). All these similarties are natural source and have various biological activitie [54- 58]. Here, there is just an example about the activity of two of these compounds. Licochalcone B (Lico B) (N-G-38) is one of the selected molecules that has a similar structure to 6-gingerol. It is a new synthesis molecule and belongs to chalcon groups extracted from licoric root also called *Glycyrrhiza* root. Chalcon groups are precursors of flavonoids. *In vitro* and *in vivo* studies have been demonstrated the therapeutic effects of licochalcone B especially as anti-inflammatory, anticancer, antioxidant, and hepatoprotective. In accordance with an *in vitro* study that has been done in 2016, reports rfere that when Oral Squamous Cell Carcinoma (OSCC) cells are treated with licochalcone B, lico B has significantly inhibited cell proliferation depending on the duration and concentration manner. Lico B treatment resulted in the up-regulation of pro-apoptotic proteins like BCL-2-associated X protein and the down-regulation of anti-apoptotic proteins like BH3 domain-only death agonist protein, B-cell lymphoma-extra large, and promoted myeloid leukemia cell differentiation protein Mcl-1 (Bax). Through the release of cytochrome C and loss of mitochondrial membrane potential, lico B induces apoptosis. These investigations also provide evidence for the activation of many caspases and the cleavage of the PARP protein following Lico B therapy. As a result, Lico B recommends as a novel natural medication to treat human oral cancer by inducing apoptosis [59]. Pratensein (N-G-39) is also another selected molecule. It is a member of the flavonoid family that is found in many plants like *Trifolium pratense,* The anticancer activity of pratensein has been demonstrated lately, that has been done by studying the anticancer effect of pratensein on breast cancer cells. The result of the study reveals that pratensein can induce Caspase-3 and Bax and increase the expression level of P53. Also, it inhibits Bcl2 activation in a time-dependent manner [60].

Table 4.1. ID and structure information of 6-gingerol and structurally similar compounds

Compound code	Compound name	CAS no	Structure
N-G-1	6-Gingerol	23513-14-6	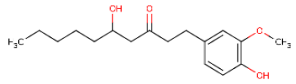
N-G-2	Ferulic acid	537-98-4	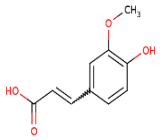
N-G-3	Eugenol	97-53-0	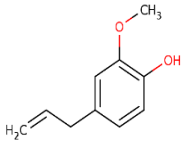
N-G-4	Vanillin	121-33-5	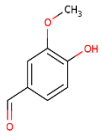
N-G-5	Curcumin	458-37-7	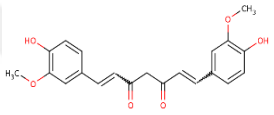
N-G-6	Methyl eugenol	93-15-2	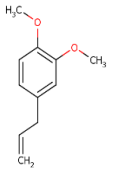
N-G-7	(E)Isoeugenol	97-54-1	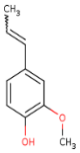
N-G-8	Ethyl vanillin	121-32-4	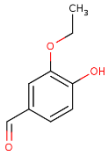
N-G-9	Vanillic acid	121-34-6	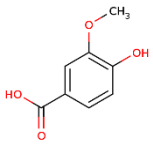

Compound code	Compound name	CAS no	Structure
N-G-10	Acetovanillone	498-02-2	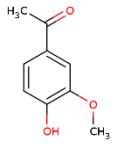
N-G-11	Dehydrozingerone	1080-12-2	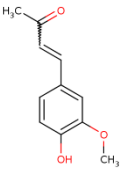
N-G-12	Calycosin	20575-57-9	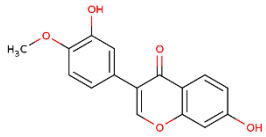
N-G-13	2-methoxy-4-propylphenol (Dihydroeugenol)	2785-87-7	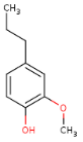
N-G-14	Vanillylmandelic acid	55-10-7	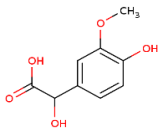
N-G-15	Shogaol	555-66-8	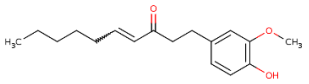
N-G-16	2-methoxyestrone	362-08-3	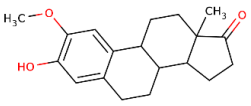
N-G-17	Matairesinol	580-72-3	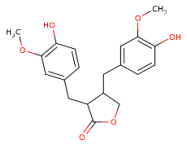
N-G-18	Vanillyl alcohol	498-00-0	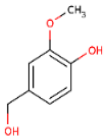
N-G-19	Zingerone	122-48-5	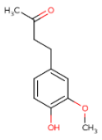

Compound code	Compound name	CAS no	Structure
N-G-20	Acetosyringone	2478-38-8	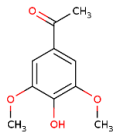
N-G-21	2-methoxy-4-methylphenol (Cresol)	93-51-6	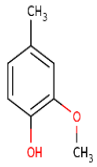
N-G-22	Homovanillic acid	306-08-1	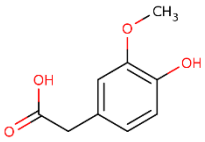
N-G-23	2-methoxy-4-vinylphenol	7786-61-0	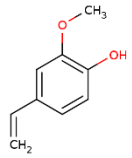
N-G-24	Demethoxycurcumin	22608-11-3	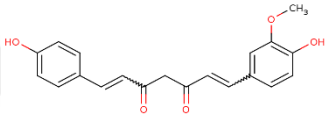
N-G-25	Coniferaldehyde	20649-42-7	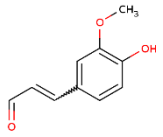
N-G-26	Coniferyl alcohol	32811-40-8	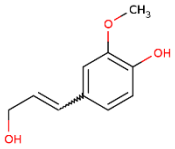
N-G-27	Terameprocol	24150-24-1	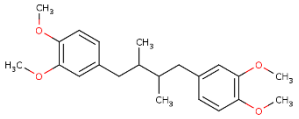
N-G-28	Dihydrocaffeic acid	1078-61-1	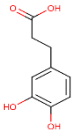
N-G-29	4-allyl-2,6-dimethoxyphenol ((Methoxyeugenol)	6627-88-9	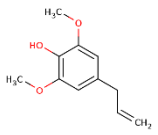

Compound code	Compound name	CAS no	Structure
N-G-30	Paradol	27113-22-0	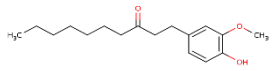
N-G-31	Secoisolariciresinol	29388-59-8	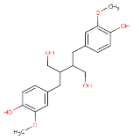
N-G-32	Arctigenin	7770-78-7	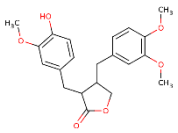
N-G-33	4-ethyl-2-methoxyphenol	2785-89-9	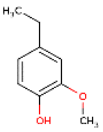
N-G-34	Methyl vanillate	3943-74-6	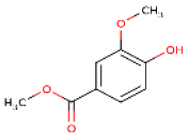
N-G-35	Ethyl vanillate	617-05-0	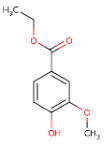
N-G-36	2-hydroxy-3-methoxybenzaldehyde	148-53-8	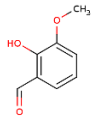
N-G-37	Vanitrope	63477-41-8	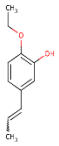
N-G-38	Licochalcone B	58749-23-8	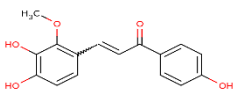
N-G-39	Pratensein	2284-31-3	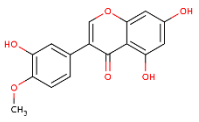

Compound code	Compound name	CAS no	Structure
N-G-40	Curcumin PE	NG	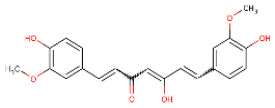
N-G-41	Tetrahydrocurcumin	36062-04-1	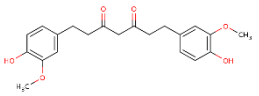
N-G-42	Vanylglycol	534-82-7	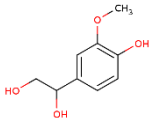
N-G-43	3-(4-Hydroxy-3-methoxyphenyl) propanal [dihydroconiferyl aldehyde]	80638-48-8	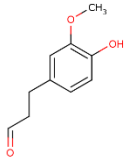
N-G-44	L- (+)-vanilmandelic acid	13244-77-4	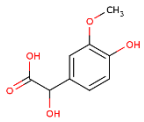
N-G-45	Piperonyl acetone	55418-52-5	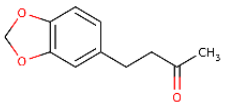
N-G-46	3-hydroxy-4-methoxybenzoıc acıd (Isovanillic acid)	645-08-9	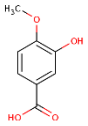
N-G-47	Isoferulic acid	25522-33-2	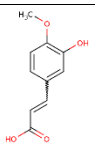
N-G-48	Homoveratric acid	93-40-3	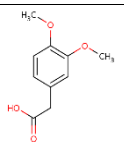
N-G-49	(3-hydroxy-4 methoxybenzaaldehyde) Isovanilline	621-59-0	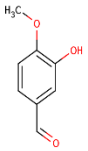

4.2 The Putative Anti-cancer Target of the Molecules

The 6-gingerol and its related compounds were used to determine the most promising target. All the anti-cancer activities of 6-gingerol were screened via using four different web servers. Then, the potential targets for small molecules (similar structures) with a 6-gingerol scaffold were screened in order to identify the most common target among them. The potential targets of the investigated molecules were predicted by PASS Online, Swiss Target Prediction, Mol Tar Pred, and SEA web servers which are depending on separate algorithms. The results from each server are represented in the appendixes (A, B, C, and D). After that, the most notable anti-cancer activities had been noticed based on the methodologies that were utilized and the results represented in the following (Table 4.2.). According to the data collection, Tyrosine Kinase [B-RAF, JAK1/2, ERK1(MAPK3), and p38γ] were mainly focused on for docking studies.

Table 4.2. Common anti-cancer targets for 6-gingerol and similar compounds via four different web servers

PASSonline	**SwissTargetPrediction**	**MolTarPred**	**SEA**
MAP Kinase Stimulant	MAP Kinase ERK1		
Apoptosis Agonist	MAP2K1		
Caspase3 Stimulant	mTOR		
Caspase8 Stimulant	STAT3		
	SYK		
JAK2 expression Inhibitor	JAK2		
	(PIK3CB) \ (PIK3CA)		
BRAF expression Inhibitor	BRAF		
AR expression Inhibitor	Androgen Receptor (AR)		
TP53 expression enhancer	p53-binding protein Mdm-2 (MDM2)		
Transcription Factor NFκB Inhibitor			NF-kappa B essential modulator
			Nuclear factor NF-kappa B p105 subunit (NF-κB1)
Beta Tubulin Antagonist	Tubulin beta-1 chain (TUBB1)		Beta-tubulin

PASSonline	SwissTargetPrediction	MolTarPred	SEA
Histone acetyltransferase Inhibitor			Histone acetyltransferase p300 (EP300)
Toll-like receptor Antagonist			Toll-like receptor 1
Beta-adrenergic receptor kinase Inhibitor			Beta-1 adrenergic receptor (ADRB1)
5-lipoxygenase Inhibitor	Arachidonate 5-lipoxygenase (ALOX5)	Arachidonate 5-lipoxygenase	Arachidonate 5-lipoxygenase (ALOX5)
	Arachidonate 15-lipoxygenase (ALOX15)		Arachidonate 15-lipoxygenase (ALOX15)

4.3 Evaluation of the Docking of the Selective Target with the Studied Molecules

6-Gingerol and its similar structures were docked into BRAF active (PDB ID: 3OG7), BRAF inactive (PBD ID: 6N0Q), JAK1 active (PDB ID: 3EYG), JAK2 active (PDB ID: 2B7A), JAK2 inactive (PDB ID: 3UGC), ERK1 (PBD ID: 2ZOQ), p38γ active (PDB ID:1CM8), and p38γ inactive (PDB ID:6UNA) proteins to reveal the potential interactions. Table 4.3. shows the docking scores for chosen compounds in the data set and their expected interactions.

Most protein kinase inhibitors that have been given approval interact with the ATP-binding pocket and are steady-state competitive enzyme antagonists with ATP. The hinge segment, which connects the amino- and carboxy-terminal kinases of the catalytic domain, interacts with the adenine ring of ATP by forming a hydrogen bond, as described previously, in all protein kinases. This interaction is essential for ATP binding and substrate phosphorylation. Hence, preventing ATP from being linked to the hinge region may be an effective method for inhibiting kinases' activity. This approach has proven its validity via determining many effective kinase inhibitors. Most BRAF inhibitors interact with the ATP-binding region and the hinge region of kinase catalytic domains (this type of inhibition mode is called type I inhibitor). Among the hinge region of B-RAF and the inhibitors, there are one or more crucial hydrogen bonds that significantly increase the binding affinity [9, 28, 61]. In general binding to BRAF in its active state (DFG-in) occurs by interaction with CYS 532 and GLN 530 of the hinge region residues. Docking studies on BRAF protein performed by using the X-ray data of 3OG7 showed that the co-crystallized ligand (PLX4032) formed two hydrogen bonds with amine backbone of CYS 532 and carbonyl backbone of GLN 530 from the azoindol ring [28, 61]. In compliance with this, 6-gingerol and its similar molecules were docked in the ATP active conformation of the V600E-BRAF kinase (PDB ID: 3O7G) to reveal which compounds will have a good inhibit effect on the protein. The results revealed that N-G-12 formed a hydrogen bond with the carbonyl backbone of CYS532, N-G-38 formed a hydrogen bond with the nitrogen backbone of CYS532, the N-G-47 forms a hydrogen bond with the carbonyl backbone of the GLN 530, and N-G-42 formed a hydrogen bonds the carbonyl backbone of the GLN 530 and a hydrogen bonds with sidechain (SH) of CYS 532 with docking scores -6.7111, -6.7236, -5.2851, and -5.341 respectively (Figure 4.1. and 4.2.). These compounds are nominated to act as type I inhibitors towards BRAF kinase.

(a) (b)

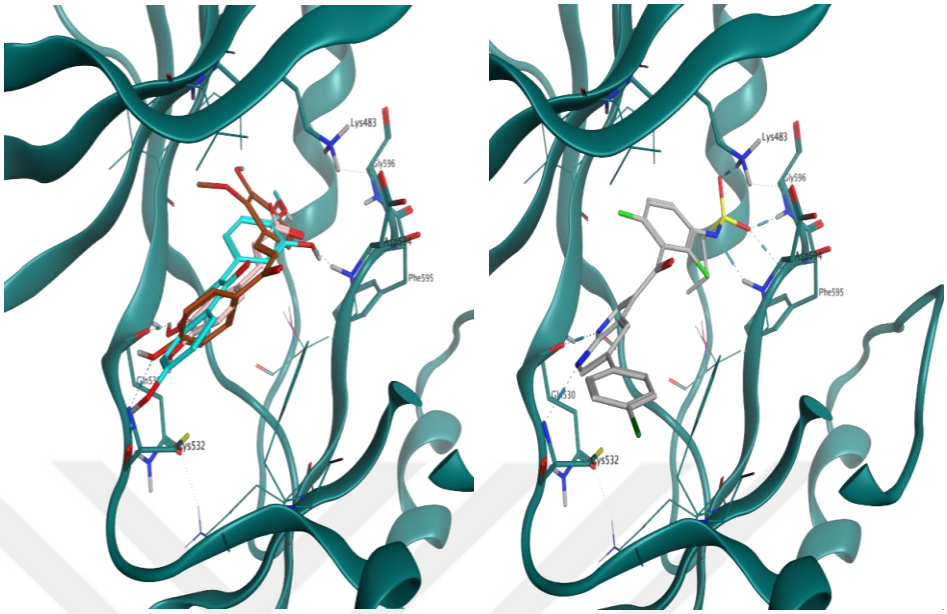

(c)

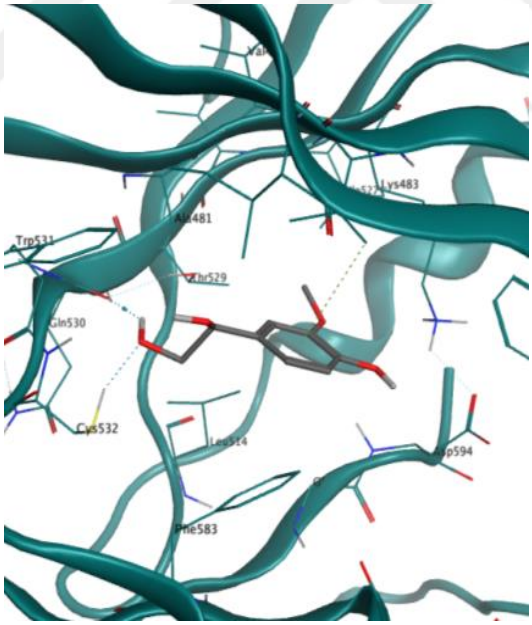

Figure 4.1. Structure of $BRAF^{V600E}$: PDB ID: 3OG7 complex with: (a) N-G-12 (cyan), N-G-38 (Brown), and N-G-47 (pink); (b) co-crystallized ligand PLX4032; (C) N-G-42 (gray).

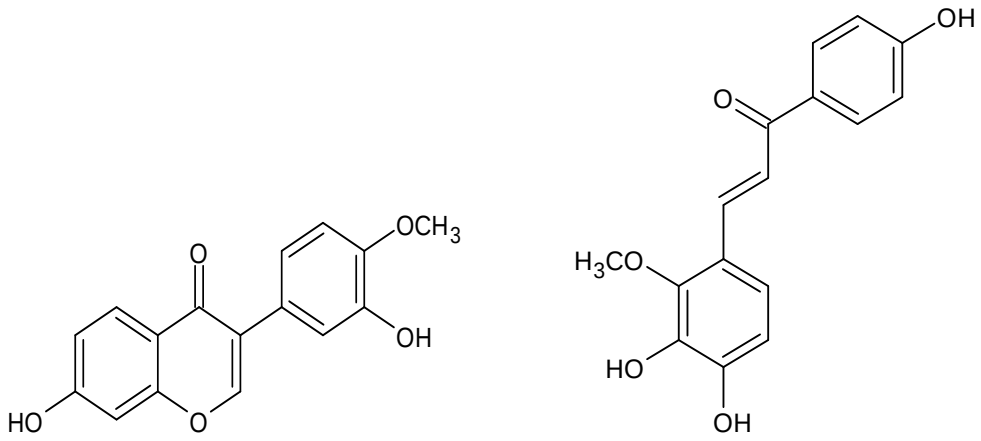

N-G-12 N-G-38

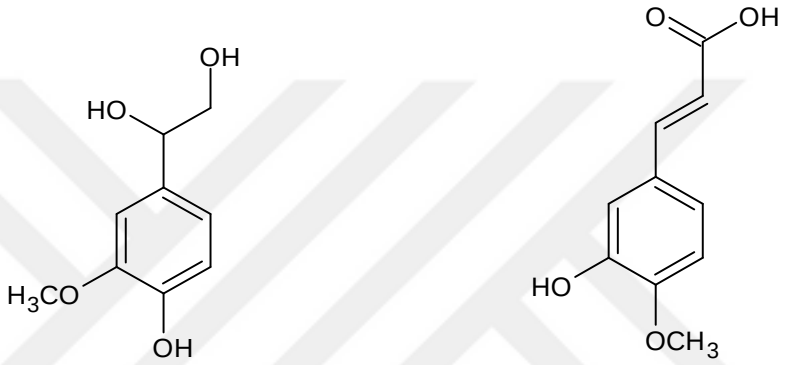

N-G-42 N-G-47

Figure 4.2. The structures of the selected compounds for the active conformer of BRAF.

Researchers always strive for obtaining highly selective BRAF inhibitors that can effectively inhibit the RAF-MEK-ERK pathway in RAS/RAF mutant tumor cells without triggering paradoxical activation. According to a structure-based approach, they observed that interacting with the DFG loop increases the potency of the inhibitor (this type of inhibition mode is called type II) [62]. The docking study that performed on 6N0Q showed that the conformer of cocrystallized ligand [N-(4-methyl-3-(1-methyl-2-oxo-2,3-dihydro-1H-benzo[d]imidazol-5-yl)phenyl)-3-(trifluoromethyl)benzamide] made H-bonds with a carbonyl backbone of Phe595, amino backbone of Asp594, and with the carboxylate group of the sidechains of αC-Glu501 [62]. In compliance with this, 6-gingerol and its similar molecules were docked into the ATP binding site of the BRAF kinase inactive form (PDB ID:6N0Q) to reveal which compounds will have a good effect on this protein. The results revealed that N-G-18 formed a hydrogen bond with the carboxylate group of the side chain of the αC-Glu 501, N-G-38 formed a hydrogen bond

with the carbonyl backbone of Cys532 and a hydrogen bond with the carboxylate group of the side chain of the αC-Glu501, and the N-G-44 formed two hydrogen bonds with nitrogen backbone of the Asp594 and hydrogen bond with the carboxylate group of the side chain of the αC-Glu501 with docking scores -5.4173, -6.71434, and -5.5003 respectively (Figure 4.3. and 4.4.). According to this result, the N-G-38 and N-G-44 may be a good selective inhibitor type II to BRAF because these molecules formed a good interaction with the inactive conformation of the protein

(a) (b)

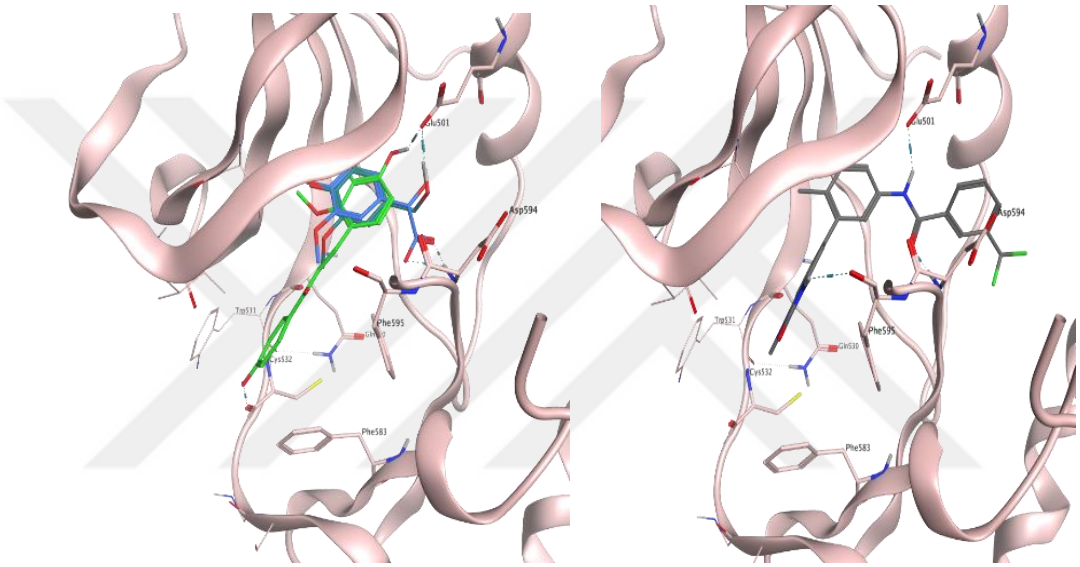

Figure 4.3. Structure of BRAF: PDB ID: 6N0Q complex with: (a) N-G-18 (green), N-G-38 (light-green), and N-G-44 (blue); (b) co-crystalized ligand [N-(4-methyl-3-(1-methyl-2-oxo-2,3-dihydro-1H-benzo[d]imidazol-5-yl)phenyl)-3-(trifluoromethyl)benzamide].

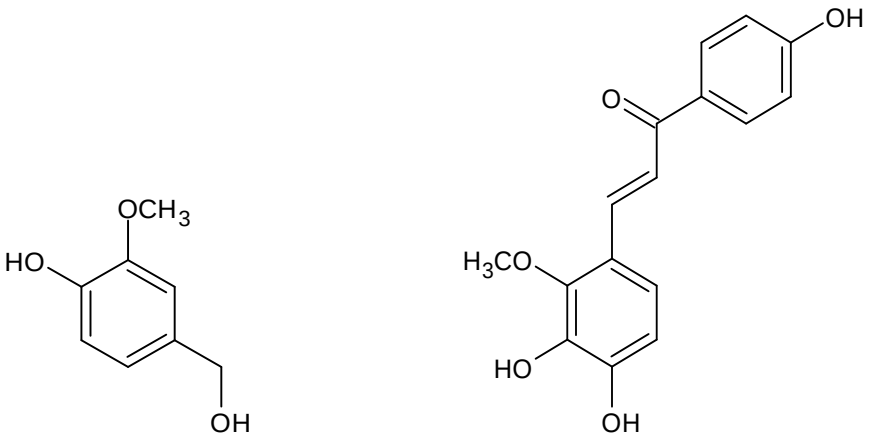

N-G-18 N-G-38

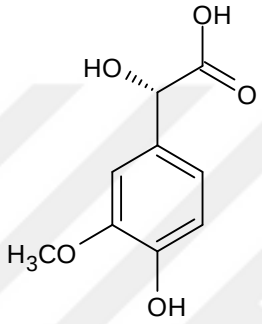

N-G-44

Figure 4.4. The structures of the selected compounds for the in active conformer of BRAF.

JAK proteins that are related to non-receptor tyrosine kinase protein are considered as essential intracellular elements for cytokine and growth factor signaling pathways [38]. The alterations in the JAK-STAT signaling cascade can lead to a variety of immunological disorders and malignancies [63, 64]. Therefore, JAK1, JAK2, and JAK3 are detected in several cancer cells, particularly JAK1 and JAK2. Accordingly, these proteins are considered as promising targets for the development of potent anticancer agents [64- 67]. The majority of the JAK inhibitors that have been found and are effective bind to ATP-pockets in its active conformation (type I inhibitors) [66]. In general, binding to JAK1 in its active state (DFG-in) occurs by interaction with Glu 957 and Leu 959 of the hinge region residues, where the interaction with the hinge residues plays a major role in kinase inhibition [35, 36]. Docking studies on JAK1 protein performed by using the X-ray data of 3EYG revealed that the co-crystallized ligand (CP-690-550) formed two hydrogen bonds with Glu 957 and Leu 959 from the pyrrolopyrimidine ring [35]. In compliance with this, 6-gingerol and its similar molecules

were docked in the ATP active conformation of the JAK1 (PDB ID: 3EYG) to reveal which compounds will have a good inhibit effect on the protein. The results revealed that N-G-1 (6-gingerol) forms a hydrogen bond with the carbonyl backbone of Leu 959, and N-G-30 forms a hydrogen bond with the carbonyl backbone of Leu 959 with docking scores -7.0641 and -6.9492 respectively.

Otherwise, to achieve a good binding to JAK2 in its active state (DFG-in), the inhibitor should form interactions with Glu 930 and Leu 932 of the hinge region residues. Where the co-crystallized ligand (CMP6) formed two hydrogen bonds with Glu 930 and Leu 932 from the pyridone ring. These interactions were investigated via the docking study on JAK2 by using the X-ray data of 2B7A [67]. The results of this study showed that the N-G-11, N-G-34, and N-G-43 formed 2 H-bonds with carbonyl backbone of Leu 932 and nitrogen backbone of Leu932, N-G-16 formed 2 H-bonds with the carbonyl backbone of Glu 930 and with nitrogen backbone of Leu932 with docking scores -5.826, -5.606, -5.478 and -6.614 respectively (Figure 4.5. and 4.6.).

(a) (b)

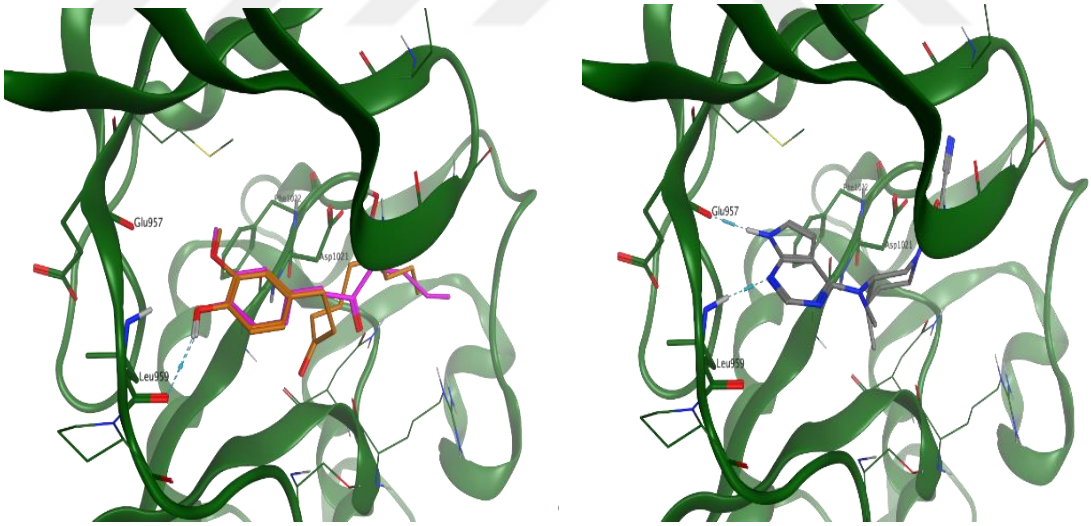

(c) (d)

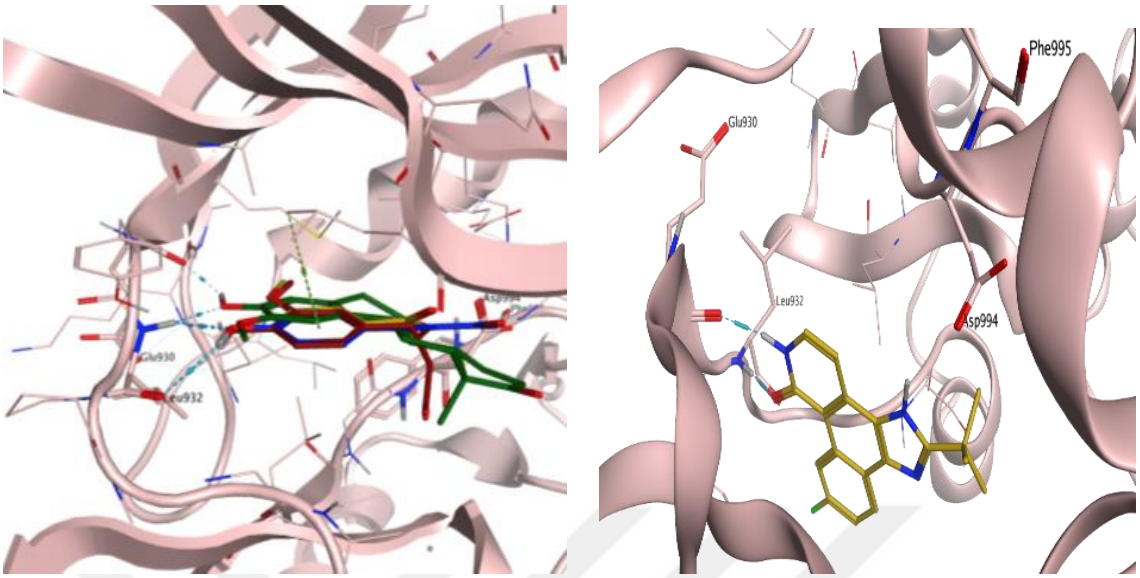

Figure 4.5. Structure of JAK1: PDB ID-3EYG complex with: (a) N-G-1 (pink) and N-G-30 (orange), (b) co-crystalized ligand CP-690-550, Structure of JAK2: PDB ID-2B7A complex with: (c) N-G-11 (blue), N-G-16 (green), N-G-34 (yellow), and N-G-43 (red), (d) co-crystallized ligand CMP6.

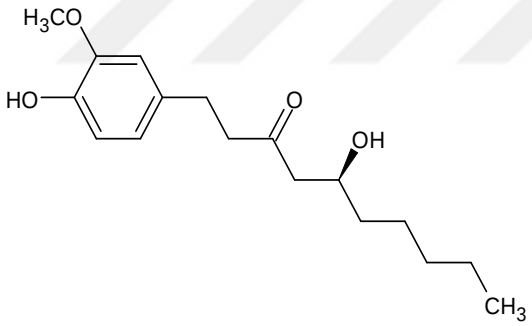

N-G-1

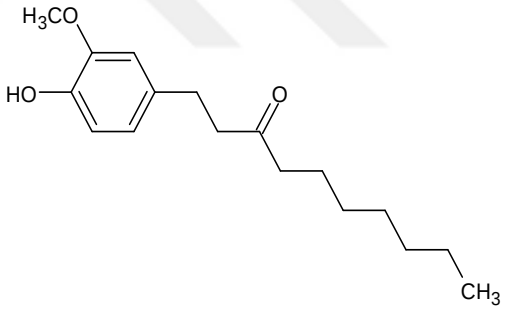

N-G-30

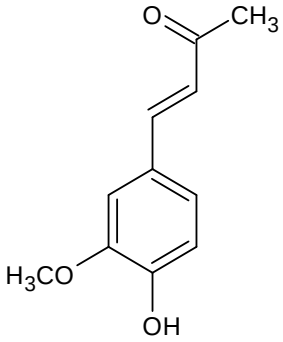

N-G-11

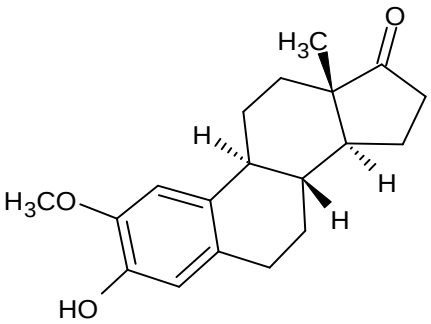

N-G-16

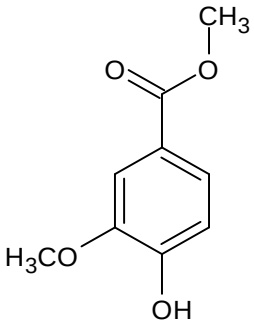

N-G-34

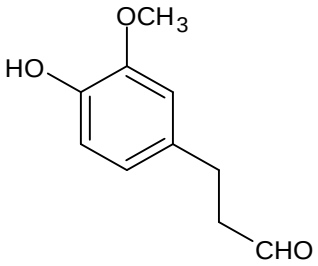

N-G-43

Figure 4.6. The structures of the selected compounds for the active conformer of each JAK1 and JAK2.

Most type I inhibitors of JAK protein can increase phosphorylation in the JAK activation loop while inhibiting the kinase function and phosphorylation of STAT protein [66]. To date, there are numerous challenges facing scientists in developing a selective JAK inhibitor relying on the conserved ATP site of the JAK family. However, they are still making many attempts to find a JAK2 selective inhibitor to avoid off-target adverse effects such as peripheral neuropathy, anemia, and thrombocytopenia [36]. Furthermore, inhibiting JAK2 activity causes numerous alterations in myeloid cell proliferation, differentiation, survival, and death. According to the studies, if the molecule binds to the inactive conformation (DFG-out) of JAK protein, it causes a decrease in phosphorylation in the activation loop, which is achieved when the molecule interacts with the Leu 932, αC-Glu898, and Asp 994, where the interaction with αC-Glu898 and Asp 994 is crucial to achieving selectivity towards JAK2. Docking studies on JAK2 protein were performed by using the X-ray data of 3UGC, where the co-crystallized ligand (NVP-BBT494) formed four hydrogen bonds, two hydrogen bonds with Leu 932, one hydrogen bonds with Asp 994, and another one with αC-Glu898 [36, 66]. The outcomes of this study revealed that N-G-1 forms two hydrogen bonds with the hydroxyl carboxyl group of the side chain of Glu898 and the nitrogen backbone of the Asp994, N-G-24 forms two hydrogen bonds with the nitrogen backbone of the Leu 932 and Asp 994, and N-G-39 form three hydrogen bonds, two hydrogen bonds with the hydroxyl carboxyl group of the side chain of Glu898 and Glu930 and one hydrogen bonds with the nitrogen backbone of the Asp 994 with docking scores -7.4223, -7.9781, and -6.5816 respectively (Figure 4.7., 4.8.).

(a) (b)

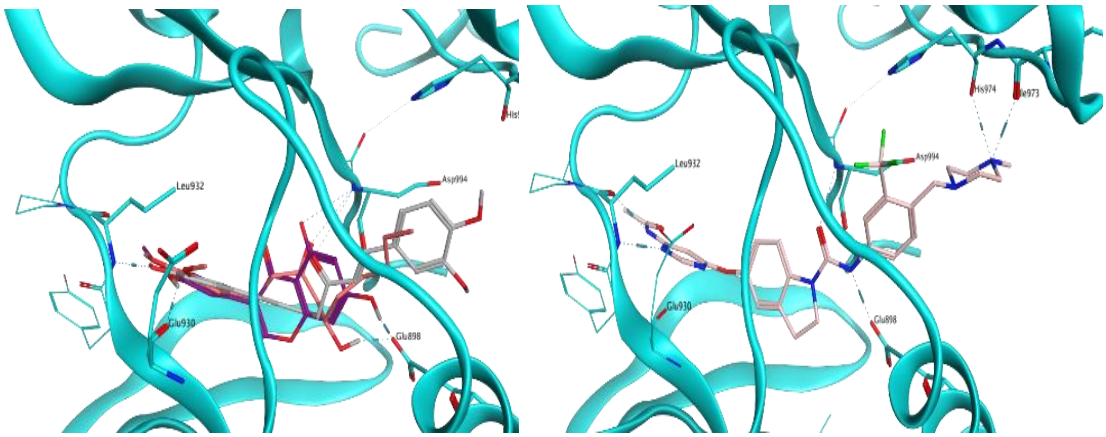

Figure 4.7. Structure of JAK2: PDB ID: 3UGC complex with: (a) N-G-1 (red), N-G-24 (gray), and N-G-39 (purple); (b) co-crystalized ligand NVP-BBT494.

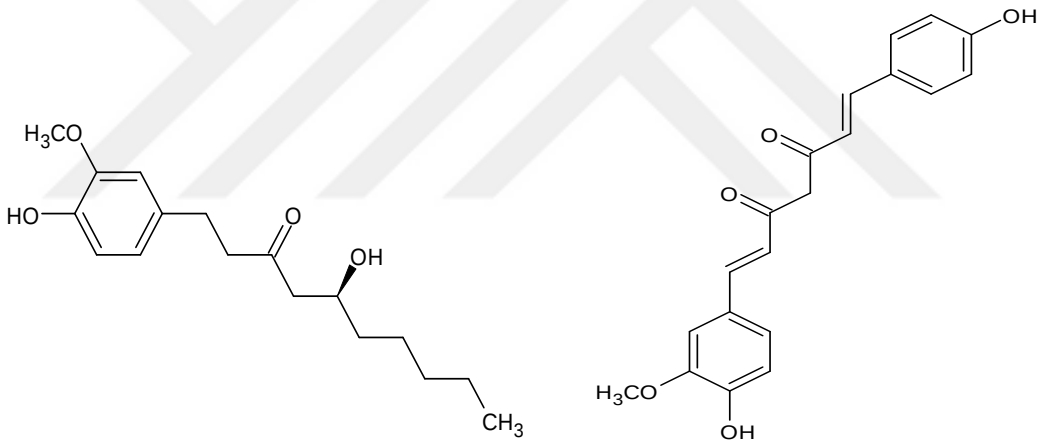

N-G-1 N-G-24

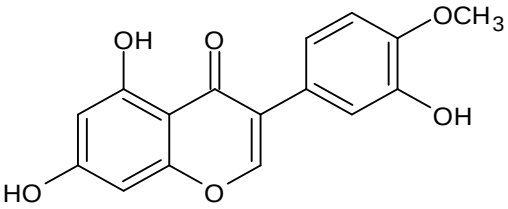

N-G-39

Figure 4.8. The structures of the selected compounds for the in active conformer of JAK2.

Mitogen-activated protein kinases (MAP kinases) are another type of protein kinase that can control cell proliferation, differentiation, and a range of other

physiological responses. Extracellular signal-regulated kinases (ERKs) are activated by MAP kinase kinases (MKK) [45]. Dysregulation of ERK signaling is linked with several cancer types, including lung, kidney, ovarian, colon, and pancreatic cancer. The two isoforms of the ERK enzyme, ERK1 and ERK2, share many biological processes but not all of them [31]. Most of the ERK1\2 inhibitors exhibited type I binding modes, because of the presence of ERK1\2 in its active conformation (DFG-in) more than in their inactive conformation (DFG-out) which is related to the residues presented in the catalytic domain and made the DFG-in state more stable than the DFG-out [69]. According to the literature, achieving a strong binding of the inhibitor is related to forming two hydrogen bonds with the hinge backbone and a hydrogen bond with Lysine K131 (ERK1 numbering) [69]. Docking studies on the ERK1 enzyme were performed by using the X-ray data of 3ZOQ. The co-crystallized ligand 5-iodotubericidin (5ID) formed two hydrogen bonds with the hinge residues (Met 125 and Asp123) and another one with Lys131. The results of our studies showed that the N-G-10, N-G-14, N-G-38, and N-G-44 form a hydrogen bond with the nitrogen sidechains of Lys 131 and the carbonyl backbone of the Met 125. The N-G-20 forms a hydrogen bond with the nitrogen backbone of Met 125 and a hydrogen bond with the nitrogen sidechain of the Lys131 and the N-G-40 forms a hydrogen bond with the carbonyl backbone of the Asp 123 and two hydrogen bonds with nitrogen sidechain of Lys 131. Also, the N-G-47 forms two hydrogen bonds with the nitrogen backbone and carbonyl backbone of Met125 and a hydrogen bond with nitrogen sidechains of Lys131 with docking scores -4.926, -6.818, -6.248, -5.305, -5.345, -7.901, and -5.413 respectively (Figure 4.9. and 4.10.).

(a) (b)

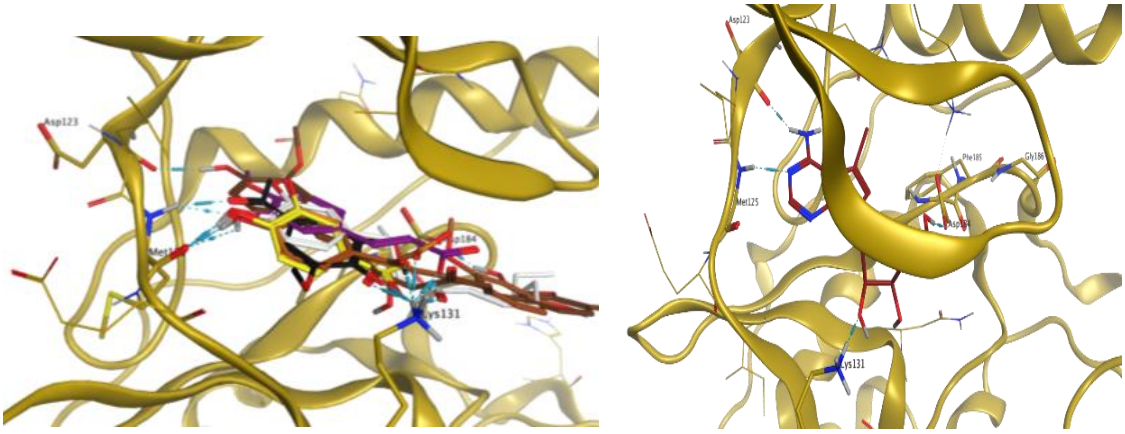

Figurel 4.9. Structure of ERK1: PDB ID: 2ZOQ complex with: (a) N-G-10 (yellow), N-G-14 (white), N-G-20 (black), N-G-38 (light-brown), N-G-40 (brown), N-G-44 (orange), and N-G-47 (purple); (b) co-crystalized ligand 5ID

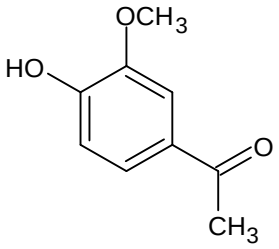

N-G-10

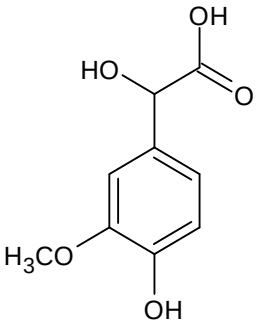

N-G-14

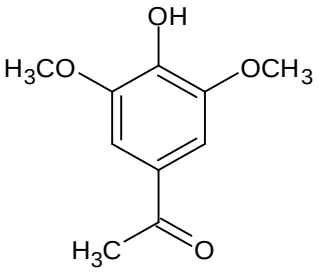

N-G-20

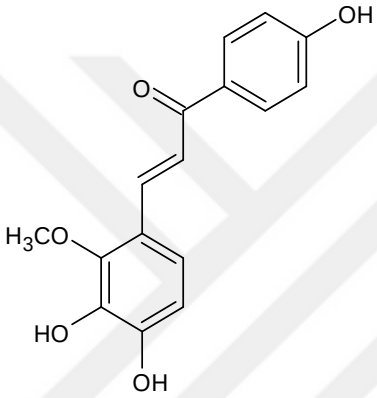

N-G-38

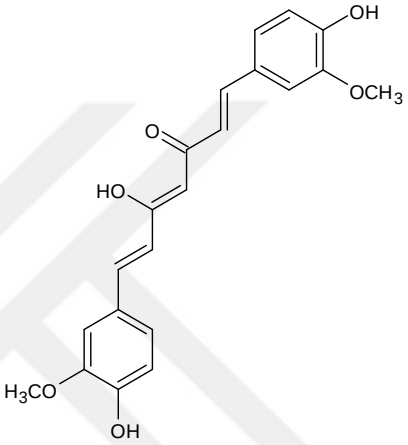

N-G-40

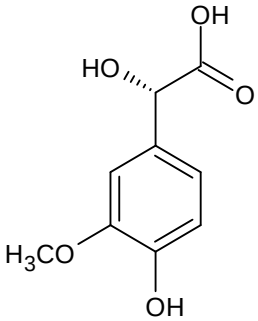

N-G-44

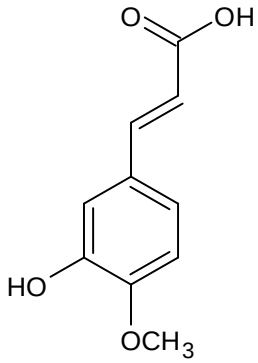

N-G-47

Figure 4.10. The structures of the selected compounds for the active conformer of ERK1.

The human p38 mitogen-activated protein kinase (MAPK) family contains four isoforms including, p38α, p38β, p38γ, and p38δ. These identical isoforms are activated via dual phosphorylation of tyrosine (Tyr) and threonine (Thr) residues in a common Thr-X-Tyr motif mediated by the MAPK. The specific function of the inflammatory response

controlled by p38 MAPK is to promote tumor development. Notably, the expression of p38γ, which is ordinarily not observable in normal T cells, is elevated in cutaneous T-cell lymphoma (CTCL), offering p38γ as a prospective therapeutic target for CTCL treatment. Also, It is demonstrated that the expression of p38γ promotes the growth of various malignancies [32, 33]. As a result, the studied compounds were docked with both conformations (active and inactive) to show how these molecules will affect this protein (Figure 4.11.). Generally, the molecule acts as a type I inhibitor for p38γ when forming H-bonds with a hinge region in the active state of the protein. Docking studies that were performed by using the X-ray data of 1CM8 revealed that AMP-PNP (a nonhydrolyzable ATP-like inhibitor) forms 2 H-bonds with the hinge residues (Met112 and Pro110) [70]. In contrast, our studies showed all compounds do not interact with any of the hinge region residues like AMP-PNP. They also interact with residue located outside of the ATP pocket.

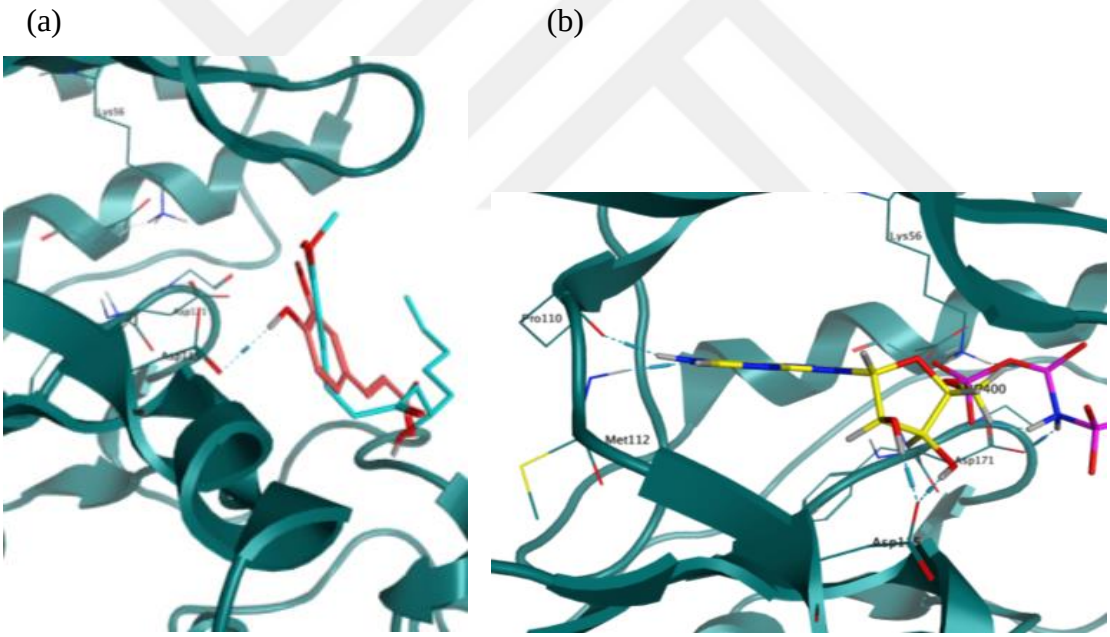

Figure 4.11. Structure of p38γ : PDB ID: 1CM8 complex with: (a) N-G-1 (cyan) and N-G-2 (dark-pink) ; (b) co-crystalized ligand ANP.

In comparison to all protein kinases, scientists are interested in investigating protein kinases in their inactive conformation to develop inhibitors more specific and potent than other inhibitors. According to the literatures, interactions with the DFG-motif and αC-Glu of inactive conformation of kinases increases the selectivity of the drugs

against protein kinases [36, 62]. These observations apply to p38 as well. Based on that, the investigated compounds were docked with 6UNA (the inactive form of p38) to examine how the chemicals interact with the protein. However, protein (6UNA) has no specific ligand. Furthermore, the binding attitude of molecules in the ATP pocket among p38 isomeres is known to be identical since these proteins share conserved residues in the ATP pocket. According to the active conformation of p38, the key residues that may interact with molecules were identified. Interactions with αC-Glu 74 and Asp171 are required for these drugs to be more selective towards the inactive conformation of p38 than the active conformation [70, 71]. Docking studies that were performed by using the X-ray data of 6UNA, showed that all molecules do interact with the ATP pocket. The N-G-16 form H-bond with carbonyl backbone of Asp171, H-bond with amine backbone of Met112, and H-bond with Phe111, the N-G-25 form H-bond with carbonyl backbone of Asp171 and H-bond with amine backbone of Met112, N-G-38 with carbonyl backbone of Asp171, H-bond with amine backbone of Met112, and H-bond with Asp115, and the N-G-40 amine backbone of Met112, H-bond with Phe111, H-bond with Asp115, and H-bond with αC-Glu 74 with docking scores -5.809, -4.875, -6.007, and -5.979 respectively (Figure 4.12.).

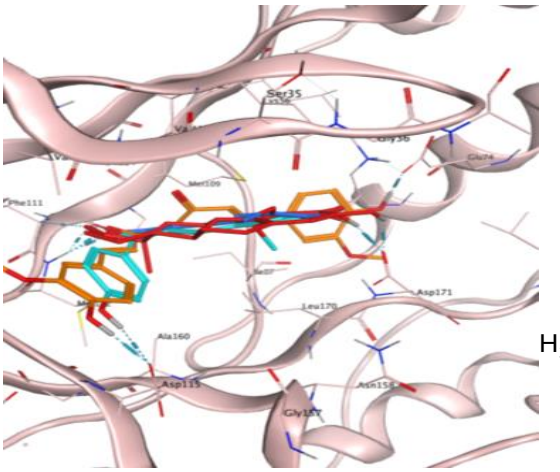

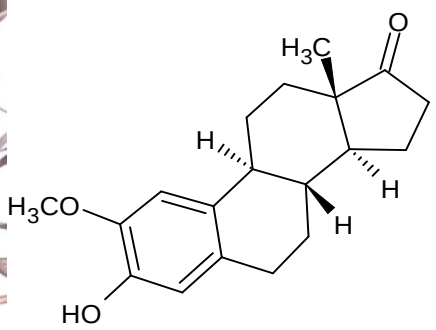

N-G-16

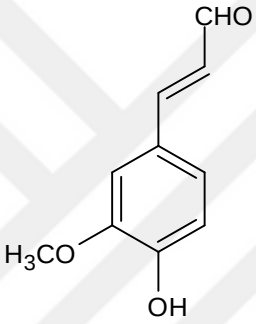

N-G-25

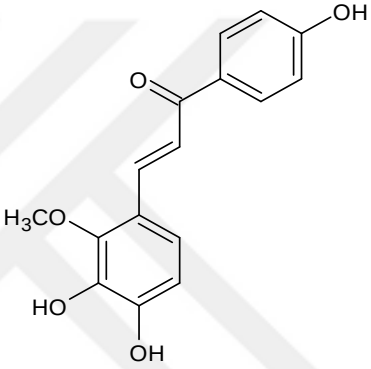

N-G-38

Figure 4.12. Structure of p38γ : PDB ID: 6UNA complex with: (a) N-G-16 (red), N-G-25 (light-blue), N-G-38 (cyan), and N-G-40 (orange).

Table 4.3. Docking scores and predicted interactions of the chosen compounds with the selected proteins

Protein ID	Selected Compounds	H-bond Interaction	Docking Score	RMSD*
BRAF (3OG7)	N-G-12	CYS532	-5.2851	
	N-G-38	CYS532	-6.7236	
	N-G-42	CYS 532 and GLN 530	-5.341	
	N-G-47	GLN 530	-5.2851	
	Co-crystalized ligand	CYS 532 and GLN 530	-7.519	1.126
BRAF (6N0Q)	N-G-18	αC-Glu 501	-5.4173	
	N-G-38	Cys532 and αC-Glu501	-6.71434	
	N-G-44	Asp594 and αC-Glu501	-5.5003	
	Co-crystalized ligand	Phe595, Asp594, and αC-Glu501	-9.362	1.282
JAK1 (3EYG)	N-G-1	Leu 959	-7.064	
	N-G-30	Leu 959	-6.949	
	Co-crystalized ligand	Glu 957 and Leu 959	-6.782	1.369
JAK2 (2B7A)	N-G-11	Leu 932	-5.826	
	N-G-16	Glu 930 and Leu 932	-6.614	
	N-G-34	Leu 932	-5.606	
	N-G-43	Leu 932	-5.478	
	Co-crystalized ligand	Glu 930 and Leu 932	-7.501	0.956

Protein ID	Selected Compounds	H-bond Interaction	Docking Score	RMSD
JAK2 (3UGC)	N-G-1	Glu898 and Asp 994	-7.4223	
	N-G-24	Leu 932 and Asp 994	-7.9781	
	N-G-39	Glu898 ,Glu930, and Asp 994	-6.5816	
	Co-crystalized ligand	Leu 932, Asp 994, and αC-Glu898	-10.644	1.418
ERK1(2ZOQ)	N-G-10	Met125 and the Lys131	-4.926	
	N-G-14	Met 125 and the Lys131	-6.818	
	N-G-20	Met 125 and the Lys131	-5.345	
	N-G-38	Met 125 and the Lys131	-6.248	
	N-G-40	Asp 123 and the Lys131	-7.901	
	N-G-44	Met 125 and the Lys131	-5.305	
	N-G-47	Met 125 and the Lys131	-5.413	
	Co-crystalized ligand	Met 125, Asp123, and Lys131	-6.971	0.828

Protein ID	Selected Compounds	H-bond Interaction	Docking Score	RMSD
P38γ(6UNA)	N-G-16	Asp171, Met112, and Phe111	-5.809	
	N-G-25	Asp171 and Met112	-4.875	
	N-G-38	Asp115, Asp171 and Met112	-6.007	
	N-G-40	Asp171, Met112, Phe111, and αC-Glu 74	-5.979	

*Root Mean Square Deviation

4.4 The Correlation Between Query and Its Similarities

The docking studies of the compounds revealed that most of the molecules have a good interaction with the active conformation of the studied proteins, except for the P38γ protein which the compounds have a good interaction with the inactive conformation.

The docking results related to the active conformation of the BRAF protein showed that the hydroxyl group of the query formed hydrogen bonds with both Cys532 and Gln530. Also, the hydroxyl group of the N-G-(12, 17, 26, 31, 38, 39, 40, 42, and 47) formed hydrogen bonds with CYS 532 (Figure 4.13.)

(a) (b)

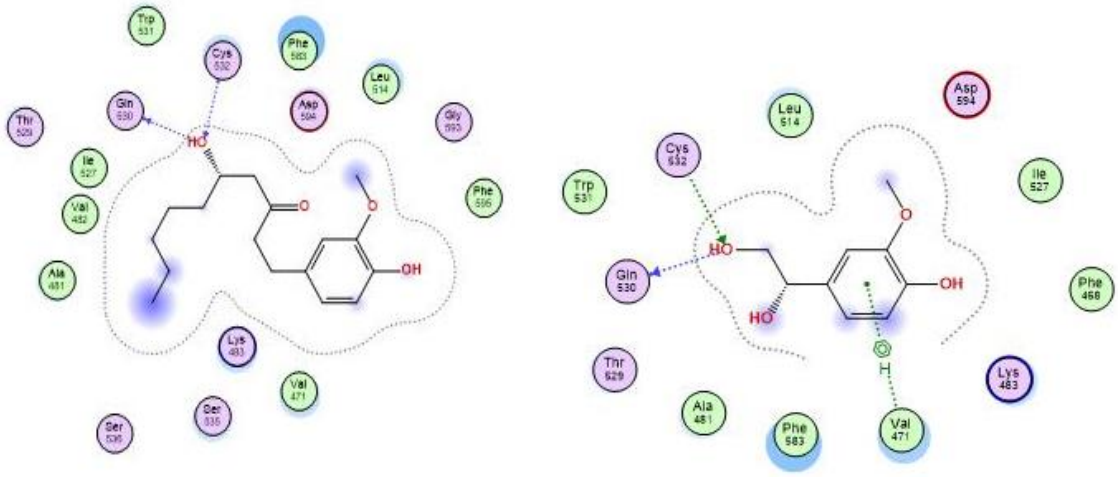

Figure 4.13. Predicted interaction of (a) N-G-1 and (b) N-G-42 with BRAF: PDB:ID: 3OG7.

The docking results related to the active conformation of the JAK1 protein showed that the hydroxy of the phenol group of the query and the majority of its similarities N-G-(2-4, 7-11, 13-15, 17-19, 20-26, 28, 30, 32-35, 37, 40, 41, 44, 47, and 49) formed one hydrogen bond with hinge region residues and specifically with Leu 959 (Figure 4.14.).

(a) (b)

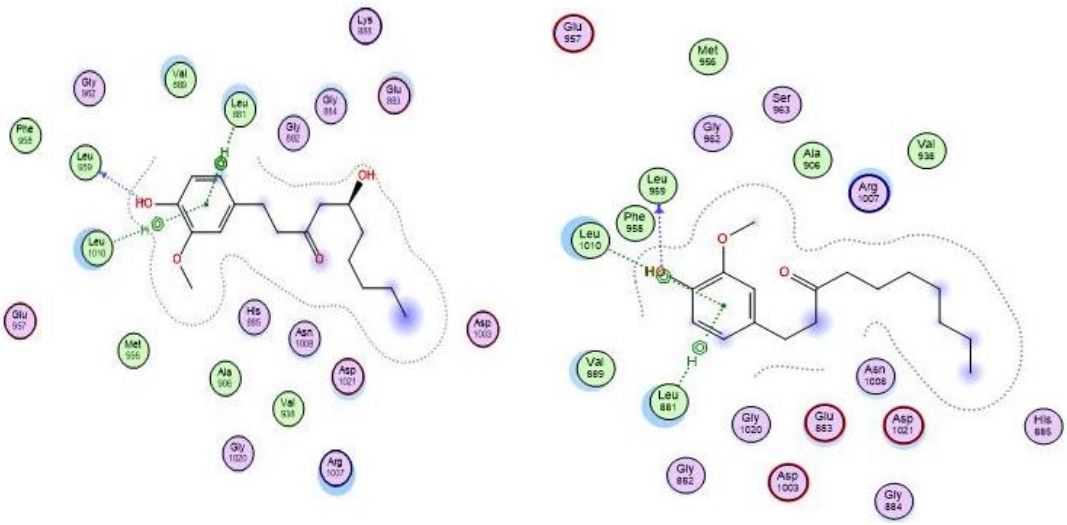

Figure 4.14. Predicted interaction of (a) N-G-1 and (b) N-G-30 with JAK 1: PDB:ID: 3EYG.

The docking results related to the active conformation of the JAK2 protein revealed that the hydroxyl group of the compounds N-G-1 and the hydroxyl of the phenol group of the compounds N-G-(2-5, 7, 8, 11, 13-23, 25, 26, 28-35, 37, 38, 42-44, and 49) formed at least one H-bond with Glu 930 and Leu 932 (Figure 4.15.).

(a) (b)

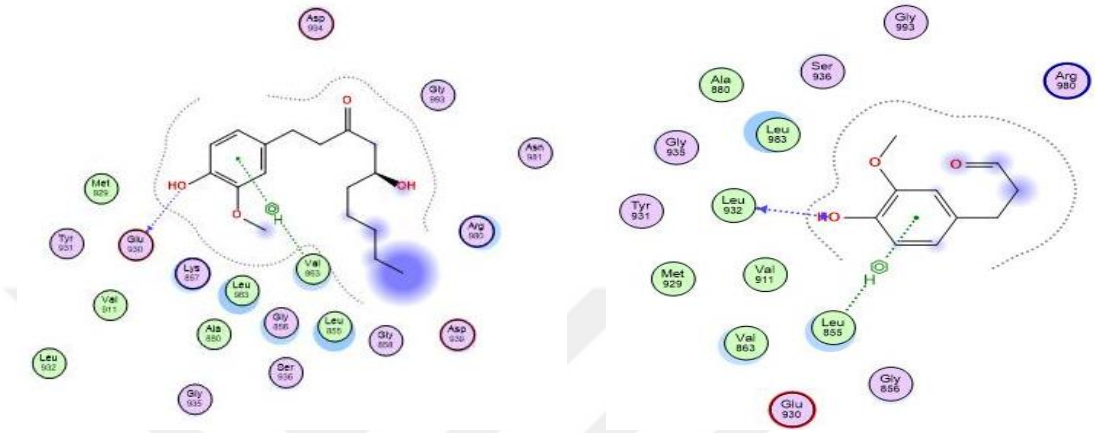

Figure 4.15. Predicted interaction of (a) N-G-1 and (b) N-G-43 with JAK 2: PDB:ID: 2B7A.

The docking results related to the active conformation of the Erk1 protein revealed that the hydroxy of the phenol group of the compound N-G-1 formed H-bond with Met 125. The hydroxy of the phenol group and carbonyl group of the compounds N-G-(12, 22, 14, 15, 38, 10, 20, and 46) formed H-bonds with both Met 125 and Lys 131. Also, the hydroxyl of the phenol group and hydroxy of the carboxylate group of the compounds N-G-(44, 47, and 31) formed H-bonds with both Met 125 and Lys131 (Figure 4.16.)

(a) (b)

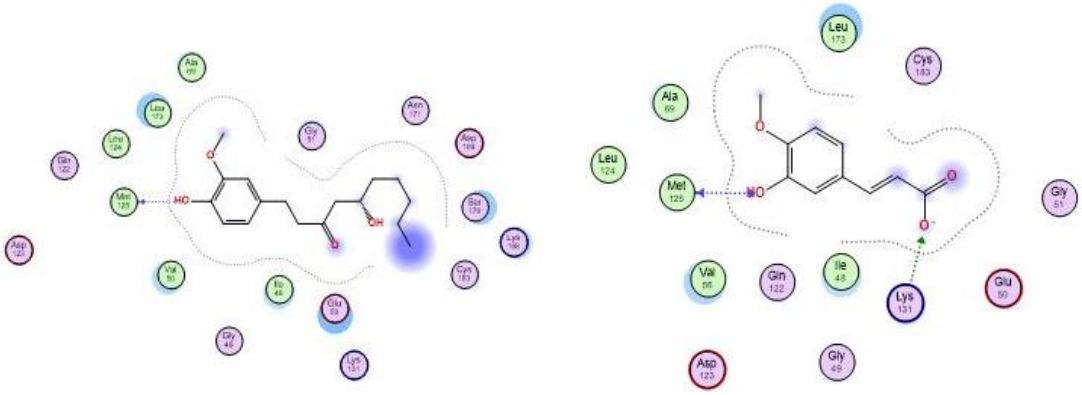

Figure 4.16. Predicted interaction of (a) N-G-1 and (b) N-G-47 with Erk 1 : PDB:ID: 2ZOQ

4.5 Prediction of Drug-likeness and Pharmacokinetics Properties of the Molecules

The drug-likeness and pharmacokinetics (ADME properties) were evaluated to make sure that the compounds are possible drugs. For this purpose, the SwissADME online tool was used, which was designed for easy submission and analysis of the results, to predict the drug-likeness and ADME properties as presented in Tables 4.4, 4.5, and 4.6**,** respectively. The 6-gingerol and the similar molecules that went through this study, meet Lipinski's and Veber's rules of five, suggesting that these molecules theoretically have ideal oral bioavailability. These physicochemical parameters are linked with acceptable aqueous solubility and intestinal permeability which are the first steps in oral bioavailability. Additionally, the bioavailability score (BA) was evaluated where most of the studied molecules have 0.55 as an obtained value, while N-G (2, 22, 46, 47, and 48) have obtained a 0.85 value. This score is depended on the probability value of a molecule to have an optimum profile of permeability and bioavailability, where 0.55 indicates the obedience of the RO5 and the rat bioavailability value is 55%, which is a higher probability value than 10% [45, 72]. Moreover, the molecules were also assessed for their synthetic accessibility, checked on a scale between 1 (simple to synthesize) to 10 (very hard and complex to synthesize) [46]. The synthetic accessibility for all the studied molecules is around 1–4 (Table 4.4), and therefore, they are easy to synthesize.

Table 4.4. Predicted drug-likeness based on the RO5 including bioavailability (BA) and synthetic accessibility (SA) of the molecules

Compound code	Mol.wt	HBA	HBD	TPSA	iLOGP	NRB	BA Score	SA
N-G-1	294.39	4	2	66.76	3.48	10	0.55	2.81
N-G-2	194.18	4	2	66.76	1.62	3	0.85	1.93
N-G-3	164.2	2	1	29.46	2.37	3	0.55	1.58
N-G-4	152.15	3	1	46.53	1.57	2	0.55	1.15
N-G-5	368.38	6	2	93.06	3.27	8	0.55	2.97
N-G-6	178.23	2	0	18.46	2.65	4	0.55	1.71
N-G-7	164.2	2	1	29.46	2.38	2	0.55	1.81
N-G-8	166.17	3	1	46.53	1.82	3	0.55	1.37
N-G-9	168.15	4	2	66.76	1.4	2	0.55	1.42
N-G-10	166.17	3	1	46.53	1.77	2	0.55	1.36
N-G-11	192.21	3	1	46.53	2.11	3	0.55	2.13
N-G-12	284.26	5	2	79.9	2.4	2	0.55	2.95
N-G-13	166.22	2	1	29.46	2.46	3	0.55	1.4
N-G-14	198.17	5	3	86.99	1.21	3	0.55	2.2
N-G-15	276.37	3	1	46.53	3.28	9	0.55	2.51
N-G-16	300.39	3	1	46.53	2.92	1	0.55	3.52
N-G-17	358.39	6	2	85.22	2.47	6	0.55	3.3
N-G-18	154.16	3	2	49.69	1.79	2	0.55	1.26
N-G-19	194.23	3	1	46.53	2.09	4	0.55	1.52
N-G-20	196.2	4	1	55.76	1.98	3	0.55	1.65
N-G-21	138.16	2	1	29.46	1.94	1	0.55	1
N-G-22	182.17	4	2	66.76	1.18	3	0.85	1.49
N-G-23	150.17	2	1	29.46	2.14	2	0.55	1.45
N-G-24	338.35	5	2	83.83	2.78	7	0.55	2.82
N-G-25	178.18	3	1	46.53	1.75	3	0.55	1.88
N-G-26	180.2	3	2	49.69	2.16	3	0.55	1.86
N-G-27	358.47	4	0	36.92	4.31	9	0.55	3.32
N-G-28	182.17	4	3	77.76	0.86	3	0.55	1.2
N-G-29	194.23	3	1	38.69	2.46	4	0.55	1.87
N-G-30	278.39	3	1	46.53	3.65	10	0.55	2.28
N-G-31	362.42	6	4	99.38	2.98	9	0.55	3.21
N-G-32	372.41	6	1	74.22	2.8	7	0.55	3.43
N-G-33	152.19	2	1	29.46	2.21	2	0.55	1.18
N-G-34	182.17	4	1	55.76	2.13	3	0.55	1.67
N-G-35	196.2	4	1	55.76	1.98	4	0.55	1.85
N-G-36	152.15	3	1	46.53	1.6	2	0.55	1.16
N-G-37	178.23	2	1	29.46	2.63	3	0.55	1.89
N-G-38	286.28	5	3	86.99	1.7	4	0.55	2.8
N-G-39	300.26	6	3	100.13	2.38	2	0.55	3.02
N-G-40	368.38	6	3	96.22	3.21	7	0.55	3.42
N-G-41	372.41	6	2	93.06	3.21	10	0.55	2.45

Compound code	Mol.wt	HBA	HBD	TPSA	iLOGP	NRB	BA Score	SA
N-G-42	184.19	4	3	69.92	1.61	3	0.55	2.11
N-G-43	180.2	3	1	46.53	1.77	4	0.55	1.4
N-G-44	198.17	5	3	86.99	1.21	3	0.56	2.2
N-G-45	192.21	3	0	35.53	2.21	3	0.55	2.03
N-G-46	168.15	4	2	66.76	0.89	2	0.85	1.24
N-G-47	194.18	4	2	66.76	1.79	3	0.85	1.9
N-G-48	196.2	4	1	55.76	1.67	4	0.85	1.62
N-G-49	152.15	3	1	46.53	1.44	2	0.55	1.05

The ADME properties of the 6-gingerol and similar compounds are summarized in (Tables 4.5 and 4.6). The gastrointestinal absorption (GI) of all the compounds of this study are characterised by a high GI absorption and this compliance with the RO5. P-glycoprotein (P-gp) considers one of the drug transporters that control the uptake and efflux of a variety of drugs. It acts like a transmembrane efflux pump, that pumps its substrates (drugs and toxins) from inside to outside the cell [61, 73]. Our results showed that the molecules N-G-(16, 27, and 31) are the only substrate for P-gp while the other molecules are not substrate for P-gp. Furthermore, the blood-brain-barrier (BBB) controls cerebral homeostasis and supplies the central nervous system (CNS) with a unique protection against the toxicity of many xenobiotics and pathogens [35, 74]. Here, the analysis of the molecules of this study showed that the compounds N-G (5, 9, 12, 14, 17, 22, 24, 28, 31, 38-42, 44, and 46) have the ability to cross the BBB while the other studied compounds are not. Additionally, according to our results, most of the compounds do not inhibit CYP2C19 while N-G-15 has just an inhibitory effect on CYP2C19. The N-G-(5, 12, 17, 24, 27, 32, 38- 41) are only affect on CYP 3A4 while the other molecules do not inhibit. The N-G-(1, 12, 15, 16, 17, 27, 30, 31, 32, 39, and 41) only inhibit the CYP 2D6 while the rest of the studied compounds do not have any effect on these isoforms. The N-G-(5, 24, 32, 38-40) are only inhibit the CYP 2C9 while the rest of the compounds do not show any effect on this isoforms. The compounds N-G-(1, 3, 6, 7, 11- 13, 15, 19, 23, 24, 29, 30, 33, 37-39, and 45) inhibit the CYP1A2 isoforms while the other compounds do not have any affect on this isoforms. Overall, the compounds N-G-(5, 12, 17, 24, 27, 32, 38-40, and 41) have an inhibition activity on more than one CYP isoform.

Table 4.5. Predicted ADME properties of molecules under study

Compound code	GI absorption	BBB permeant	Pgp substrate	CYP1A2 inhibitor	CYP2C19 inhibitor	CYP2C9 inhibitor	CYP2D6 inhibitor	CYP3A4 inhibitor
N-G-1	High	+	-	+	-	-	+	-
N-G-2	High	+	-	-	-	-	-	-
N-G-3	High	+	-	+	-	-	-	-
N-G-4	High	+	-	-	-	-	-	-
N-G-5	High	-	-	-	-	+	-	+
N-G-6	High	+	-	+	-	-	-	-
N-G-7	High	+	-	+	-	-	-	-
N-G-8	High	+	-	-	-	-	-	-
N-G-9	High	-	-	-	-	-	-	-
N-G-10	High	+	-	-	-	-	-	-
N-G-11	High	+	-	+	-	-	-	-
N-G-12	High	-	-	+	-	-	+	+
N-G-13	High	+	-	+	-	-	-	-
N-G-14	High	-	-	-	-	-	-	-
N-G-15	High	+	-	+	+	-	+	-
N-G-16	High	+	+	-	-	-	+	-
N-G-17	High	-	-	-	-	-	+	+
N-G-18	High	+	-	-	-	-	-	-
N-G-19	High	+	-	+	-	-	-	-
N-G-20	High	+	-	-	-	-	-	-
N-G-21	High	+	-	-	-	-	-	-
N-G-22	High	-	-	-	-	-	-	-
N-G-23	High	+	-	+	-	-	-	-
N-G-24	High	-	-	+	-	+	-	+
N-G-25	High	+	-	-	-	-	-	-
N-G-26	High	+	-	-	-	-	-	-
N-G-27	High	+	+	-	-	-	+	+
N-G-28	High	-	-	-	-	-	-	-
N-G-29	High	+	-	+	-	-	-	-
N-G-30	High	+	-	+	-	-	+	-
N-G-31	High	-	+	-	-	-	+	-
N-G-32	High	+	-	-	-	+	+	+
N-G-33	High	+	-	+	-	-	-	-
N-G-34	High	+	-	-	-	-	-	-
N-G-35	High	+	-	-	-	-	-	-
N-G-36	High	+	-	-	-	-	-	-
N-G-37	High	+	-	+	-	-	-	-
N-G-38	High	-	-	+	-	+	-	+
N-G-39	High	-	-	+	-	+	+	+
N-G-40	High	-	-	-	-	+	-	+
N-G-41	High	-	-	-	-	-	+	+
N-G-42	High	-	-	-	-	-	-	-
N-G-43	High	+	-	-	-	-	-	-
N-G-44	High	-	-	-	-	-	-	-
N-G-45	High	+	-	+	-	-	-	-
N-G-46	High	-	-	-	-	-	-	-
N-G-47	High	+	-	-	-	-	-	-
N-G-48	High	+	-	-	-	-	-	-
N-G-49	High	+	-	-	-	-	-	-

In the case of excretion, clearance was calculated as the sum of hepatic clearance and renal clearance. Also, it refers to a constant that explains the relationship between the drug concentration in the body and the rate of elimination of the drug. A low total clearance value corresponds to a higher drug persistence in the body. Here in this study, most of the compounds showed low clearance. However, the compounds N-G-(1, 2, 4, 8-10, 15, 16, 20, 30, 34, 35, 38, 46, 47, and 49) showed high clearance (Table 4.6). The renal uptake transporter known as Organic Cation Transporter 2 (OCT2) is crucial for medication clearance and endogenous substance clearance. OCT2 substrates may also have possibility for a negative interactions with coadministered OCT2 inhibitors [47]. Non of the studied compounds are substrate for OCT2. Accordingly, these compounds will not interact or have a negative effect on the OCT2 inhibitors.

Table 4.6. The excretion properties of the studied compounds

Compound code	Total Clearance Log (ml/min/kg)	Renal OCT2 substrate
N-G-1	1.339	No
N-G-2	0.623	No
N-G-3	0.282	No
N-G-4	0.601	No
N-G-5	-0.002	No
N-G-6	0.338	No
N-G-7	0.221	No
N-G-8	0.642	No
N-G-9	0.628	No
N-G-10	0.62	No
N-G-11	0.16	No
N-G-12	0.18	No
N-G-13	0.244	No
N-G-14	0.446	No
N-G-15	1.44	No
N-G-16	0.719	No
N-G-17	0.147	No
N-G-18	0.215	No
N-G-19	0.307	No
N-G-20	0.641	No
N-G-21	0.202	No
N-G-22	0.246	No
N-G-23	0.233	No
N-G-24	0.026	No
N-G-25	0.183	No
N-G-26	0.233	No
N-G-27	0.197	No
N-G-28	0.245	No
N-G-29	0.293	No
N-G-30	1.411	No
N-G-31	0.248	No
N-G-32	0.214	No

Compound code	Total Clearance Log (ml/min/kg)	Renal OCT2 substrate
N-G-33	0.232	No
N-G-34	0.687	No
N-G-35	0.769	No
N-G-36	0.159	No
N-G-37	0.268	No
N-G-38	0.555	No
N-G-39	0.165	No
N-G-40	0.089	No
N-G-41	0.23	No
N-G-42	0.206	No
N-G-43	0.325	No
N-G-44	0.446	No
N-G-45	0.158	No
N-G-46	0.626	No
N-G-47	0.621	No
N-G-48	0.304	No
N-G-49	0.599	No

4.6 Prediction of the Toxicities Profiles of the Molecules

Appendix E shows the cytotoxicity predictions (Way2Drug) on the tumor and non-tumor cell lines of the compounds with a probability of greater than 0.50. 21 compounds are predicted to be effective on various tumor cell lines. 21 different cell lines of 8 different tissues. Coniferaldehyde was predicted to be the most effective compound (6 cell lines). Vanylglycol had the highest predicted activity (0.747) on PC-3. However, the majority of the compounds do not have an effect on non-tumor cells when their probability is greater than 0.50, with only 6 compounds having an adverse effect on non-tumor cells. Hepatotoxicity predictions made via ProTox-II revealed the majority of compounds expected to be safe (Appendix F). The compounds predicted as positive had low probabilities (between 50%- 52%). Also, Appendix G shows the toxicity effect (hepatotoxicity, hERG I inhibitor, and hERG II inhibitor) of the compounds that were predicted by using pkCSM where most of the compounds show no effect on hepatotoxicity, hERG I inhibitor, and hERG II inhibitor. Additionally, the ProTox-II mutagenicity, carcinogenicity, cytotoxicity, and immunotoxicity prediction revealed that all compounds are not expected to have a mutagenicity or cytotoxicity effect. There are only two compounds that do have a positive mutagenicity result with a low probability (between 53% and 67 %). The results of the immunotoxicity effect of the compounds revealed that 17 chemicals, including the query compound, have high probability of influence on the immune system (79%- 98%). In regard to the carcinogenicity effect of the compounds, methyl eugenol showed the greatest ability to induce tumors, with a probability of 76%. The majority of the compounds is not toxic to MMP and P53. However, 7 compounds predicted to be positive on MMP have higher probabilities between (78%- 100%) and 2 compounds predicted to be positive on P53 have a higher probabilities between (80%- 100%), where curcumin showed the highest toxicity effect on MMP and P53 with a probability of 100%.

5. CONCLUSION

Taking it all together, an *in silico* target Prediction was presented depending on a ligand-based virtual screening workflow that could identify both new lead compounds and molecular targets for natural chemical entities, here 6-gingerol and its similar compounds. Natural products are a vital component of drug discovery. In particular, the detection of the phenotypic change caused by the studied natural product in cell-based assays, like the suppression of cancer cell growth is the major motive for screening natural products of interest in target-based assays [75]. In this respect, *in silico* approaches offer adaptable equipment for screen analysis and qualitative and quantitative descriptions of the variety, predicted activity, and even potential toxicity of natural chemicals [76]. The anti-cancer targets of 6-gingerol and its similar compounds have been predicted by using four different target fishing servers. Their effect on the kinases protein as an anti-cancer target were focused specifically on due to its essential role in controlling signaling pathways in cells. Also, the knowledge that the dysregulation and mutations of protein kinases are linked with a multiplicity of human diseases like cancer [6, 9]. According to our results that are represented in (Table 4. 3.), the 6-gingerol and its similar molecules were investigated with these kinases including [B-RAF, JAK1/2, ERK1(MAPK3), and p38γ] via molecular docking studies using MOE [13]. Generally, the results of the study on the BRAF protein showed that the majority of studied compounds act as type I inhibitors because they formed a hydrogen bond with the major residues located in the hinge region (Cys 532 and Gln 530). 13 molecules formed a hydrogen bond with just αC-Glu501 which showed good selectivity towards the inactive conformation. While the molecule N-G-44 (L-(+)-vanilmandelic acid) was the most selective molecule as a type II inhibitor for BRAF because it formed two hydrogens bond with both Asp 594 and αC-Glu501.

For the JAK 1/2 protein, the docking results revealed that the majority of the compounds act as type I inhibitors for the active conformation of the JAK 1/2 and JAK 2 isoform was focused on due to its overexperssion linked with various type of cancer. All the studied molecules formed at least one hydrogen bond with basic hinge region residues (Glu 930 and Leu 932). Moreover, some of the studied compounds act as type II inhibitors for the inactive conformation of JAK 2 where these compounds formed a hydrogen bond with Asp 994 and αC-Glu 898 which considered the most crucial residues for the interaction with JAK2 (in active conformation) and make the molecule highly selective toward JAK2.

Additionally, all compounds have revealed a positive interaction with the ERK1 in its active conformation forming at least one hydrogen bond with the hinge residues (Met 125 and Asp123) and with Lys131 which promot the interaction between molecules and the target [4]. The compounds N-G-10 (Acetovanillone), N-G-14 (Vanillylmandelic acid), N-G-20 (Acetosyringone), N-G-38 (Licochalcone B), N-G-44 (L-(+)-vanilmandelic acid), and N-G-47 (Isoferulic acid) formed two hydrogen bonds with Met 125 and Lys131.

The docking studies on the last studied protein p38γ showed that none of the studied compounds interact with any of the hinge region residues Met112 or Pro110. The compounds do not have any inhibitory effect on p38γ in its active conformation. Meanwhile, the compounds showed an interaction with the residues that may play a vital role in inhibiting the inactive conformation of the protein αC-Glu 74 and Asp171 [70]. Additionally, most of the compounds made interaction with the hinge region residues. The molecules N-G-16 (2-methoxyestrone), N-G-25 (Coniferaldehyde), and N-G-38 (Licochalcone B) formed hydrogen bonds with Asp171 and the other hydrogen bonds with the hinge region residues. According to these results, these molecules may act as potent and selective inhibitors toward the inactive conformation of p38γ. However, the molecules N-G-40 (Curcumin PE) formed hydrogen bonds with both αC-Glu 74 and Asp171. Also, it interacted with the hinge residues. These interactions make N-G-40 (Curcumin PE) the most nominating molecule inhibiting the p38γ (inactive) and for further studies, especially since the p38γ (inactive) does not have an exact ligand.

The drug-likeness is the precondition for a bioactive molecule to enter into the drug development process. In our study 6-gingerol and the similar molecules that went through this study, meet Lipinski’s and Veber's rules of five, suggesting that these molecules theoretically have ideal oral bioavailability. Additionally, all the molecules have a good bioavailability score (BA) over 0.55. Properties related to absorption, distribution, metabolism, excretion, and toxicity (ADMET) have become one of the most important issues to assess the effects or risks of bioactive compounds on the human body [77]. According to the ADMET properties of the studied compounds all the compounds showed a high absorption and distribution. However, N-G-(5, 12, 17, 24, 27, 32, 38- 40, and 41) have an inhibition activity on more than one CYP isoform. Here in this study, most of the compounds showed low clearance. Whereas, the compounds N-G-(1, 2, 4, 8-10, 15, 16, 20, 30, 34, 35, 38, 46, 47, and 49) showed high clearance, non of these compounds act as substrate for OTC2.

The toxicity of the studied compounds was determined by using three different computational approaches to identify the potential cytotoxicity and adverse effect of chemical structures on both normal cells and tumor cells, as well as organs in general. It also assists in determining the molecules that may boost efficacy and therapeutic success [52]. All the compounds do not have cytotoxicity on the normal cell with the only exception of the 6 molecules that have toxicity on a normal cell. However, 21 molecules had toxicity on the cancer cell line. N-G-25 (Coniferaldehyde) was the most molecule effect on six different cell lines. It also has good potency as a type I inhibitor towards JAK2 and ErK1 and showed good interaction with the inactive conformation of p38γ. N-G-42 (Vanylglycol) had affected on three different cell lines with the highest predicted activity on PC-3 cell line (0.747). In addition to its highest potency as V600E-BRAF inhibitors in its active conformation. N-G-44 (L-(+)-vanilmandelic acid) had toxicity on DMS-114 with the best selectivity towards JAK2 (inactive), BRAF(inactive), and Erk1 which promote its anti-cancer activities. N-G-16 (2-methoxyestrone) had a toxicity effect on two cell lines SF-539 and MDA-MB-231. It is also high potency as a type I inhibitor for JAK2 and as a type II inhibitor for p38γ**.** N-G-11 (Dehydrozingerone), N-G-34 (Methyl vanillate), and N-G-43 (dihydroconiferyl aldehyde) had cytotoxicity on one cell line, in compliance with their potency as type I inhibitors for JAK2. The N-G-10 (Acetovanillone), N-G-14 (Vanillylmandelicacid), N-G-20 (Acetosyringone), N-G-38 (Licochalcone B), and N-G-47 (Isoferulic acid) had cytotoxicity on one cell line, in compliance to their potency as type I inhibitor for ErK1. Also, N-G-38 (Licochalcone B) had potency towards BRAF (active) and p38γ (inactive). The N-G-40 (Curcumin PE) had cytotoxicity on one cell line, in compliance with its potency as typeII inhibitors for both JAk2 and p38γ and type I inhibitors for ErK1, according to the PASS CLC Pred. Also, 6-gingerol and its similar molecules showed that they do not have any hepatotoxicity, hERG I inhibitor, and hERG II inhibitor effect on the liver and hearts which are the organs affected by the drugs according to the prediction by both ProTox-II. The mutagenicity and carcinogenicity effect of the studied compounds showed that all compounds do not have a mutagenicity or cytotoxicity effect, and just two compounds had a positive mutagenicity effect with a low probability. Additionally, 17 molecules had a high probability of influencing the immune system (79% -98%). The molecules N-G-(40, 38, 47, 16, and 11) that had potency towards studied proteins had toxicities on the immune systems. However, seven compounds had a positive effect on MMP with higher probabilities between (78%-100%). While, the molecules N-G-(38, 39, and 40) that

showed potency towards the protein have toxicity on MMP. Also, two of the compounds were expected to be positive on P53 with higher probabilities between (80%-100%), where curcumin showed the highest toxicity effect on MMP and P53 with a probability of 100%.

To end, our study that depends on target prediction workflow revealed that the vanylglycol, L-(+)-vanillylmandelic acid, dehydrozingerone, 2-methoxyestrone, methylvanillate, dihydroconiferyl aldehyde, pratensein, acetovanillone, acetosyringone, licochalcone B, isoferulic acid, curcumin PE, and coniferaldehyde are potential anticancer candidates which could play a desirable role in future lead optimization studies.

6. REFERENCES

[1] Rayan A, Raiyn J, Falah M. Nature is the best source of anticancer drugs: Indexing natural products for their anticancer bioactivity. *PLoS One*. 2017;12(11):1-12. doi:10.1371/journal.pone.0187925

[2] Rastogi N, Duggal S, Singh SK, et al. Proteasome inhibition mediates p53 reactivation and anticancer activity of 6-Gingerol in cervical cancer cells. *Oncotarget*. 2015; 6(41): 43310-43325. doi:10.18632/oncotarget.6383

[3] Mao QQ, Xu XY, Cao SY, et al. Bioactive compounds and bioactivities of ginger (zingiber officinale roscoe). *Foods*. 2019; 8(6): 1-21. doi:10.3390/foods8060185

[4] Wang S, Zhang C, Yang G, Yang Y. Biological properties of 6-Gingerol: A brief review. *Nat Prod Commun*. 2014;9(7):1027-1030. doi:10.1177/1934578x1400900736

[5] Zhang F, Zhang JG, Qu J, Zhang Q, Prasad C, Wei ZJ. Assessment of anti-cancerous potential of 6-gingerol (Tongling White Ginger) and its synergy with drugs on human cervical adenocarcinoma cells. *Food Chem Toxicol*. 2017;109:910-922.

[6] Wang B, Wu H, Hu C, et al. An overview of kinase downregulators and recent advances in discovery approaches. *Signal Transduct Target Ther*. 2021;6(1):1-19. doi:10.1038/s41392-021-00826-7

[7] Schwarz D, Merget B, Deane C, Fulle S. Modeling conformational flexibility of kinases in inactive states. *Proteins Struct Funct Bioinforma*. 2019;87(11):943-951. doi:10.1002/prot.25756

[8] Modi V, Dunbrack RL. Defining a new nomenclature for the structures of active and inactive kinases. *Proc Natl Acad Sci USA*. 2019;116(14):6818-6827. doi:10.1073/pnas.1814279116

[9] Roskoski R. Classification of small molecule protein kinase inhibitors based upon the structures of their drug-enzyme complexes. *Pharmacol Res*. 2016;103:26- 48. doi:10.1016/j.phrs.2015.10.021

[10] Singh N, Chaput L, Villoutreix BO. Virtual screening web servers: Designing chemical probes and drug candidates in the cyberspace. *Brief Bioinform*. 2021;22(2): 1790-1818. doi:10.1093/bib/bbaa034

[11] Surabhi S, Singh B. Computer Aided Drug Design: an Overview. *J Drug Deliv Ther*. 2018;8(5):504-509. doi:10.22270/jddt.v8i5.1894

[12] F. Sousa S, M.F.S.A. Cerqueira N, A. Fernandes P, Joao Ramos M. Virtual Screening in Drug Design and Development. *Comb Chem High Throughput Screen*. 2010; 13(5):442-453. doi:10.2174/138620710791293001

[13] Bielska E, Lucas X, Czerwoniec A, Kasprzak JM, Kaminska KH, Bujnicki JM. Virtual screening strategies in drug design - methods and applications. *Biotechnologia*. 2011;92(3):249-264. doi:10.5114/bta.2011.46542

[14] Manikandan S, Ansarali S, Priyadharshini M; Lakshmanan G.M.A. pharmacoinformatics approach of identified biological compounds from selected plectranthus (L) species in tamil nadu, india: an in-silico approach. *Int Res J Pharm*. 2021;12(7).

[15] Ekins S, Mestres J; Testa B. In silico pharmacology for drug discovery: applications to targets and beyond. *Br J Pharmacol*. 2007;152, 21-37.

[16] Stewart B, Weiderpass E, Wild C. *World Cancer Report Cancer research for cancer prevention*. Lyon: International Agency for Research on Cancer; 2020.

[17] Cabral C, Efferth T, M.Pires I, Severino P,F.L. Lemos, M. Natural Products as a Source for New Leads in Cancer Research and Treatment. *eCAM*. 2018; 1–2.

[18] de Lima RMT, dos Reis AC, de Menezes AAPM, et al. Protective and therapeutic potential of ginger (Zingiber officinale) extract and [6]-gingerol in cancer: A comprehensive review. *Phyther Res*. 2018;32(10):1885-1907. doi:10.1002/ptr.6134

[19] Tripathi P, Singh A. Natural resources from plants in the treatment of cancer: An update. *Asia J Pharm Clin Res*. 2017;10(7):11-20. doi:10.22159/ajpcr.2017.v10i7.17399

[20] Maneikyte J, Bausys A, Leber B, et al. Dietary glycine prevents folfox chemotherapy-induced heart injury: A colorectal cancer liver metastasis treatment model in rats. *Nutrients*. 2020; 12(9): 1-16. doi:10.3390/nu12092634

[21] Prša P, Karademir B, Biçim G, et al. The potential use of natural products to negate hepatic, renal and neuronal toxicity induced by cancer therapeutics. *Biochem Pharmacol*. 2020;173(June 2019):113551. doi:10.1016/j.bcp.2019.06.007

[22] Unuofin, J. O., Masuku, N. P., Paimo, O. K., and Lebelo, S. L. Ginger from farmyard to town: Nutritional and pharmacological applications. *Front Pharmacol*. 2021;12.

[23] Ahmed SHH, Gonda T, Hunyadi A. Medicinal chemistry inspired by ginger: exploring the chemical space around 6-gingerol. *RSC Adv*. 2021;11(43):26687-26699. doi:10.1039/d1ra04227k

[24] Prasad, S., and Tyagi, A. K. Ginger and its constituents: Role in prevention and treatment of gastrointestinal cancer. *Gastroenterol Res Pract* . 2015; 2015: 1–11.

[25] Liu, C.-M., Kao, C.-L., Tseng, Y.-T., Lo, Y.-C., and Chen, C.-Y. Ginger phytochemicals inhibit cell growth and modulate drug resistance factors in docetaxel resistant prostate cancer cell. *Molecules*. 2017;22(9):1477.

[26] Zivarpour, P., Nikkhah, E., Maleki Dana, P., Asemi, Z., and Hallajzadeh, J. Molecular and biological functions of Gingerol as a natural effective therapeutic drug for cervical cancer. *J Ovarian Res*. 2021;14(1): 2021.

[27] Vijayan R, He P, Modi V et al. Conformational Analysis of the DFG-Out Kinase Motif and Biochemical Profiling of Structurally Validated Type II Inhibitors. *J Med Chem*. 2014;58(1):466-479.

[28] Umar, A.B., Uzairu, A., Shallangwa, G.A. *et al*. Docking-based strategy to design novel flavone-based arylamides as potent V600E-BRAF inhibitors with prediction of their drug-likeness and ADMET properties. *Bull Natl Res Cent*. 2020;44:179.

[29] Xie P, Streu C, Qin J et al. The Crystal Structure of BRAF in Complex with an Organoruthenium Inhibitor Reveals a Mechanism for Inhibition of an Active Form of BRAF Kinase. *Biochemistry.* 2009;48(23):5187-5198.

[30] Pegram L, Liddle J, Xiao Y et al. Activation loop dynamics are controlled by conformation-selective inhibitors of ERK2. *Proceedings of the National Academy of Sciences*. 2019;116(31):15463-15468.

[31] Halder A, Giri A, Cordeiro M. Multi-Target Chemometric Modelling, Fragment Analysis and Virtual Screening with ERK Inhibitors as Potential Anticancer Agents. *Molecules*. 2019; 24(21):3909.

[32] Sahu V, Nigam L, Agnihotri V et al. Diagnostic Significance of p38 Isoforms (p38α, p38β, p38γ, p38δ) in Head and Neck Squamous Cell Carcinoma: Comparative Serum Level Evaluation and Design of Novel Peptide Inhibitor Targeting the Same. *Cancer Res Treat*. 2019;51(1):313-325.

[33] Zhang X, Chen C, Li H et al. Targeting the non-ATP-binding pocket of the MAP kinase p38γ mediates a novel mechanism of cytotoxicity in cutaneous T-cell lymphoma (CTCL). *FEBS Lett.* 2021;595(20):2570-2592.

[34] Martínez-Limón A, Joaquin M, Caballero M, Posas F, de Nadal E. The p38 Pathway: From Biology to Cancer Therapy. *Int J Mol Sci.* 2020;21(6):1913.

[35] Williams N, Bamert R, Patel O et al. Dissecting Specificity in the Janus Kinases: The Structures of JAK-Specific Inhibitors Complexed to the JAK1 and JAK2 Protein Tyrosine Kinase Domains. *J Mol Biol*. 2009; 387(1):219-232.

[36] Lin T, HuangFu W, Chao M et al. A Novel Selective JAK2 Inhibitor Identified Using Pharmacological Interactions. *Front Pharmacol.* 2018;9.

[37] Backman TW, Cao Y, Girke T. ChemMine tools: an online service for analyzing and clustering small molecules. *Nucl Acids Res*. 2011; 39(Web Server issue): W486-W491. doi:10.1093/nar/gkr320

[38] Filimonov D, Lagunin A, Gloriozova T et al. Prediction of the Biological Activity Spectra of Organic Compounds Using the Pass Online Web Resource. *Chem Heterocycl Compd*. 2014;50(3): 444- 457.

[39] Daina A, Michielin O and Zoete V. SwissTargetPrediction: updated data and new features for efficient prediction of protein targets of small molecules, *Nucl Acids Res*. 2019;47(Web Server issue): W357–W364.

[40] http://moltarpred.marseille.inserm.fr/ (9\11\2021).

[41] Keiser MJ, Roth BL, Armbruster BN, Ernsberger P, Irwin JJ, Shoichet BK. Relating protein pharmacology by ligand chemistry. *Nat Biotech.* 2007;25 (2),197- 206.

[42] Wang Z, Liang L, and Yin Z, Lin J. Improving chemical similarity ensemble approach in target prediction. *J Cheminform*. 2016; 8(1). doi:10.1186/s13321-016-0130-x

[43] Irwin J, Gaskins G, Sterling T, Mysinger M, Keiser M. Predicted Biological Activity of Purchasable Chemical Space. *J Chem Inf Model*. 2018;58(1):148-164. doi:10.1021/acs.jcim.7b00316

[44] H.M. Berman, J. Westbrook, Z. Feng, G. Gilliland, T.N. Bhat, H. Weissig, I.N. Shindyalov, P.E. Bourne. The Protein Data Bank. *Nucl Acids Res*. 2000; 28:235-242.

[45] Molecular Operating Environment (MOE), 2019.01; Chemical Computing Group ULC, 1010 Sherbooke St. West, Suite #910, Montreal, QC, Canada, H3A 2R7, 2021

[46] Daina, A., Michielin, O., and Zoete, V. SwissADME: a free web tool to evaluate pharmacokinetics, drug-likeness and medicinal chemistry friendliness of small molecules. *Scientific reports.* 2017;7(1): 1-13.

[47] Pires, D. E., Blundell, T. L., and Ascher, D. B. pkCSM: predicting small-molecule pharmacokinetic and toxicity properties using graph-based signatures. *J Med Chem*. 2015; 58(9):4066-4072.

[48] Leeson P.D, and Young R.J. Molecular Property Design: Does Everyone Get It? *ACS Med Chem Lett.* 2015;6:722-725.

[49] Bickerton GR, Paolini GV, Besnard J, Muresan S, Hopkins AL. Quantifying the chemical beauty of drugs. *Nat Chem*. 2012;4(2):90-8.

[50] Veber DF, Johnson SR, Cheng H-Y, Smith BR, Ward KW, Kopple KD. Molecular properties that influence the oral bioavailability of drug candidates. *J Med Chem*. 2002; 45(12):2615–2623.

[51] Capuzzi S, Politi R, Isayev O, Farag S, Tropsha A. QSAR Modeling of Tox21 Challenge Stress Response and Nuclear Receptor Signaling Toxicity Assays. *Front Environ Sci*. 2016;4.

[52] Lagunin A.A., Dubovskaja V.I., Rudik A.V., Pogodin P.V., Druzhilovskiy D.S., Gloriozova T.A., Filimonov D.A., Sastry G.N., Poroikov V.V. CLC-Pred: a freely available web-service for in silico prediction of human cell line cytotoxicity for drug-like compounds. *PLOS One*. 2018;13(1).

[53] Banerjee, P., Eckert, A. O., Schrey, A. K., and Preissner, R. ProTox-II: a webserver for the prediction of toxicity of chemicals. *Nucleic acids Res*. 2018;46(W1): W257-W263.

[54] Tian W, Wang Z, Yuan B, Bao Y. Calycosin induces apoptosis in osteosarcoma cell line via ERβ-mediated PI3K/Akt signaling pathways. *Mol Med Rep*. 2020;21:2349-2356.

[55] Benvenuto M, Albonici L, Focaccetti C et al. Polyphenol-Mediated Autophagy in Cancer: Evidence of In Vitro and In Vivo Studies. *Int J Mol Sci*. 2020; 21(18): 6635.

[56] Srinivasulu C, Ramgopal M, Ramanjaneyulu G, Anuradha C, Suresh Kumar C. Syringic acid (SA) –A Review of Its Occurrence, Biosynthesis, Pharmacological and Industrial Importance. *Biomedicine & Pharmacotherapy*. 2018;108:547-557.

[57] Jung H, Song Y, Lim C, Park E. Anti-angiogenic, anti-inflammatory and anti-nociceptive activities of vanillyl alcohol. *Arch Pharm Res*. 2008; 31(10): 1275-1279.

[58] Carvalho A, Andrade L, de Sousa É, de Sousa D. Antitumor Phenylpropanoids Found in Essential Oils. *Biomed Res Int*. 2015;2015:1-21.

[59] Maria Pia GD, Sara F, Mario F, Lorenza S. Biological Effects of Licochalcones. *Mini-Reviews Med Chem*. 2018;19(8):647-656.

[60] Behbahani M, Moghaddam M. Study of Anticancer Activity of Pratensein and Pratensein Glycoside Isolated from Cuscuta kotchiana. *J Mol Biol Res*. 2020;10(1): 73.

[61] Wang GM, Wang X, Zhu JM, et al. Docking-based structural splicing and reassembly strategy to develop novel deazapurine derivatives as potent B-Raf^{V600E} inhibitors. *Acta Pharmacol Sin*. 2017;38(7):1059-1068.

[62] Ramurthy S, Taft BR, Aversa RJ, et al. Design and Discovery of N-(3-(2-(2-Hydroxyethoxy)-6-morpholinopyridin-4-yl)-4-methylphenyl)-2 (trifluoromethyl) isonicotinamide, a Selective, Efficacious, and Well-Tolerated RAF Inhibitor Targeting RAS Mutant Cancers: The Path to the Clinic. *J Med Chem*. 2020;63(5): 2013-2027.

[63] L. Alicea-Velazquez N, J. Boggon T. The Use of Structural Biology in Janus Kinase Targeted Drug Discovery. *Curr Drug Targets*. 2011;12(4):546-555.

[64] Sanachai K, Mahalapbutr P, Choowongkomon K, Poo-arporn R, Wolschann P, Rungrotmongkol T. Insights into the Binding Recognition and Susceptibility of Tofacitinib toward Janus Kinases. *ACS Omega*. 2020; 5(1):369-377.

[65] Hornakova T, Springuel L, Devreux J et al. Oncogenic JAK1 and JAK2-activating mutations resistant to ATP-competitive inhibitors. *Haematologica*. 2011;96(6):845-853.

[66] Andraos R, Qian Z, Bonenfant D et al. Modulation of Activation-Loop Phosphorylation by JAK Inhibitors Is Binding Mode Dependent. *Cancer Discov*. 2012;2(6):512-523.

[67] Lucet I, Fantino E, Styles M et al. The structural basis of Janus kinase 2 inhibition by a potent and specific pan-Janus kinase inhibitor. *Blood*. 2006;107(1):176-183.

[68] Kinoshita T, Yoshida I, Nakae S et al. Crystal structure of human mono-phosphorylated ERK1 at Tyr204. *Biochem Biophys Res Commun*. 2008;377(4): 1123-1127.

[69] Chaikuad A, M C Tacconi E, Zimmer J et al. A unique inhibitor binding site in ERK1/2 is associated with slow binding kinetics. *Nat Chem Biol*. 2014;10(10):853-860.

[70] Bellon S, Fitzgibbon M, Fox T, Hsiao H, Wilson K. The structure of phosphorylated P38γ is monomeric and reveals a conserved activation-loop conformation. *Structure*. 1999;7(9):1057-1065.

[71] Aoto P, Stanfield R, Wilson I, Dyson H, Wright P. A Dynamic Switch in Inactive p38γ Leads to an Excited State on the Pathway to an Active Kinase. *Biochemistry*. 2019;58(51):5160-5172.

[72] Martin YC. A bioavailability score. *J Med Chem*. 2005;48(9):3164–3170.

[73] Finch, A., & Pillans, P. P-glycoprotein and its role in drug-drug interactions. *Australian Prescriber*. 2014;37(4):137–139.

[74] Weiss, N., Miller, F., Cazaubon, S., & Couraud, P.-O. The blood brain barrier in brain homeostasis and neurological diseases. *Biochimica et Biophysica Acta*. 2009; 1788(4):842–857.

[75] Rodrigues T. A Toolbox for the Identification of Modes of Action of Natural Products. *Prog Chem Org Nat Prod. 110*. 2019:73-97.

[76] Prieto-Martínez F, Norinder U, Medina-Franco J. Cheminformatics Explorations of Natural Products. *Prog Chem Org Nat Prod. 110*. 2019:1-35.

[77] Cheng, F., Li, W., Liu, G., & Tang, Y. In silico ADMET prediction: Recent advances, current challenges and future trends. *Curr Top Med Chem*. 2013:13(11),1273–1289.

7. APPENDIXES

Appendix A (PASS online)

Compounds	Gluconate 2-dehydrogenase (acceptor) inhibitor	TP53 expression enhancer	Preneoplastic conditions treatment	GST A substrate	GST M substrate	Lipid peroxidase inhibitor	JAK2 expression inhibitor	NOS2 expression inhibitor	TNF expression inhibitor
N-G-1	0,765	0,600	0,772	0,717	0,687	0,670	0,679	0,632	0,633
N-G-2	0,833	0,788	0,903	0,768	0,673	0,618	0,915	0,560	0,819
N-G-3	0,797	0,724	0,803	0,633	0,543	0,501	0,873	0,618	0,525
N-G-4	0,737	0,608	0,777	0,532	0,572	0,711	0,886	0,465	0,546
N-G-5	0,833	0,671	0,676	0,778	0,777	0,598	0,369	0,649	0,764
N-G-6	0,825	0,649	0,748	0,632	0,437	0,383	0,819	0,545	0,437
N-G-7	0,772	0,766	0,879	0,719	0,730	0,613	0,942	0,724	0,852
N-G-8	0,496	0,549	0,637	0,622	0,439	0,729	0,710	0,378	0,433
N-G-9	0,794	0,713	0,905	0,537	0,535	0,564	0,871	0,485	0,670
N-G-10	0,780	0,681	0,798	0,584	0,542	0,467	0,883	0,531	0,691
N-G-11	0,927	0,745	0,905	0,861	0,888	0,582	0,953	0,801	0,847
N-G-12	0,759	0,797	0,571	0,314	0,541	0,734	0,837	0,567	0,453
N-G-13	0,747	0,686	0,861	0,638	0,630	0,535	0,876	0,527	0,638
N-G-14	0,823	0,652	0,794	0,560	0,472	0,426	0,821	0,418	0,758
N-G-15	0,759	0,757	0,873	0,730	0,707	0,603	0,828	0,544	0,754
N-G-16	0,698	0,755	0,351		0,246	0,501	0,964	0,505	0,568
N-G-17	0,646	0,536	0,683	0,304	0,395	0,371	0,709	0,426	0,483
N-G-18	0,747	0,720	0,796	0,523	0,549	0,587	0,876	0,591	0,618
N-G-19	0,921	0,744	0,841	0,655	0,641	0,602	0,870	0,600	0,715
N-G-20	0,768	0,680	0,740	0,594	0,468	0,463	0,845	0,474	0,618
N-G-21	0,772	0,739	0,814	0,544	0,585	0,614	0,924	0,606	0,723
N-G-22	0,831	0,775	0,878	0,668	0,560	0,517	0,836	0,512	0,647
N-G-23	0,916	0,723	0,824	0,700	0,609	0,462	0,922	0,597	0,613
N-G-24	0,822	0,693	0,950	0,751	0,802	0,627	0,978	0,674	0,901
N-G-25	0,706	0,830	0,834	0,830	0,864	0,438	0,925	0,540	0,634
N-G-26	0,715	0,735	0,867	0,711	0,661	0,560	0,919	0,595	0,804
N-G-27	0,755	0,584	0,593	0,480	0,431	0,339	0,798	0,389	0,549
N-G-28	0,801	0,699	0,816	0,771	0,574	0,507	0,747	0,405	0,580
N-G-29	0,788	0,723	0,746	0,642	0,468	0,496	0,832	0,559	0,451
N-G-30	0,797	0,760	0,892	0,646	0,625	0,726	0,811	0,577	0,678
N-G-31	0,658	0,633	0,859	0,468	0,459	0,420	0,801	0,458	0,589
N-G-32	0,646	0,536	0,683	0,304	0,395	0,371	0,709	0,426	0,483
N-G-33	0,765	0,725	0,848	0,598	0,622	0,497	0,888	0,548	0,620
N-G-34	0,757	0,652	0,872	0,531	0,548	0,584	0,871	0,501	0,628
N-G-35	0,727	0,652	0,825	0,469	0,416	0,631	0,784	0,453	0,605
N-G-36	0,770	0,541	0,706	0,568	0,498	0,580	0,848	0,387	0,447
N-G-37	0,525	0,711	0,786	0,767	0,614	0,616	0,868	0,620	0,749
N-G-38	0,706	0,657	0,754	0,584	0,569	0,697	0,882	0,640	0,563
N-G-39	0,727	0,857	0,507	0,244	0,464	0,797	0,792	0,612	0,492
N-G-40	0,825	0,686	0,883	0,721	0,720	0,403	0,941	0,589	0,788
N-G-41	0,822	0,744	0,874	0,555	0,573	0,405	0,913	0,599	0,639
N-G-42	0,688	0,647	0,727	0,469	0,460	0,543	0,827	0,459	0,736
N-G-43	0,672	0,716	0,783	0,670	0,670	0,375	0,839	0,444	0,478
N-G-44	0,823	0,652	0,794	0,560	0,472	0,426	0,821	0,418	0,758
N-G-45	0,902	0,572	0,479	0,569	0,324	0,468	0,546	0,330	0,587
N-G-46	0,794	0,713	0,905	0,537	0,535	0,564	0,871	0,485	0,670
N-G-47	0,833	0,788	0,903	0,768	0,673	0,618	0,915	0,560	0,819
N-G-48	0,864	0,738	0,851	0,694	0,482	0,422	0,784	0,457	0,581
N-G-49	0,737	0,608	0,777	0,532	0,572	0,711	0,886	0,465	0,546

Appendix A (continued)

Compounds	Free radical scavenger	Prostaglandin-A1 DELTA-isomerase inhibitor	Antimutagenic	Caspase 3 stimulant	GST P substrate	GST P1-1 substrate	Nitric oxide antagonist	Apoptosis agonist
N-G-1	0,617	0,602	0,597	0,575	0,546	0,511	0,494	0,518
N-G-2	0,731	0,431	0,900	0,749	0,541	0,521	0,324	0,702
N-G-3	0,563	0,309	0,878	0,873	0,491	0,467	0,335	0,743
N-G-4	0,546	0,387	0,618	0,754	0,379	0,350	0,247	0,705
N-G-5	0,766	0,294	0,814	0,747	0,184	0,188	0,346	0,803
N-G-6	0,536	0,362	0,807	0,840	0,465	0,438	0,297	0,726
N-G-7	0,717	0,365	0,805	0,778	0,538	0,517	0,329	0,733
N-G-8	0,481	0,380	0,469	0,651	0,356	0,305	0,189	0,588
N-G-9	0,643	0,731		0,640	0,358	0,330	0,258	0,512
N-G-10	0,560	0,446	0,609	0,658	0,384	0,356	0,284	0,547
N-G-11	0,704	0,322	0,848	0,819	0,654	0,640	0,280	0,760
N-G-12	0,506	0,221	0,864	0,603	0,220	0,216	0,454	0,779
N-G-13	0,528	0,477	0,783	0,734	0,393	0,364	0,249	0,482
N-G-14	0,482		0,575	0,439	0,386	0,351	0,220	0,405
N-G-15	0,743	0,344	0,851	0,551	0,676	0,663	0,475	0,711
N-G-16	0,440		0,335	0,737			0,253	0,484
N-G-17	0,330	0,249	0,372	0,582	0,202	0,192	0,207	0,422
N-G-18	0,579	0,394	0,816	0,787	0,364	0,325	0,270	0,562
N-G-19	0,551	0,376	0,796	0,659	0,364	0,336	0,315	0,488
N-G-20	0,547	0,439	0,573	0,534	0,323	0,299	0,282	0,578
N-G-21	0,546	0,447	0,730	0,756	0,375	0,346	0,271	0,600
N-G-22	0,612	0,530	0,748	0,634	0,393	0,364	0,266	0,471
N-G-23	0,540	0,342	0,791	0,768	0,784	0,772	0,362	0,663
N-G-24	0,785	0,269	0,834	0,719	0,813	0,803	0,356	0,861
N-G-25	0,487	0,276	0,752	0,945	0,765	0,754	0,277	0,871
N-G-26	0,565	0,281	0,796	0,784	0,529	0,491	0,305	0,590
N-G-27	0,340	0,454	0,356	0,529	0,200	0,199	0,138	0,326
N-G-28	0,516	0,758	0,818	0,401	0,413	0,384	0,249	0,363
N-G-29	0,652	0,304	0,868	0,816	0,459	0,432	0,336	0,794
N-G-30	0,631	0,438	0,789	0,544	0,420	0,392	0,350	0,538
N-G-31	0,439	0,303	0,523	0,543	0,315	0,269	0,194	0,436
N-G-32	0,330	0,249	0,372	0,582	0,202	0,192	0,207	0,422
N-G-33	0,529	0,456	0,769	0,761	0,366	0,338	0,284	0,516
N-G-34	0,575	0,542	0,700	0,728	0,356	0,329	0,263	0,521
N-G-35	0,539	0,462	0,628	0,657	0,318	0,271	0,243	0,440
N-G-36	0,503	0,387	0,435	0,647	0,285	0,267	0,175	0,889
N-G-37	0,643	0,336	0,715	0,698	0,520	0,480	0,275	0,648
N-G-38	0,737	0,276	0,650	0,805	0,389	0,361	0,640	0,829
N-G-39	0,593		0,896	0,660	0,178	0,181	0,590	0,844
N-G-40	0,562	0,269	0,736	0,626	0,632	0,618	0,253	0,799
N-G-41	0,710	0,353	0,718	0,539	0,675	0,662	0,406	0,625
N-G-42	0,518	0,315	0,486	0,483	0,361	0,304	0,216	0,513
N-G-43	0,390	0,324	0,650	0,700	0,530	0,509	0,220	0,435
N-G-44	0,482	0,475	0,575	0,439	0,386	0,351	0,220	0,405
N-G-45	0,408	0,401	0,245	0,646			0,243	0,371
N-G-46	0,643	0,731	0,834	0,640	0,358	0,330	0,258	0,512
N-G-47	0,731	0,431	0,900	0,749	0,541	0,521	0,324	0,702
N-G-48	0,520	0,638	0,630	0,570	0,350	0,323	0,223	0,394
N-G-49	0,546	0,387	0,618	0,754	0,379	0,350	0,247	0,705

Appendix A (continued)

Compounds	Platelet derived growth factor receptor kinase inhibitor	Histone acetyltransferase inhibitor	MAP kinase stimulant	Prostaglandin-E2 9-reductase inhibitor	Caspase 8 stimulant	Histidine kinase inhibitor	Anticarcinogenic	Myc inhibitor
N-G-1	0,509	0,470	0,482	0,461	0,433	0,390	0,364	0,350
N-G-2		0,555	0,709	0,464	0,551	0,400	0,616	0,357
N-G-3		0,457	0,735	0,298	0,598	0,331	0,459	0,476
N-G-4		0,284	0,744	0,240	0,525	0,473	0,388	0,307
N-G-5		0,305	0,737	0,235	0,487	0,317	0,611	0,313
N-G-6		0,350	0,663	0,285	0,566		0,362	0,492
N-G-7		0,524	0,806	0,324	0,545	0,344	0,408	0,350
N-G-8		0,432	0,597	0,195	0,449	0,443	0,353	0,278
N-G-9		0,619	0,717	0,702	0,573	0,405	0,413	0,358
N-G-10		0,470	0,764	0,510	0,519	0,467	0,341	0,343
N-G-11	0,400	0,584	0,756	0,241	0,491	0,315	0,609	0,319
N-G-12		0,170	0,794	0,167	0,536	0,937	0,703	0,327
N-G-13	0,346	0,561	0,781	0,435	0,566	0,435	0,367	0,390
N-G-14		0,333	0,608	0,389	0,505	0,433	0,370	0,464
N-G-15	0,559	0,614	0,564	0,454	0,536	0,389	0,475	0,386
N-G-16			0,547	0,875	0,521	0,259	0,496	0,444
N-G-17		0,210	0,578		0,487	0,251	0,566	0,337
N-G-18		0,357	0,720	0,342	0,649	0,372	0,469	0,392
N-G-19	0,854	0,399	0,728	0,257	0,478	0,360	0,419	0,346
N-G-20		0,390	0,691	0,513	0,474	0,473	0,341	0,350
N-G-21	0,379	0,397	0,838	0,438	0,606	0,407	0,402	0,398
N-G-22		0,414	0,733	0,705	0,608	0,706	0,453	0,389
N-G-23		0,502	0,810	0,324	0,610	0,342	0,402	0,370
N-G-24		0,703	0,760	0,248	0,461	0,388	0,649	0,299
N-G-25		0,362	0,735	0,196	0,498	0,385	0,498	0,286
N-G-26		0,565	0,711	0,332	0,550	0,298	0,595	0,369
N-G-27		0,227	0,721	0,439	0,470		0,270	0,431
N-G-28		0,501	0,652	0,705	0,482	0,553	0,412	0,367
N-G-29		0,378	0,660	0,301	0,553	0,326	0,459	0,488
N-G-30	0,630	0,471	0,647	0,350	0,507	0,438	0,415	0,359
N-G-31		0,344	0,691	0,379	0,506	0,307	0,477	0,407
N-G-32		0,210	0,578		0,487	0,251	0,566	0,337
N-G-33	0,286	0,377	0,826	0,401	0,644	0,410	0,394	0,471
N-G-34		0,567	0,717	0,453	0,608	0,376	0,364	0,392
N-G-35	0,268	0,684	0,630	0,386	0,511	0,323	0,341	0,339
N-G-36		0,218	0,660	0,271	0,461	0,493	0,353	0,391
N-G-37		0,624	0,673	0,237	0,461	0,326	0,367	0,302
N-G-38		0,511	0,644	0,315	0,351	0,457	0,382	0,219
N-G-39			0,744		0,570	0,954	0,781	0,329
N-G-40		0,503	0,682	0,187	0,432	0,289	0,455	0,284
N-G-41	0,680	0,475	0,733	0,241	0,472	0,359	0,495	0,330
N-G-42		0,344	0,610	0,268	0,504	0,331	0,421	0,475
N-G-43	0,251	0,277	0,707	0,208	0,484	0,430	0,341	0,316
N-G-44		0,333	0,608	0,389	0,505	0,433	0,370	0,464
N-G-45	0,850	0,159	0,658		0,481	0,235	0,251	
N-G-46		0,619	0,717	0,702	0,573	0,405	0,413	0,358
N-G-47		0,555	0,709	0,464	0,551	0,400	0,616	0,357
N-G-48		0,348	0,675	0,735	0,579	0,675	0,381	0,396
N-G-49		0,284	0,744	0,240	0,525	0,473	0,388	0,307

Appendix A (continued)

Compounds	AR expression inhibitor	Transcription factor NF kappa B inhibitor	BRAF expression inhibitor	Endothelial growth factor antagonist	G-protein-coupled receptor kinase inhibitor	Beta-adrenergic receptor kinase inhibitor	Pin1 inhibitor	DNA polymerase I inhibitor
N-G-1	0,339	0,264	0,273	0,297	0,332	0,332	0,340	0,277
N-G-2	0,627	0,407	0,395	0,386	0,641	0,641	0,562	0,253
N-G-3	0,608	0,488	0,126	0,376	0,807	0,807	0,607	0,249
N-G-4	0,582	0,378	0,176	0,377	0,753	0,753	0,617	0,258
N-G-5	0,527	0,399	0,219	0,375	0,427	0,427	0,567	0,237
N-G-6	0,529	0,405	0,162	0,388	0,811	0,811	0,585	
N-G-7	0,702	0,520	0,296	0,414	0,539	0,539	0,612	0,252
N-G-8	0,465	0,451	0,185	0,290	0,882	0,882	0,479	0,237
N-G-9	0,594	0,296	0,172	0,393	0,698	0,698	0,606	0,289
N-G-10	0,666	0,290	0,188	0,424	0,388	0,388	0,631	0,292
N-G-11	0,697	0,422	0,230	0,479	0,407	0,407	0,556	0,229
N-G-12	0,871	0,332		0,264			0,680	0,245
N-G-13	0,559	0,246	0,230	0,490	0,447	0,447	0,674	0,302
N-G-14	0,560	0,133	0,183	0,370	0,562	0,562	0,507	0,303
N-G-15	0,570	0,452	0,217	0,382	0,406	0,406	0,428	0,271
N-G-16	0,846	0,255		0,216	0,256	0,256	0,398	0,315
N-G-17	0,393	0,155		0,383	0,290	0,290	0,467	0,240
N-G-18	0,529	0,288	0,148	0,416	0,617	0,617	0,654	0,354
N-G-19	0,551	0,272	0,145	0,747	0,309	0,309	0,620	0,260
N-G-20	0,664	0,278	0,243	0,487	0,392	0,392	0,620	0,268
N-G-21	0,634	0,356	0,270	0,685	0,541	0,541	0,660	0,318
N-G-22	0,544	0,207	0,206	0,447	0,515	0,515	0,668	0,288
N-G-23	0,639	0,375	0,152	0,349	0,551	0,551	0,630	0,235
N-G-24	0,810	0,560	0,193	0,343	0,425	0,425	0,534	
N-G-25	0,675	0,289	0,447	0,302	0,419	0,419	0,542	
N-G-26	0,598	0,458	0,181	0,370	0,675	0,675	0,589	0,276
N-G-27	0,526	0,189	0,172	0,411	0,323	0,323	0,631	
N-G-28	0,494	0,133	0,413	0,361	0,749	0,749	0,611	0,269
N-G-29	0,605	0,474	0,163	0,432	0,810	0,810	0,596	
N-G-30	0,504	0,267	0,193	0,433	0,319	0,319	0,522	0,292
N-G-31	0,492	0,177		0,356	0,401	0,401	0,630	0,294
N-G-32	0,393	0,155		0,383	0,290	0,290	0,467	0,240
N-G-33	0,619	0,281	0,196	0,481	0,417	0,417	0,715	0,291
N-G-34	0,561	0,350	0,141	0,418	0,628	0,628	0,606	0,316
N-G-35	0,496	0,547	0,115	0,355	0,655	0,655	0,580	0,266
N-G-36	0,566	0,253	0,176	0,413	0,755	0,755	0,657	0,233
N-G-37	0,612	0,559	0,260	0,311	0,788	0,788	0,492	0,230
N-G-38	0,648	0,497	0,170	0,259	0,359	0,359	0,542	
N-G-39	0,905	0,471		0,308			0,616	0,275
N-G-40	0,642	0,295	0,160	0,318	0,337	0,337	0,478	
N-G-41	0,596	0,406	0,122	0,552	0,305	0,305	0,638	0,260
N-G-42	0,524	0,141	0,107	0,354	0,598	0,598	0,534	0,323
N-G-43	0,575	0,188	0,227	0,359	0,316	0,316	0,605	0,247
N-G-44	0,560	0,133	0,183	0,370	0,562	0,562	0,507	0,303
N-G-45	0,242	0,130	0,187	0,422			0,487	
N-G-46	0,594	0,296	0,172	0,393	0,698	0,698	0,606	0,289
N-G-47	0,627	0,407	0,395	0,386	0,641	0,641	0,562	0,253
N-G-48	0,473	0,167	0,303	0,459	0,582	0,582	0,664	0,247
N-G-49	0,582	0,378	0,176	0,377	0,753	0,753	0,617	0,258

Appendix A (continued)

Compounds	Leukopoiesis inhibitor	Toll-Like receptor antagonist	Transcription factor inhibitor	Tumour necrosis factor alpha release inhibitor	Glutamate decarboxylase inhibitor	Antineoplastic (breast cancer)	Transcription factor NF kappa A inhibitor	Antineoplastic (cervical cancer)
N-G-1	0,288	0,166	0,243	0,200	0,162	0,210	0,228	0,151
N-G-2	0,431		0,329		0,263	0,467	0,338	0,308
N-G-3	0,434		0,410	0,171	0,202	0,419	0,351	0,276
N-G-4	0,443		0,379		0,191	0,466	0,329	0,139
N-G-5	0,335		0,334		0,175	0,528	0,325	0,323
N-G-6	0,476		0,377	0,270	0,151	0,402	0,316	0,315
N-G-7	0,427		0,494	0,160	0,148	0,463	0,377	0,318
N-G-8	0,312		0,425		0,146	0,365	0,341	
N-G-9	0,570		0,304		0,513	0,298	0,371	0,155
N-G-10	0,582		0,415	0,176	0,225	0,413	0,382	0,264
N-G-11	0,348		0,339		0,153	0,552	0,342	0,512
N-G-12	0,300		0,361		0,097	0,565	0,294	0,355
N-G-13	0,499		0,254	0,158	0,183	0,252	0,366	0,181
N-G-14	0,443				0,360		0,292	
N-G-15	0,254		0,334		0,134	0,256	0,268	0,148
N-G-16	0,317		0,229			0,563	0,353	0,163
N-G-17	0,777					0,231	0,278	0,115
N-G-18	0,477		0,296		0,172	0,384	0,357	0,271
N-G-19	0,414		0,253	0,124	0,189	0,242	0,316	0,400
N-G-20	0,605		0,389	0,138	0,229	0,401	0,357	0,280
N-G-21	0,571		0,406	0,163	0,185	0,399	0,387	0,267
N-G-22	0,558		0,190		0,478	0,181	0,333	0,113
N-G-23	0,395		0,340	0,174	0,191	0,411	0,341	0,320
N-G-24	0,304		0,504		0,184	0,547	0,310	0,309
N-G-25	0,321		0,239		0,203	0,279	0,316	0,331
N-G-26	0,364		0,379		0,128	0,357	0,400	0,280
N-G-27	0,488	0,137	0,257	0,215	0,105	0,282	0,368	0,190
N-G-28	0,514	0,124	0,166		0,603		0,363	
N-G-29	0,465		0,384	0,136	0,206	0,410	0,327	0,292
N-G-30	0,305	0,121	0,255	0,137	0,194	0,227	0,288	0,254
N-G-31	0,381	0,122	0,181	0,131	0,126	0,179	0,398	0,103
N-G-32	0,777					0,231	0,278	0,115
N-G-33	0,588		0,305	0,171	0,192	0,302	0,371	0,229
N-G-34	0,647		0,382	0,145	0,248	0,349	0,404	0,259
N-G-35	0,652	0,145	0,519	0,140	0,177	0,309	0,357	0,164
N-G-36	0,510		0,295		0,173	0,437	0,298	0,177
N-G-37	0,307		0,535	0,159	0,120	0,391	0,379	0,179
N-G-38	0,283		0,449		0,183	0,597	0,320	0,537
N-G-39	0,252		0,468	0,131	0,092	0,602	0,267	0,376
N-G-40	0,293		0,245		0,146	0,727	0,307	0,406
N-G-41	0,423		0,375	0,134	0,202	0,250	0,305	0,156
N-G-42	0,374				0,195	0,174	0,348	
N-G-43	0,379				0,250		0,291	0,140
N-G-44	0,443				0,360		0,292	
N-G-45			0,210		0,172		0,231	0,345
N-G-46	0,570		0,304		0,513	0,298	0,371	0,155
N-G-47	0,431		0,329		0,263	0,467	0,338	0,308
N-G-48	0,597	0,119		0,137	0,358		0,307	0,107
N-G-49	0,443		0,379		0,191	0,466	0,329	0,139

Appendix A (continued)

Compounds	Antineoplastic (endocrine cancer)	Phosphomevalonate kinase inhibitor	Tubulin antagonist	Nucleotidase inhibitor	Glutaminase inhibitor	Antineoplastic (thyroid cancer)	Antineoplastic (bone cancer)	Antineoplastic (non-Hodgkin's lymphoma)
N-G-1	0,171	0,115	0,121	0,126	0,180	0,161	0,205	0,295
N-G-2		0,482	0,283	0,137	0,335	0,163	0,219	0,424
N-G-3	0,172	0,170	0,344		0,214	0,189	0,206	
N-G-4		0,619	0,480		0,287		0,272	
N-G-5		0,267	0,238		0,274	0,160	0,211	0,387
N-G-6	0,174	0,115	0,315		0,201	0,188		
N-G-7		0,297	0,514		0,259	0,165	0,230	0,420
N-G-8		0,523	0,248		0,392	0,150	0,261	
N-G-9		0,320	0,254	0,194	0,594	0,168	0,235	0,388
N-G-10	0,187	0,171	0,347		0,316	0,176	0,222	0,432
N-G-11		0,264	0,272		0,313	0,163	0,208	0,426
N-G-12		0,129	0,327		0,178		0,274	
N-G-13	0,167	0,184	0,248		0,293	0,151	0,242	0,382
N-G-14		0,203	0,169	0,153	0,346	0,176	0,211	0,348
N-G-15		0,135	0,154		0,176		0,206	0,352
N-G-16			0,371			0,228	0,214	
N-G-17	0,187	0,112	0,172		0,162	0,173		0,336
N-G-18		0,205	0,271	0,120	0,322	0,160	0,251	0,467
N-G-19		0,164	0,203		0,351		0,209	0,356
N-G-20	0,205	0,138	0,383		0,309	0,172	0,192	0,444
N-G-21		0,197	0,447		0,352	0,178	0,246	0,415
N-G-22		0,233	0,231	0,150	0,390	0,150	0,225	0,362
N-G-23	0,189	0,233	0,521		0,254	0,208	0,232	0,316
N-G-24		0,286	0,234		0,253	0,153	0,209	0,375
N-G-25	0,175	0,292	0,288		0,202	0,179	0,253	0,320
N-G-26		0,313	0,384		0,305	0,159	0,227	0,442
N-G-27	0,155	0,093	0,176		0,227		0,258	0,315
N-G-28		0,344		0,226	0,618		0,206	0,400
N-G-29	0,186	0,140	0,377		0,208	0,187		
N-G-30		0,138	0,151		0,279	0,171	0,227	0,327
N-G-31		0,171	0,167		0,284		0,246	0,378
N-G-32	0,187	0,112	0,172		0,162	0,173		0,336
N-G-33	0,176	0,181	0,327		0,305	0,157	0,244	0,431
N-G-34		0,233	0,365	0,131	0,423	0,195	0,219	0,366
N-G-35	0,165	0,203	0,234	0,111	0,507	0,191	0,219	0,401
N-G-36		0,411	0,502		0,305		0,257	
N-G-37		0,260	0,326		0,351	0,165	0,216	0,391
N-G-38	0,166	0,229	0,353		0,202	0,184		0,319
N-G-39		0,114	0,386		0.171		0,272	
N-G-40		0,257	0,186		0,236			0,320
N-G-41		0,171	0,179		0,297	0,171	0,206	0,288
N-G-42		0,176	0,183		0,316	0,173	0,220	0,376
N-G-43	0,167	0,186	0,187		0,233	0,161	0,253	
N-G-44		0,203	0,169	0,153	0,346	0,176	0,211	0,348
N-G-45			0,179		0,282			0,339
N-G-46		0,320	0,254	0,194	0,594	0,168	0,235	0,388
N-G-47		0,482	0,283	0,137	0,335	0,163	0,219	0,424
N-G-48		0,201	0,184	0,163	0,410		0,212	0,297
N-G-49		0,619	0,480		0,287		0,272	

Appendix A (continued)

Compounds	Prostaglandin F2 alpha antagonist	Antineoplastic (liver cancer)	Aspartate kinase inhibitor	Antineoplastic	Dual specificity protein phosphatase VHR inhibitor	Glutamate dehydrogenase (NADP+) inhibitor	Prostaglandin EP2 antagonist	Adenylate kinase inhibitor
N-G-1	0,063	0,175	0,115	0,241	0,062	0,081	0,043	0,127
N-G-2	0,051	0,241	0,121	0,601		0,133	0,055	0,148
N-G-3		0,239		0,461	0,057		0,029	0,135
N-G-4		0,190	0,115	0,636	0,050	0,160		0,136
N-G-5	0,045	0,194		0,672		0,065		
N-G-6		0,245		0,417			0,037	0,144
N-G-7	0,046	0,205	0,097	0,679				0,121
N-G-8			0,148	0,448		0,192		0,148
N-G-9		0,250	0,193	0,326	0,079	0,207		0,258
N-G-10		0,234	0,117	0,404	0,075			0,132
N-G-11	0,043	0,216		0,773		0,078		0,146
N-G-12				0,708				
N-G-13	0,042	0,208	0,126	0,222	0,071	0,072		0,129
N-G-14	0,042		0,134			0,090		0,149
N-G-15	0,015	0,230		0,338	0,066	0,062	0,019	0,152
N-G-16				0,731				
N-G-17		0,183		0,574	0,056			
N-G-18		0,258	0,121	0,509	0,062	0,082		0,157
N-G-19		0,190	0,100	0,383	0,055	0,090		0,143
N-G-20		0,213	0,134	0,513	0,079	0,076		0,151
N-G-21		0,244	0,117	0,478	0,065	0,070		0,145
N-G-22	0,043	0,217	0,145		0,054	0,118		0,225
N-G-23		0,220		0,617	0,057			0,143
N-G-24	0,045	0,193		0,678				
N-G-25	0,042	0,202	0,113	0,551		0,060		0,150
N-G-26	0,046	0,232	0,107	0,674		0,069		0,118
N-G-27		0,160	0,118					
N-G-28	0,058	0,165	0,214		0,050	0,262	0,070	0,252
N-G-29		0,220		0,564	0,059		0,031	0,155
N-G-30	0,042	0,219	0,110	0,268	0,076	0,109		0,127
N-G-31		0,230	0,114	0,247				
N-G-32		0,183		0,574	0,056			
N-G-33		0,259	0,116	0,329	0,063	0,064		0,130
N-G-34		0,242	0,148	0,378	0,116	0,099		0,239
N-G-35		0,196	0,185	0,270	0,088	0,091		0,214
N-G-36		0,187	0,115	0,693	0,052	0,166		0,141
N-G-37	0,046		0,117	0,545		0,066		0,129
N-G-38	0,043			0,786			0,030	
N-G-39		0,161		0,775				
N-G-40	0,042			0,888				
N-G-41				0,260	0,053	0,064		0,118
N-G-42		0,170	0,118	0,287		0,065		0,119
N-G-43		0,174	0,153	0,250	0,050			0,146
N-G-44	0,042		0,134			0,090		0,149
N-G-45				0,236		0,088		0,144
N-G-46		0,250	0,193	0,326	0,079	0,200		0,258
N-G-47	0,051	0,241	0,121	0,601		0,133	0,055	0,148
N-G-48	0,042	0,218	0,164			0,143	0,019	0,261
N-G-49		0,190	0,115	0,636	0,050	0,160		0,136

Appendix A (continued)

Compounds	Glutamate-tRNA ligase inhibitor	Glutamate synthase (ferredoxin) inhibitor	Beta tubulin antagonist	5-Lipoxygenase inhibitor
N-G-1	0,198	0,129	0,050	0,064
N-G-2	0,291	0,172	0,163	0,172
N-G-3	0,203		0,237	0,154
N-G-4	0,254	0,149	0,462	0,094
N-G-5	0,217	0,143	0,168	0,156
N-G-6	0,221		0,195	0,113
N-G-7	0,225	0,136	0,387	0,210
N-G-8	0,239	0,145	0,227	0,089
N-G-9	0,457	0,274	0,150	0,105
N-G-10	0,264	0,161	0,169	0,166
N-G-11	0,199	0,138	0,189	0,135
N-G-12			0,145	0,156
N-G-13	0,255	0,152	0,173	0,131
N-G-14	0,324	0,180	0,058	0,068
N-G-15			0,085	0,141
N-G-16			0,251	
N-G-17			0,074	0,086
N-G-18	0,292	0,163	0,168	0,122
N-G-19	0,226	0,155	0,095	0,089
N-G-20	0,284	0,174	0,180	0,165
N-G-21	0,279	0,179	0,321	0,138
N-G-22	0,337	0,197	0,104	0,121
N-G-23	0,231	0,135	0,442	0,150
N-G-24	0,202	0,133	0,169	0,152
N-G-25	0,191		0,218	0,140
N-G-26	0,204	0,151	0,312	0,158
N-G-27	0,313	0,156	0,063	0,102
N-G-28	0,501	0,280		0,118
N-G-29	0,219	0,127	0,265	0,153
N-G-30		0,157	0,060	0,095
N-G-31	0,235	0,159	0,071	0,072
N-G-32			0,074	0,086
N-G-33	0,262	0,157	0,219	0,115
N-G-34	0,335	0,194	0,208	0,116
N-G-35	0,277	0,186	0,139	0,120
N-G-36	0,259	0,151	0,498	0,104
N-G-37	0,217	0,131	0,226	0,190
N-G-38	0,191		0,251	0,378
N-G-39			0,203	0,193
N-G-40		0,125	0,107	0,102
N-G-41	0,233	0,153	0,096	0,090
N-G-42	0,229	0,158	0,071	0,086
N-G-43	0,217	0,124	0,125	0,077
N-G-44	0,324	0,180	0,058	0,068
N-G-45	0,245	0,132	0,049	
N-G-46	0,457	0,274	0,150	0,105
N-G-47	0,291	0,172	0,163	0,172
N-G-48	0,387	0,212	0,059	0,091
N-G-49	0,254	0,149	0,462	0,094

Appendix B (Swiss Target Prediction)

Target																										
	N-G-1	N-G-2	N-G-3	N-G-4	N-G-5	N-G-6	N-G-7	N-G-8	N-G-9	N-G-10	N-G-11	N-G-12	N-G-13	N-G-14	N-G-15	N-G-16	N-G-17	N-G-18	N-G-19	N-G-20	N-G-21	N-G-22	N-G-23	N-G-24	N-G-25
ESR1	+						+		+		+	+	+		+	+	+		+		+				+
ALOX5	+	+			+		+			+	+	+	+	+	+	+	+		+			+		+	+
ALOX15	+	+	+			+					+	+	+			+	+		+		+	+			
LYPLA1	+															+	+		+						
LYPLA2	+															+	+		+						
PDE4B	+																								
PPARG	+											+				+	+								
MAP2K1	+																+		+						
NR3C1	+												+			+	+		+		+				
CHEK1	+		+		+		+			+	+	+	+		+		+		+	+	+			+	
WEE1	+				+						+	+			+		+		+					+	
PTGES	+			+	+						+													+	+
KIF11	+																								
PIK3CB	+					+									+										
PIK3CG	+			+						+	+				+		+		+	+					
PIK3CA	+			+		+									+				+	+					
CDK2	+		+										+	+			+		+		+				
MTOR	+														+									+	
KDR	+		+			+	+			+					+	+				+	+		+		
ERN1	+							+	+	+					+					+	+		+		
RET	+									+						+				+					
ITK	+																								
PDK1	+				+										+		+								
PARP1	+	+	+	+		+	+				+		+		+		+		+			+	+		+
PIK3C2B	+																								
STAT3	+	+			+		+				+		+											+	+
PIM2	+							+		+	+	+			+		+		+	+		+			+
PIM3	+			+				+		+	+	+								+					+
IGF1R	+								+				+			+	+		+		+				
PIK3CD	+			+											+		+			+					
SYK	+																+						+		
MAPK3	+															+									
LIMK1	+																								
LRRK2	+			+		+		+		+						+				+					
AR	+		+			+	+						+		+										
CDK2 CCNA1 CCNA2	+				+			+		+	+					+			+	+	+		+	+	+
JAK3	+					+				+					+	+			+	+					
JAK1	+		+		+	+	+			+										+	+		+		
JAK2	+		+		+	+	+			+						+			+	+	+		+		
TYK2	+		+			+	+			+										+	+		+		
CDK5R1 CDK5	+				+			+		+	+				+	+					+		+	+	+
CCNE1 CDK2	+																		+		+				
CDK7 CCNH	+																								
CDK9 CCNT1	+									+											+		+		
PRKDC	+			+											+				+	+	+				
PDPK1	+							+							+						+		+		
FLT1	+																			+					
ROCK2	+														+	+									
ROCK1	+																+							+	
TUBB1	+	+	+	+			+		+		+		+						+	+			+		+
BRAF	+		+		+	+	+					+	+		+	+	+							+	
TNK2	+																								
EPHB4	+																								
HSP90AA1	+								+			+					+		+						
GAK	+																								
MDM2	+																								
CCND1 CDK4	+																				+				
CDK1 CCNB1	+						+	+			+													+	+
CCNE2 CDK2 CCNE1	+					+		+			+					+					+		+		+
GSK3B	+	+			+					+	+					+	+							+	+
GSK3A	+							+			+				+				+	+	+		+		

Appendix B (continued)

Target																										
	N-G-26	N-G-27	N-G-28	N-G-29	N-G-30	N-G-31	N-G-32	N-G-33	N-G-34	N-G-35	N-G-36	N-G-37	N-G-38	N-G-39	N-G-40	N-G-41	N-G-42	N-G-43	N-G-44	N-G-45	N-G-46	N-G-47	N-G-48	N-G-49
ESR1		+	+		+	+	+					+	+	+		+		+			+			+
ALOX5		+	+		+	+	+					+	+	+	+	+		+	+	+		+		
ALOX15		+	+	+	+	+	+	+	+	+				+	+	+		+		+		+	+	
LYPLA1			+			+	+									+								
LYPLA2			+			+	+									+								
PDE4B							+																	
PPARG			+		+		+							+		+					+			
MAP2K1		+	+		+	+	+									+								
NR3C1		+	+		+	+		+								+		+		+				
CHEK1					+	+	+		+	+	+		+	+	+	+		+		+				
WEE1					+	+	+						+	+		+		+						
PTGES					+		+								+	+								
KIF11																								
PIK3CB		+			+	+	+						+											+
PIK3CG		+			+	+	+				+							+		+				+
PIK3CA		+			+	+	+				+	+	+			+				+				+
CDK2			+	+	+	+	+									+			+	+				
MTOR						+	+						+							+				+
KDR		+		+	+	+				+		+			+	+					+			+
ERN1			+			+	+	+	+	+	+		+								+			+
RET					+		+		+	+						+		+						
ITK					+	+																		
PDK1													+			+								
PARP1			+	+	+	+	+	+				+						+		+		+	+	
PIK3C2B																								
STAT3															+	+						+		
PIM2							+				+							+					+	+
PIM3									+		+							+		+				+
IGF1R		+	+		+	+							+	+		+		+		+	+			
PIK3CD		+				+	+				+									+				+
SYK							+					+				+								
MAPK3						+																		
LIMK1																				+				
LRRK2																								+
AR			+	+	+	+				+						+								
CDK2 CCNA1 CCNA2				+	+			+	+	+	+					+		+		+				
JAK3				+			+		+	+		+								+				
JAK1				+			+	+	+											+				
JAK2				+			+	+	+	+										+				
TYK2				+				+	+											+				
CDK5R1 CDK5				+	+		+	+	+			+		+				+		+				
CCNE1 CDK2				+		+							+					+		+				
CDK7 CCNH						+																		
CDK9 CCNT1				+		+		+	+	+		+								+				
PRKDC		+									+									+				+
PDPK1		+		+			+	+										+						
FLT1					+		+																	
ROCK2						+																		
ROCK1																		+						
TUBB1		+		+	+		+	+	+	+	+	+	+			+		+		+	+	+		+
BRAF					+		+	+					+		+	+		+		+				
TNK2																								
EPHB4																								
HSP90AA1				+	+	+	+							+		+		+			+		+	
GAK																								
MDM2																								
CCND1 CDK4				+										+						+		+		
CDK1 CCNB1													+					+						
CCNE2 CDK2 CCNE1				+			+								+			+		+				
GSK3B						+	+			+					+						+			
GSK3A				+	+				+	+	+									+				+

Appendix C (Mol Tar Pred)

Target	N-G-1	N-G-2	N-G-3	N-G-4	N-G-5	N-G-6	N-G-7	N-G-8	N-G-9	N-G-10	N-G-11	N-G-12	N-G-13	N-G-14	N-G-15	N-G-16	N-G-17	N-G-18	N-G-19	N-G-20	N-G-21	N-G-22	N-G-23	N-G-24	N-G-25
Vanilloid receptor	+														+				+						
Arachidonate 5-lipoxygenase	+		+	+	+		+			+	+		+		+			+	+	+		+	+	+	+

Target	N-G-26	N-G-27	N-G-28	N-G-29	N-G-30	N-G-31	N-G-32	N-G-33	N-G-34	N-G-35	N-G-36	N-G-37	N-G-38	N-G-39	N-G-40	N-G-41	N-G-42	N-G-43	N-G-44	N-G-45	N-G-46	N-G-47	N-G-48	N-G-49
Vanilloid receptor					+											+		+		+				
Arachidonate 5-lipoxygenase	+			+	+			+					+		+	+		+				+		

Appendix D (SEA)

Target	N-G-1	N-G-2	N-G-3	N-G-4	N-G-5	N-G-6	N-G-7	N-G-8	N-G-9	N-G-10	N-G-11	N-G-12	N-G-13	N-G-14	N-G-15	N-G-16	N-G-17	N-G-18	N-G-19	N-G-20	N-G-21	N-G-22	N-G-23	N-G-24	N-G-25
APP	+	+	+	+	+	+	+	+	+	+	+		+	+	+		+	+	+	+	+	+	+	+	+
NDUFAB1	+	+	+		+				+	+	+		+	+	+		+	+	+		+	+		+	
Adrb1	+		+	+	+	+			+	+			+	+	+		+	+	+		+	+	+	+	+
ADRB1	+					+											+		+						
EP300	+	+	+	+	+		+	+	+	+	+		+	+	+		+	+	+		+	+	+	+	+
GPR174	+																								
LPAR1	+								+						+										
IKBKG	+	+	+	+	+	+	+	+	+	+	+		+	+	+		+	+	+	+	+	+	+	+	+
NFE2L2	+	+	+	+	+	+	+	+	+	+	+		+	+	+		+	+	+	+	+	+	+	+	+
NFKB1	+	+	+	+	+	+	+	+	+	+	+		+	+	+		+	+	+	+	+	+	+	+	+
Ptger2	+														+										
beta-tubulin	+		+	+					+	+			+		+			+	+	+	+	+		+	
CXCL12	+	+	+	+	+		+	+	+	+	+		+	+	+		+	+	+	+	+	+	+	+	+
MAPT	+	+	+	+	+		+	+	+	+	+	+	+	+	+		+	+	+	+	+	+	+	+	+
TLR1	+								+				+		+					+		+			
Tlr1	+		+	+	+				+	+			+	+	+	+	+	+	+	+	+	+			
Tlr2	+		+	+	+				+	+			+	+	+	+	+	+	+	+	+	+			
YWHAG	+												+		+			+	+			+			
NDUFAF1	+	+	+		+				+	+	+		+	+	+		+	+	+		+	+			
Enpp2	+																								
FOS	+	+	+	+	+	+	+	+	+	+	+		+	+	+		+	+	+	+	+	+	+	+	+
ALOX15	+	+	+	+	+	+	+			+	+	+	+		+			+	+		+	+		+	+
ALOX5	+	+	+	+	+		+	+	+	+	+	+	+		+		+	+	+	+	+	+	+	+	+
Alox5	+	+	+	+	+		+	+	+	+	+	+	+	+	+		+	+	+	+	+	+	+	+	+
Trpv2	+	+	+	+	+		+	+	+	+	+		+	+	+		+	+	+		+	+	+	+	+

Appendix D (continued)

Target																									
	N-G-26	N-G-27	N-G-28	N-G-29	N-G-30	N-G-31	N-G-32	N-G-33	N-G-34	N-G-35	N-G-36	N-G-37	N-G-38	N-G-39	N-G-40	N-G-41	N-G-42	N-G-43	N-G-44	N-G-45	N-G-46	N-G-47	N-G-48	N-G-49
APP	+	+	+	+	+	+	+	+	+	+	+	+	+		+	+	+	+	+		+	+	+	+
NDUFAB1	+				+	+	+	+	+	+						+	+	+	+					
Adrb1	+	+	+		+	+	+	+	+	+	+					+	+	+	+		+		+	+
ADRB1		+						+		+						+	+	+					+	
EP300	+				+	+	+	+	+	+					+	+	+	+	+		+	+	+	+
GPR174					+																			
LPAR1					+																+			
IKBKG	+			+	+	+	+	+	+	+	+	+	+		+	+	+	+	+		+	+	+	+
NFE2L2	+			+	+	+	+	+	+	+	+	+	+		+	+	+	+	+		+	+	+	+
NFKB1	+			+	+	+	+	+	+	+	+	+	+		+	+	+	+	+		+	+	+	+
Ptger2			+		+															+				
beta-tubulin	+				+	+		+	+	+	+					+		+			+		+	
CXCL12	+				+	+		+	+	+	+	+	+		+	+	+	+	+	+	+	+	+	+
MAPT	+	+		+	+	+	+	+	+	+	+	+	+		+	+	+	+	+		+	+	+	+
TLR1					+			+	+	+											+			
Tlr1	+			+	+	+		+	+	+	+		+	+		+	+	+	+		+		+	+
Tlr2	+			+	+	+		+	+	+	+		+	+		+	+	+	+		+		+	+
YWHAG			+		+			+		+						+		+		+			+	
NDUFAF1	+				+	+	+	+	+	+						+	+	+	+					
Enpp2																								
FOS	+	+		+	+	+	+	+	+	+	+				+	+	+	+	+		+	+	+	+
ALOX15	+	+	+	+	+	+		+	+	+	+			+		+	+	+				+	+	
ALOX5	+			+	+			+	+	+				+	+	+		+			+	+	+	+
Alox5	+		+		+	+	+	+	+	+	+	+	+	+	+	+	+	+	+	+	+	+	+	+	+
Trpv2	+				+	+	+	+	+	+					+	+	+	+	+		+	+	+	+

Appendix E

Cell-line	NCI-H322M	NCI-H226	PC-6	HOP-18	NCI-H187	DMS-114	Malme-3M	M14	SK-MEL-	M19-MEL
Full name	Non-small cell l	Non-small cell l	Small cell lun	Non-small cell	Small cell lung ca	Lung carcin	Melanoma	Melanoma	Melanoma	Melanoma
Tissue	Lung	Lung	Lung	Lung	Lung	Lung	Skin	Skin	Skin	Skin
N-G-1	-									
N-G-2	-									
N-G-3	-									
N-G-4	-				0.537					
N-G-5	-									
N-G-6	-									
N-G-7	-									
N-G-8	-									
N-G-9	-									
N-G-10	-									
N-G-11	-									
N-G-12	-									
N-G-13	-									
N-G-14	-					0.539				
N-G-15	-									
N-G-16	-									
N-G-17	-									
N-G-18	-									
N-G-19	-									
N-G-20	-									
N-G-21	-			0.587						0.514
N-G-22	-									
N-G-23	-									
N-G-24	-									
N-G-25	0.7	0.64					0.646	0.564	0.514	
N-G-26	-									
N-G-27	-									
N-G-28	-									
N-G-29	-									
N-G-30	-									
N-G-31	-									
N-G-32	-									
N-G-33	-		0.628							
N-G-34	-		0.534							
N-G-35	-									
N-G-36	-				0.741					
N-G-37	-									
N-G-38	-									
N-G-39	-									
N-G-40	-									
N-G-41	-									
N-G-42	-					0.512				
N-G-43	-									
N-G-44	-					0.539				
N-G-45	-									
N-G-46	-									
N-G-47	-									
N-G-48	-									
N-G-49	-									

Appendix E (continued)

Cell-line	RPMI-8226	K562	Hs 683	SF-539	MDA-MB	MCF7	OVCAR-8	IGROV-1	PC-3	DU-145	SN12C	SNB-75	cytoxicity on non-tumor cell line when pa>0.5
Full name	Multiple myeloma	Erythroleu	Oligodendr	Glioblastor	Breast ade	nocarcinor	Ovarian ad	Ovarian ad	Prostate c	Prostate c	Renal carc	Glioblastor	
Tissue	Haematopoietic and lymphc	Haematop	Brain	Brain	Breast	Breast	Ovarium	Ovarium	Prostate	Prostate	Kidney	Nervous s	
N-G-1													no
N-G-2		0.542						0.529					no
N-G-3													no
N-G-4													no
N-G-5													no
N-G-6													no
N-G-7													no
N-G-8													no
N-G-9													no
N-G-10		0.53											no
N-G-11		0.586											no
N-G-12													no
N-G-13													no
N-G-14													no
N-G-15					0.601								no
N-G-16				0.528	0.53						0.524		yes (on endothelium)
N-G-17													yes (on lung)
N-G-18			0.612										no
N-G-19													no
N-G-20		0.517								0.503			no
N-G-21			0.591										no
N-G-22													yes (on lung)
N-G-23													no
N-G-24													no
N-G-25	0.578												no
N-G-26													no
N-G-27													no
N-G-28													no
N-G-29													no
N-G-30													no
N-G-31													no
N-G-32													yes (on lung)
N-G-33													no
N-G-34													no
N-G-35													no
N-G-36			0.512										no
N-G-37													no
N-G-38		0.646											no
N-G-39													no
N-G-40									0.733				no
N-G-41													no
N-G-42							0.53		0.747				no
N-G-43					0.551								no
N-G-44													no
N-G-45			0.598									0.535	yes (on lung)
N-G-46													no
N-G-47		0.542						0.529					no
N-G-48													yes (on lung)
N-G-49													no

Appendix F

	Organ Toxicity	Toxicity end points				Tox21 Stress response pathways	
Compound code	Hepatotoxicity	Carcinogenicity	Immunotoxicity	Mutagenicity	Cytotoxicity	(MMP)	p53
N-G-1	inactive(0.83)	inactive(0.76)	active(0.95)	inactive(0.65)	inactive(0.88)	inactive(0.59)	inactive(0.69)
N-G-2	inactive(0.51)	inactive(0.61)	active(0.91)	inactive(0.96)	inactive(0.88)	inactive(0.92)	inactive(0.93)
N-G-3	inactive(0.67)	inactive(0.73)	inactive(0.83)	inactive(0.97)	inactive(0.90)	inactive(0.98)	inactive(0.99)
N-G-4	inactive(0.52)	inactive(0.60)	inactive(0.55)	inactive(0.98)	inactive(0.94)	inactive(0.99)	inactive(1.0)
N-G-5	inactive(0.61)	inactive(0.84)	active(0.92)	inactive(0.88)	inactive(0.88)	active(1.0)	active(1.0)
N-G-6	inactive(0.65)	active(0.76)	inactive(0.92)	inactive(0.86)	inactive(0.89)	inactive(0.99)	inactive(0.99)
N-G-7	inactive(0.67)	active(0.55)	active(0.85)	inactive(0.97)	inactive(0.85)	inactive(0.97)	inactive(0.99)
N-G-8	inactive(0.69)	inactive(0.70)	inactive(0.68)	inactive(0.92)	inactive(0.90)	inactive(0.97)	inactive(0.99)
N-G-9	inactive(0.55)	inactive(0.64)	inactive(0.97)	inactive(0.96)	inactive(0.93)	inactive(0.93)	inactive(0.98)
N-G-10	inactive(0.52)	inactive(0.57)	inactive(0.78)	inactive(0.99)	inactive(0.94)	inactive(0.97)	inactive(0.99)
N-G-11	active(0.51)	inactive(0.59)	active(0.87)	inactive(0.87)	inactive(0.91)	inactive(0.96)	inactive(0.98)
N-G-12	inactive(0.72)	inactive(0.59)	active(0.92)	inactive(0.71)	inactive(0.89)	active(0.89)	inactive(0.88)
N-G-13	inactive(0.65)	inactive(0.54)	inactive(0.72)	inactive(0.83)	inactive(0.87)	inactive(0.91)	inactive(0.98)
N-G-14	inactive(0.6)	inactive(0.52)	inactive(0.95)	inactive(0.95)	inactive(0.92)	inactive(0.95)	inactive(0.99)
N-G-15	inactive(0.72)	inactive(0.74)	active(0.86)	active(0.67)	inactive(0.75)	inactive(0.68)	inactive(0.92)
N-G-16	inactive(0.73)	inactive(0.68)	active(0.98)	inactive(0.86)	inactive(0.83)	inavtive(0.53)	inactive(0.76)
N-G-17	inactive(0.78)	inactive(0.61)	active(0.98)	inactive(0.72)	inactive(0.92)	active(0.63)	inactive(0.70)
N-G-18	inactive(0.87)	inactive(0.64)	inactive(0.78)	inactive(0.88)	inactive(0.93)	inactive(0.93)	inactive(0.98)
N-G-19	inactive(0.51)	inactive(0.73)	inactive(0.90)	inactive(0.89)	inactive(0.89)	inactive(0.93)	inactive(0.98)
N-G-20	inactive(0.55)	inactive(0.61)	inactive(0.78)	inactive(0.95)	inactive(0.94)	inactive(0.81)	inactive(0.99)
N-G-21	inactive(0.71)	active(0.61)	inactive(0.95)	inactive(0.98)	inactive(0.86)	inactive(0.99)	inactive(1.0)
N-G-22	inactive(0.61)	inactive(0.79)	inactive(0.94)	inactive(0.92)	inactive(0.91)	inactive(0.95)	inactive(0.98)
N-G-23	inactive(0.66)	inactive(0.61)	active(0.59)	inactive(0.97)	inactive(0.88)	inactive(0.98)	inactive(0.99)
N-G-24	inactive(0.61)	inactive(0.82)	active(0.94)	inactive(0.79)	inactive(0.85)	active(0.94)	active(0.80)
N-G-25	active(0.50)	inactive(0.63)	active(0.79)	inactive(0.85)	inactive(0.90)	inactive(0.97)	inactive(0.98)
N-G-26	inactive(0.82)	inactive(0.68)	active(0.76)	inactive(0.81)	inactive(0.93)	inactive(0.92)	inactive(0.96)
N-G-27	inactive(0.63)	inactive(0.57)	inactive(0.80)	inactive(0.75)	inactive(0.93)	active(0.52)	inactive(0.89)
N-G-28	inactive(0.67)	inactive(0.64)	inactive(0.99)	inactive(0.79)	inactive(0.86)	inactive(0.88)	inactive(0.95)
N-G-29	inactive(0.64)	inactive(0.63)	inactive(0.73)	inactive(0.72)	inactive(0.93)	inactive(0.97)	inactive(0.96)
N-G-30	inactive(0.71)	inactive(0.75)	active(0.62)	active(0.53)	inactive(0.80)	inactive(0.69)	inactive(0.93)
N-G-31	inactive(0.87)	inactive(0.70)	inactive(0.71)	inactive(0.80)	inactive(0.94)	inactive(0.58)	inactive(0.80)
N-G-32	inactive(0.74)	inactive(0.60)	active(0.98)	inactive(0.72)	inactive(0.94)	active(0.55)	inactive(0.84)
N-G-33	inactive(0.71)	active(0.53)	inactive(0.82)	inactive(0.93)	inactive(0.88)	inactive(0.98)	inactive(0.99)
N-G-34	active(0.52)	inactive(0.70)	inactive(0.92)	inactive(0.95)	inactive(0.96)	inactive(0.96)	inactive(0.99)
N-G-35	inactive(0.70)	inactive(0.74)	inactive(0.94)	inactive(0.87)	inactive(0.94)	inactive(0.91)	inactive(0.98)
N-G-36	inactive(0.55)	inactive(0.62)	inactive(0.68)	inactive(0.96)	inactive(0.93)	inactive(0.98)	inactive(1.0)
N-G-37	inactive(0.76)	inactive(0.62)	active(0.87)	inactive(0.78)	inactive(0.88)	inactive(0.92)	inactive(0.99)
N-G-38	inactive(0.62)	inactive(0.57)	active(0.97)	inactive(0.61)	inactive(0.86)	active(0.85)	inactive(0.53)
N-G-39	inactive(0.72)	inactive(0.68)	active(0.66)	inactive(0.94)	inactive(0.95)	active(0.92)	inactive(0.86)
N-G-40	inactive(0.58)	inactive(0.69)	active(0.93)	inactive(0.69)	inactive(0.97)	active(0.94)	active(0.56)
N-G-41	inactive(0.70)	inactive(0.71)	inactive(0.91)	inactive(0.75)	inactive(0.85)	active(0.78)	inactive(0.59)
N-G-42	inactive(0.94)	inactive(0.79)	active(0.52)	inactive(0.83)	inactive(0.92)	inactive(0.94)	inactive(0.97)
N-G-43	inactive(0.55)	inactive(0.72)	inactive(0.69)	inactive(0.87)	inactive(0.91)	inactive(0.92)	inactive(0.98)
N-G-44	inactive(0.6)	inactive(0.52)	inactive(0.95)	inactive(0.95)	inactive(0.92)	inactive(0.95)	inactive(0.99)
N-G-45	inactive(0.68)	active(0.64)	inactive(0.91)	inactive(0.79)	inactive(0.88)	inactive(0.96)	inactive(0.98)
N-G-46	inactive(0.55)	inactive(0.64)	inactive(0.96)	inactive(0.96)	inactive(0.93)	inactive(0.93)	inactive(0.98)
N-G-47	inactive(0.51)	inactive(0.61)	active(0.95)	inactive(0.96)	inactive(0.88)	inactive(0.92)	inactive(0.93)
N-G-48	active(0.50)	inactive(0.80)	inactive(0.97)	inactive(0.93)	inactive(0.92)	inactive(0.95)	inactive(0.97)
N-G-49	inactive(0.52)	inactive(0.60)	active(0.63)	inactive(0.98)	inactive(0.94)	inactive(0.99)	inactive(1.0)

Appendix G

Compound code	Hepatotoxicity	hERG I inhibitor	hERG II inhibitor
N-G-1	no	no	no
N-G-2	no	no	no
N-G-3	no	no	no
N-G-4	no	no	no
N-G-5	no	no	no
N-G-6	no	no	no
N-G-7	yes	no	no
N-G-8	no	no	no
N-G-9	no	no	yes
N-G-10	no	no	no
N-G-11	no	no	no
N-G-12	no	no	no
N-G-13	yes	no	no
N-G-14	no	no	no
N-G-15	no	no	yes
N-G-16	no	no	no
N-G-17	no	no	yes
N-G-18	no	no	no
N-G-19	yes	no	no
N-G-20	no	no	no
N-G-21	no	no	no
N-G-22	no	no	no
N-G-23	no	no	no
N-G-24	no	no	yes
N-G-25	no	no	no
N-G-26	no	no	no
N-G-27	no	no	yes
N-G-28	yes	no	no
N-G-29	no	no	no
N-G-30	no	no	yes
N-G-31	no	no	yes
N-G-32	no	no	no
N-G-33	yes	no	no
N-G-34	no	no	no
N-G-35	no	no	no
N-G-36	no	no	no
N-G-37	no	no	no
N-G-38	no	no	no
N-G-39	no	no	no
N-G-40	no	no	no
N-G-41	no	no	yes
N-G-42	no	no	no
N-G-43	yes	no	no
N-G-44	no	no	no
N-G-45	yes	no	no
N-G-46	no	no	no
N-G-47	no	no	no
N-G-48	no	no	no
N-G-49	no	no	no

8. Curriculum Vitae

Personal Informations

Name	Nour	**Surname**	Al-Massri
Place of Birth		**Date of Birth**	
Nationality		**TR ID Number**	
E-mail		**Phone number**	

Education

Degree	Department	The name of the Institution Graduated From	Graduation year
Doctorate			
Master			
University	Damascus	Faculty of Pharmacy	2019
High school	-		2014

Languages	Grades (#)
English	6.5
Turkish	B1

All the grades must be listed if there is more than one (KPDS, ÜDS, TOEFL; EELTS vs),

Work Experience (Sort from present to past)

Position	Institute	Duration (Year - Year)
Pharmacist	Nour Pharmacy	8 months
Pharmacist	Atfeh Pharmacy	3 years

Computer Skills

Program	**Level**
Microsoft Office	Excellent
Molecular Operating Environment (MOE)	Excellent

***Excellent, good, average, or basic**